An Innovative Method for Evaluating Power Distribution System Reliability

by

Mohammad Almuhaini

A Dissertation Presented in Partial Fulfillment
of the Requirements for the Degree
Doctor of Philosophy

Approved August 2012 by the
Graduate Supervisory Committee:

Gerald Heydt, Chair
Raja Ayyanar
Esma Gel
Daniel Tylavsky

ARIZONA STATE UNIVERSITY

December 2012

ABSTRACT

The reliability assessment of future distribution networks is an important issue in power engineering for both utilities and customers. This is due to the increasing demand for more reliable service with less interruption frequency and duration. This research consists of two main parts related to the evaluation of the future distribution system reliability. An innovative algorithm named the encoded Markov cut set (EMCS) is proposed to evaluate the reliability of the networked power distribution system. The proposed algorithm is based on the identification of circuit minimal tie sets using the concept of Petri nets. Prime number encoding and unique prime factorization are then utilized to add more flexibility in communicating between the systems states, and to classify the states as tie sets, cut sets, or minimal cut sets. Different reduction and truncation techniques are proposed to reduce the size of the state space. The Markov model is used to compute the availability, mean time to failure, and failure frequency of the network. A well-known Test Bed is used to illustrate the analysis (the Roy Billinton test system (RBTS)), and different load and system reliability indices are calculated. The method shown is algorithmic and appears suitable for off-line comparison of alternative secondary distribution system designs on the basis of their reliability.

The second part assesses the impact of the conventional and renewable distributed generation (DG) on the reliability of the future distribution system. This takes into account the variability of the power output of the renewable DG, such as wind and solar DGs, and the chronological nature of the load demand.

The stochastic nature of the renewable resources and its influence on the reliability of the system are modeled and studied by computing the adequacy transition rate. Then, an integrated Markov model that incorporates the DG adequacy transition rate, DG mechanical failure, and starting and switching probability is proposed and utilized to give accurate results for the DG reliability impact. The main focus in this research is the conventional, solar, and wind DG units. However, the technique used appears to be applicable to any renewable energy source.

DEDICATION

Dedicated to my parents, my wife, and my children, Mohanad and Seba,

for their infinite love, support, and encouragement.

ACKNOWLEDGMENTS

I am grateful to Allah for his guidance and protection throughout my life and for giving me courage, patience, and strength to carry out this work.

Acknowledgement is also due to King Fahd University of Petroleum & Minerals and the Electrical Engineering Department for providing support for this research.

I would like to express my deepest appreciation and thanks to my advisor, Prof. Gerald Heydt, for his invaluable support, discussions, criticism, and guidance throughout this research. Without his guidance and encouragement, this study would not have been possible. I truly appreciate and enjoyed the opportunity to be part of his research group and learn from his fascinating personality, teaching philosophy, and unlimited knowledge. It has been an honor to be his PhD student, and I will always remain indebted to him.

I thankfully acknowledge the PhD advisory committee members, Dr. Raja Ayyanar, Dr. Esma Gel, and Dr. Daniel Tylavsky, for their time, critical reviews, and suggestions. Their academic support and helpful comments are greatly appreciated.

I would also like to thank all the faculty, staff, friends, and colleagues at Arizona State University who have supported me during my PhD program. I am grateful for time spent with my close friends, Bharadwaj R. Sathyanarayana, Daniel Haughton, and Sara Eftekharnejad. Special thanks go to Mr. Clayton "Clay" Javurek, the instructional laboratory manager, for his friendship, support, and shared passion for sports. I am very grateful to all the faculty and students

who have supported me during the medical crises that I had in 2010, especially Prof. Gerald Heydt, Dr. Daniel Talavsky, Mr. Clayton Javurek, and Dr. Joseph Palais. I appreciate all you did and thank you from the bottom of my heart.

I would like to thank my parents, brothers, and sisters for their love, concern, and moral support throughout my research. Their encouragement was always a source of motivation for me, and they deserve more thanks than I can give.

Last, but certainly not least, I especially want to thank my wife, my son Mohanad, and my daughter Seba for their love and continuous support in the good times and the bad times. Thank you for being who you are and for being the best part of me. Words are insufficient to express gratitude to my wife and children for their unconditional love and support.

TABLE OF CONTENTS

Page

CHAPTER Page

LIST OF TABLES

Table Page

LIST OF FIGURES

Figure Page

Figure Page

Figure Page

NOMENCLATURE

A	Availability
A_{DG}	Distributed generation availability
AID	Average interruption duration
AID^{eq}	Equivalent average interruption duration
AID_l	Average interruption duration lower bound
AID_u	Average interruption duration upper bound
AIF	Averaged interruption frequency
AIF^{eq}	Equivalent averaged interruption frequency
AIF_l	Averaged interruption frequency lower bound
AIF_u	Averaged interruption frequency upper bound
A_l	Availability lower bound
ARMA	Auto-regressive and moving average
ASAI	Average system availability index
$ASAI_l$	Average system availability index lower bound
$ASAI_u$	Average system availability index upper bound
ASUI	Average system unavailability index
$ASUI_l$	Average system unavailability index lower bound
$ASUI_{pu}$	Average system unavailability index in per unit
$ASUI_u$	Average system unavailability index upper bound
A_{sys}	System availability
A^T	Connection matrix
A_u	Availability upper bound
B	Total number of buses
c	Customer
CAIDI	Customer average interruption duration index
$CAIDI_l$	Customer average interruption duration index lower bound
$CAIDI_u$	Customer average interruption duration index upper bound

C_i	*i*th minimal cut set
C_j	DG capacity of the level *j*
COT	Capacity outage table
CPT	Capacity probability table
CS	Cut set
CTMC	Continuous time Markov chains
d	Number of down states
DG	Distributed generation
DPLVC	Daily peak load variation curve
DPT	Demand probability table
DTMC	Discrete time Markov chain
D_x	Total time spent in *x*
$E[T_{br}]$	Expected time between residences
$E[T_c]$	Expected cycle time
$E[T_r]$	Expected residence time
EMCS	Encoded Markov cut set
ENS	Energy not supplied
ENS_l	Energy not supplied lower bound
ENS_{pu}	Energy not supplied in per unit
ENS_u	Energy not supplied upper bound
f	Failure frequency
FD	Failure duration
FD_l	Failure duration lower bound
FD_u	Failure duration upper bound
f_{ij}	Frequency of occurrence from state *i* to state *j* and
f_m	Merged frequency
f_p	Equivalent frequency (parallel components)
f_s	Equivalent frequency (series components)

f_{system}	System frequency
I	Identity matrix
I	Transition input arc weight (Petri nets)
ID	Identification number
IEEE	Institute of electrical and electronics engineers
L	Total number of loads in the system
l	Lower bound
$L(t)$	Hourly load in per unit
LDC	Load duration curve
L_i	Load level i
LOLE	Loss of load expectation
LOLF	Loss of load frequency
LOLP	Loss of load probability
LP	Load point
M	Column vector of the change in marking (Petri nets)
m	Total number of minimal cut sets
m	Total number of levels in capacity probability table
MC	Monte Carlo
MCS	Minimal cut set
ML	Master list
M_o	Initial marking (Petri nets)
MP	Markov process
MTBF	Mean time between failures
MTS	Minimal tie set
MTTF	Mean time to failure
$MTTF_m$	Distributed generation mechanical mean time to failure
MTTR	Mean time to repair
$MTTR_m$	Distributed generation mechanical mean time to repair

N	Total number of columns in the connection matrix
n	Total number of segments
N-matrix	Fundamental matrix of the absorbing Markov chains
N_T	Total number of customers in the system
N_{xy}	Number of observed transitions from x to y
O	Transition output arc weight (Petri nets)
P	Probability
P	Places (Petri nets)
P_{avg}	Average power
P_d	Percentage of the daily load in terms of the weekly peak load
P_{DG}	Distributed generation power output
P_h	Percentage of the hourly load in terms of the daily peak
P-matrix	Stochastic transitional probability matrix
PN	Petri nets
P_{SS}	Probability to start and switch the distributed generation
PV	Photovoltaic
P_w	Percentage of weekly load in terms of the annual peak load
Q-matrix	Coefficients matrix of the Markov differential equations
R1	Reduction level 1: Irrelevant load points
R2	Reduction level 2: Series and parallel sections
R3	Reduction level 3: Irrelevant sections
R4	Reduction level 4: Sections of the irrelevant load points
RBTS	Roy Billinton test system
RCR	Rated capacity ratio
RI	Reliability index
R-matrix	Probability to enter the absorbing states matrix
S	State
SAIDI	System average interruption duration index

$SAIDI_l$	System average interruption duration index lower bound
$SAIDI_{pu}$	System average interruption duration index in per unit
$SAIDI_u$	System average interruption duration index upper bound
SAIFI	System average interruption frequency index
$SAIFI_l$	System average interruption frequency index lower bound
$SAIFI_{pu}$	System average interruption frequency index in per unit
$SAIFI_u$	System average interruption frequency index upper bound
S-matrix	Truncated matrix associated with stochastic transitional probability matrix
STD	State transition diagram
STM	State transition matrix
T	Transitions (Petri nets)
T1	Truncation level: Maximum simultaneous failures
T_f	Mean time to failure
T_f^{eq}	Equivalent time to fail
T_{fr}	Mean time between failures
T_{frs}	Equivalent failure cycle (series components)
T_{fs}	Equivalent time to fail (series components)
T_r	Mean time to repair
T_r^{eq}	Equivalent time to repair
Trs	Equivalent time to repair (series components)
TS	Tie set
u	Number of up states
u	Upper bound
U	Unavailability
U_{DG}	Distributed generation unavailability
U_l	Unavailability lower bound
U_u	Unavailability upper bound
w_i	Weight for each i index

x	Working state where the generated power is greater than the demand
y	Failed state where the load demand is greater than the generated power
y	Year
μ	Repair rate
μ_{ds}	Distribution system repair rate
μ_m	Distributed generation mechanical repair rate
μ_p	Equivalent repair rate (parallel components)
μ_s	Equivalent repair rate (series components)
μ_{ss}	DG starting and switching repair rate
λ	Failure rate
λ_{ds}	Distribution system failure rate
λ_m	Distributed generation mechanical failure rate
λ_p	Equivalent failure rate (parallel components)
λ_s	Equivalent failure rate (series components)
λ_{xy}	Transition of change from the working state x to the failed state y
λ_{yx}	Transition of change from the failed state y to the working state x
Σ	Column vector for the firing count (Petri nets)
σ_{ij}	Transition rates or rates of departure from i to j
σ-*matrix*	Transition rates matrix
Ω_L	Set of additional lines in tie set

Chapter 1

RELIABILITY OF POWER DISTRIBUTION SYSTEMS

1.1 The Configuration of Power Distribution Systems

The configuration of a distribution system can follow different arrangements based on the cost vs. reliability requirements. The distribution system can have multiple configurations including simple radial, primary selective, secondary selective, or secondary network. Each design will provide increasing reliability as well as increasing installation and operational costs. Distribution systems are typically of radial configuration, as shown in Fig. 1.1.

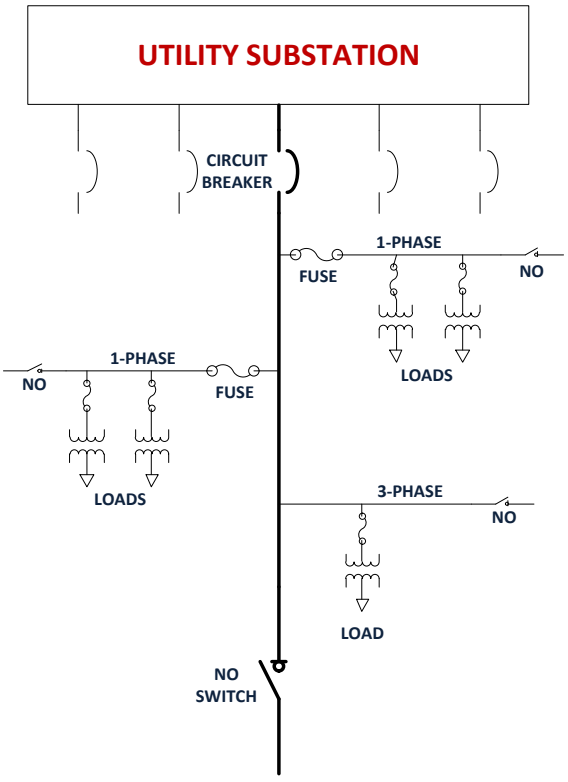

Fig. 1.1 Typical radial distribution system

The radial configuration is the simplest and perhaps least reliable design of load distribution, where the power is flowing in one direction from one substation to the loads. The radial system consists of one substation with one or more main feeders and many laterals connecting the transformers and load points. The radial configuration is less reliable than a secondary networked configuration, but it is also less expensive and less complex due to fewer connections and protection devices. Radial configuration is usually located in the suburban and rural areas where the density of customers is low and their reliability requirement is not very high. The radial feeders in these areas are either in overhead lines or in underground cables. All system feeders and laterals are designed to operate in their full rated capacity. With the absence of an alternative power supply, there is not much redundancy with this arrangement. If there is any failure in the main feeder, the circuit breaker on the transformer side or the reclosers in the feeder will clear the fault and interrupt the loads downstream of the protection device.

The secondary network is described as a configuration in which all the loads are connected via two or more alternative routes to the main supply. A secondary network is designed to provide highly reliable service to customers. Unlike the radial configuration, there are multiple transformers serving each network. The reliability of this secondary network is very high, and every load point in the network is supplied by two or more alternative power supplies. If a fault occurs on one of the transformers or primary feeders, there will not be any interruption to any load point and, therefore, no network interruption. This type of network can usually be found in downtown areas (central business districts)

where the density of loads is very high and the interruption cost is expensive. The installation cost of the secondary network is 175–200% of the cost of radial configuration [1]. This increased cost is because of the additional secondary connections, the overrated size of lines and transformers, and the protection devices.

Radial systems have been in widespread use for almost 100 years, and a considerable level of engineering expertise has resulted from this basic design configuration. Nonetheless, it is prudent to look to the next generation of distribution systems, often referred to as ‘smart grids’, by incorporating networks, DG, energy storage, electronic controls, self-healing designs, and improved protection systems [2-4].

The term “smart grid” is defined and used in several ways, but a common characteristic is the growth usage of advanced information technology (IT) in electric distribution systems. The future grid will bring smaller DGs into the grid and the grid should be more flexible to any changes from the renewable sources in the system. The renewable resources are expected to be integrated at any location in the grid. Furthermore, the widespread use of DG will force the distribution system to become bidirectional, thereby creating more challenges in designing and operating the system.

Another advanced aspect of the future grid will be the smart communications among the devices in the system. This can be done by building a processor in every protection device, transformer, switch, etc., and making them capable of communicating with each other. The live communication is also

between the customers and the utilities so that the customers can manage their energy consumption. Some key changes to the future systems include integrating small-scale distributed generators and renewable energy, greater level of storage, and demand response. Fig. 1.2 shows the key factors of the next generation smart grids.

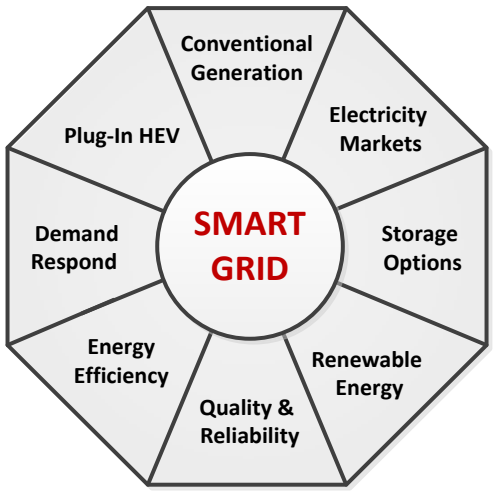

Fig. 1.2 Smart grid key factors

One of the main incentives for smart grids is to enhance the reliability of the power system by integrating small-scale resources and reconfiguring the distribution system to be a unidirectional network. The complexity of the future distribution systems will require enhanced techniques to evaluate the reliability and minimize the frequency and duration of the outages. Several studies discussed the effect of the DG in the load and system reliability indices [5, 6]. When a fault occurs in the smart grid, the system then will break into islanded areas or clusters where each area has the capability to survive based on its resources and connections until the system can regroup into a complete system.

In general, the reliability of the future distribution systems can be improved by enhancing the fault detection techniques, fault isolation, restoration capabilities, and incorporating smarter information technologies in controlling and operating the system [7].

1.2 Reliability of Power Distribution Systems

Reliability has been a subject of great interest in most of the manufacturing and services applications [8]. The reliability definition based on the IEEE 90 standard is "*the ability of a system or component to perform its required functions under stated conditions for a specified period of time*" [9]. In electric power distribution systems, reliability is a key issue in design and operation—especially in view of sensitive, digitally controlled loads.

Analyzing and evaluating the distribution system's reliability is important to improve the operational and maintenance performance of the system and provide highly reliable electricity with high quality. Some sources of power problems are in nature form, such as, tornadoes, lightning, wind, earthquakes, and snow. Manmade problems include automotive accidents, vandalism, and inadvertent contact with overhead conductors, distribution operator errors, and fires. These factors are extremely difficult to predict or control, thereby making it hard to avoid power outages. Some factors that can be controlled or optimized include vehicle or construction accidents, overloads, animal contacts, and equipment failure or wear out. Most power problems can be reduced by implementing underground connections, but this result in increased cost and maintenance inflexibility.

The overall reliability evaluation of power systems should include generation, transmission, and distribution reliability studies. In reference [10], the reliability of distribution systems is evaluated by considering the impact of the failures from the generation and transmission subsystems. In practice, all reliability studies are conducted in relatively small local subsystems since the complete network from the source to the load is enormous. In reality, it is also difficult to collect the necessary data for reliability evaluations. Utilities are conservative or sometimes reluctant to release actual reliability data and failure rates. Several references have investigated methods to collect and categorize data that can be used in reliability studies [11, 12].

The performance of distribution systems may be quantified by measures of voltage regulation and classical power distribution engineering issues including evaluation of losses, power factor, overhead versus underground designs [13-15], counts of anomalous events [16-19], and power quality at the point of end use [20, 21]. Reference [17] specifically addresses the value of ‘count indices’ (i.e., counting undesired events such as outages or low voltage cases) for the purpose of standardized distribution system planning. Reference [18] addresses the probabilistic analysis of these indices. In recent years, the move to use DG resources in the distribution system and the impact of these resources on distribution system reliability has also been considered, as shown in [22–27]. References [21, 28, 29] are samples of distribution system engineering analysis and design—an area that has received considerable attention for over 100 years.

These references are only a small sample of the literature since the full literature is voluminous.

The reliability evaluation can be divided into two parts: modeling of the reliability characteristics of the components, and the calculation of the reliability of the system. In modeling the components reliability data, it is a common practice to assume that the failures are independent of each other. Each component of the system is modeled with a different number of states (commonly, two or three states). The two states include the up state (working condition) and the down state (repair condition), and the additional third state can be the planned or scheduled maintenance state.

To evaluate the reliability of a system, a mathematical or graphical model of the system should be used and designed to reflect its reliability characteristics. The models can be either analytical or simulation. Analytical models represent the system by a set of exact or approximate mathematical models and evaluate the reliability based on this mathematical representation of each state. The Markov model is one of the popular analytical techniques to evaluate the reliability of the power system. All transition rates between the states are assumed, making it possible to evaluate the steady-state probability of the states. The Markov chain is one of the best models that can represent the dynamic behavior of the system, but it is also very complicated to construct the transition matrix for a large number of components.

Another widely used technique for reliability assessment in many fields is Monte Carlo (MC) simulation. In MC simulation, the reliability is evaluated

repeatedly using parameters drawn from random distributions to simulate the stochastic problems [19, 30, 31]. Usually, MC simulation is used when other deterministic methods failed to apply and can be useful in evaluating the mean time to failure for very complicated or large scale systems.

The advantage of the MC simulation is that it can simulate almost any system and any failure mode. The disadvantages, on the other hand, are that it requires long runs (i.e., many samples) and the accuracy of the output may depend on the number of runs and variables in the system.

In applications of complex systems, analytical techniques usually include some simplifications or assumptions. However, the simulation technique can simulate and include any system behavior with less approximation. The analytical models give the same numerical results each run since the model contains a fixed mathematical representation for the system, whereas the results from the simulation models differ in each run since the system characteristics are randomly changing in each run [32]. The solution time for the analytical techniques are relatively shorter than that of the simulation run time. The simulation time can be very high in complex systems and in applications where several reliability indices are required.

1.3 Motivation for This Research

The massive blackout in the northeastern United States and Canada on August 2003 brought more public interest in the reliability of the grid. Moreover, the power industry has become a competitive environment under deregulation, and the continuity of power supply to the customers is significant. Deregulation

seeks to create a competitive environment in the power area to obtain better service and lower cost. Therefore, utilities are seeking more accurate data and predictions about the electrical service and its availability to keep their customers satisfied.

A distribution system is highly complex and contains a large number of connections and components, which make it the greatest contributor to the unavailability of power supply to the customers. In fact, the distribution system accounts for almost 40% of the overall power system and 80% of customer reliability problems [33]. Moreover, contemporary loads are often digital in nature, and these loads are frequently sensitive to interruptions and, indeed, many other power quality problems. The customers themselves are perhaps becoming more sensitive to interruptions due to the possibility of industrial manufacturing interruption, commercial loss of sales, and residential nuisance. Sophisticated control systems may actually exacerbate the impact of service interruptions. Competition in power marketing may be impacted as well—industrial customers may seek to locate places where power system reliability is high. For these reasons, distribution system design and operation is critical for the power industry. One common characteristic among industrial and commercial customers is that the cost of downtime is enormous. As the availability and the reliability of the power system become more sensitive to the customers and utilities, more research and techniques are needed to evaluate the reliability of power system.

Distribution systems are now in a significant transitional phase; the system is shifting from passive distribution systems with unidirectional power flow to

active distribution networks with bidirectional flow and small scale generators. This can present an extraordinary challenge for the business of electric generation and delivery. Future distribution systems are often referred to as “smart grids”, where more intelligent technologies are integrated to the system to monitor, control, and operate the system. Therefore, the reliability of the future grids is expected to become more challenging issue in the near future, with more complex configurations and an increase in small scale units.

Taking into account the ongoing deregulation process in many countries and the rapid development in the DG technologies, there may be a need to reconsider or to extend and enhance the traditional approach to evaluate the reliability of the distribution system. Furthermore, the increased demand for more reliability introduces more networked secondary systems, making it complicated to evaluate the reliability of the distribution systems. Conventional methods to evaluate the reliability of the secondary networks will be more complex and time consuming. Enhanced or new methods are needed to accelerate the evaluation process and increase its process.

1.4 Scope and Objectives of This Research

The central objective of this research is to examine and develop engineering methods to evaluate and increase the reliability of the next generation of power distribution systems. The following are key components of this work:

- To examine, quantify, and develop engineering designs for networked distribution systems. Analyzing the reliability of a network means evaluating the ability of two or more connected nodes to ‘communicate’

successfully given the failure probability of all components or elements in the system. Such analysis is usually complicated and consumes substantial computation time since it requires an analysis of the states of the failed components and analysis of the routing within the network in a combinatorial fashion.

- To utilize advanced circuit analytical techniques such as Petri nets and Markov process analysis to analyze the reliability of the networked systems. In power systems, as in many practical systems, the system has different discrete states and operates in one state and can change its state at any time. The reliability of these systems can be analyzed using continuous time Markov chains (CTMC). The Petri nets concept can also be used to solve the connectivity problem in complex systems. The minimal tie sets can be found using this concept, and these sets are used in Markov models to evaluate the reliability.
- To propose different reduction and truncation techniques to reduce the system connections and its state space for ease in analysis. The reduction techniques are used to exclude irrelevant load buses and their associated connections from the reliability model of each load point under study. The truncation method is used to reduce the state space by excluding states that are considered rare events.
- To use prime number theory to code the design of power distribution systems. In the application of prime number encoding to the evaluation of distribution reliability, prime numbers are used to encode the sections of

the power distribution network to classify the state space as minimal tie sets, tie sets, minimal cut sets, and cut sets. Prime number encoding-decoding adds more flexibility in finding and categorizing the states in the Markov model.

- To examine networked distribution systems. A reliability evaluation study quantifies reliability based on component reliability data and can be used to evaluate past performance and to identify the weak points or components in the system that introduce a high number of power problems to the whole network. To increase the reliability of the system, it can be reconfigured or the component can be replaced. Moreover, the reliability assessment is used to evaluate the reliability for different network designs during the design phase. Then, the designer can compare the configurations and select the optimal design.
- To assess the conventional and renewable DGs impact on the reliability of the networked distribution system. The stochastic nature of the renewable resources and its effect on the reliability of the system are modeled and studied. Then, the DG model and the load demand model are integrated to the distribution system reliability model to evaluate the load and system reliability indices.

All the techniques used in this report are interconnected in an algorithm named encoded Markov cut sets (EMCS) and will be explained in detail in Chapter 3. This algorithm will be used to evaluate the reliability of future distribution systems. A roadmap for the complete analysis is shown in Fig. 1.3.

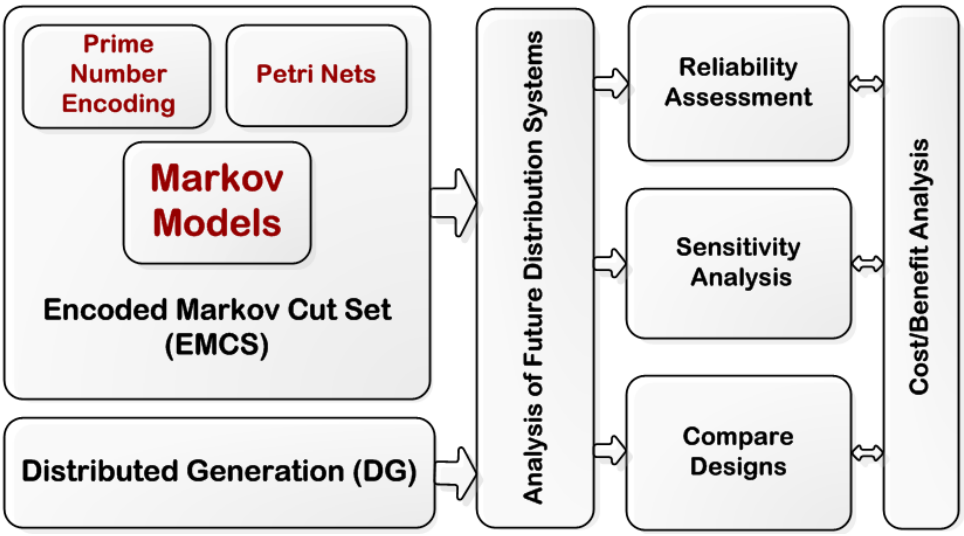

Fig. 1.3 Roadmap for evaluating the reliability of future distribution system using EMCS

Chapter 2

DISTRIBUTION POWER SYSTEM RELIABILITY CALCULATIONS

2.1 Quantification of Distribution System Reliability

Reliability is an important issue in any designed system or product. Customers and users do not expect any failure or interruption of the service since the failure can be expensive or insecure. It is important to differentiate between the power quality and system reliability. System reliability is more concerned with the continuity of the service (sustained and momentary interruptions), whereas power quality pertains to other power problems such as voltage fluctuations, harmonic distortion, and variations in the wave shape or magnitude.

A typical reliability study focuses on the probability of a component or a system to operate as intended or to fail. This probability does not provide specific definitive information regarding exactly when or how long an outage will occur. For this reason, it is important to introduce other indices that will reveal the frequency and duration of outages.

In practice, system average interruption frequency index (SAIFI) and system average interruption duration index (SAIDI) are two commonly used indices used to evaluate the frequency and duration of the interruptions that customers experience in the period of study (typically one year). These two indices are related to the configuration of a system and the probability of each component in the system to fail. The indices are used in reliability evaluation to study the effect of components on reliability and to compare different configurations based on their reliability performance. One important route to the

examination of reliability relates to the probabilistic modeling of networks and systems in general. For example, Billinton and others (e.g., [34–37]) have employed the basic properties of the probability of failure of components in series and parallel (including vector-matrix operational analysis) to quantify the probability of failure of a system or network.

Major events such as severe weather conditions are usually excluded when calculating the reliability indices since the weather conditions can have a major effect on the indices based on the location and configuration of the system. Excluding major events allow the utilities to respond to the real changes of the system's reliability. Utilities used different approaches to define and exclude the major events from the reliability indices. One approach to classify any event as a major event is when the event causes 10% of the utility customers to lose service for 24 hours [38]. Another approach to classify the major events is when 15% of the customers experience an outage during the severe weather condition [38].

The duration and frequency of mis-operation are significant in evaluating the reliability of a device or system. In this report, *the event count indices* will be studied, principally the SAIDI and the SAIFI,

$$SAIDI = \frac{Total\ duration\ of\ all\ interruptions}{Total\ number\ of\ customers\ connected}$$

$$SAIFI = \frac{Total\ number\ of\ all\ interruptions}{Total\ number\ of\ customers\ connected}.$$

The SAIDI index reveals the average *time* the customer is interrupted in minutes (or hours) in one year. The SAIFI index reveals how *often* these interruptions occur on the average for each customer. Both indices have been

widely used in North America as measures of the effectiveness of distribution systems [16, 33]. Both indices are carried out (i.e., averaged) typically over a one-year interval; SAIDI is usually expressed in hours per customer, and SAIFI in failures per customer. (Further system reliability indices can be found in Appendix A)

Most utilities have to report their reliability indices to regulatory bodies. In a 2008 survey, 35 states and Washington DC required routine reporting of SAIDI and SAIFI from the utilities to the public utility commission [39]. Most utilities exclude severe weather outages and planned outages from reliability indices because in most storm outages, the utility cannot control the incident or severity of the storms. Customers also may be notified before any planned outages (e.g., maintenance) so that the impact of the outage will be minimized.

2.2 Calculating the Reliability Using System Theoretic Concepts

Even though availability and reliability are used interchangeably in several papers in the literature, they are not the same in concept and values. The reliability basically represents the probability that a component or a system will perform its designed function without any failure under the normal working environment. The reliability does not reflect or contain any time to repair the failed component. It mainly reflects how long the system is expected to work at a specific time before it fails.

The availability, on the other hand, is the probability that the component or the system is working as expected during its operational cycle. It shows how

share of time the system is working. Availability depends on both the expected time to fail and time to repair the component or the system. The availability is,

$$Avaliability = \frac{UP\ TIME}{UP\ TIME + DOWN\ TIME}.$$

For continuously operating systems such as power systems, it is more informative to study the availability of the components and system to address the quality of service provided to the customers. The term "reliability" will be used in this report as a general word that represents all aspects of the study (e.g., availability, unavailability, failure frequency, duration) rather than a quantity or a value. Generally speaking, system reliability can be defined as the probability of at least one minimal set of components working properly between the input and output. This set of components is called tie or path set in graph theory.

The life of the power system equipment may be divided into three intervals: infant mortality, useful life, and wear out period. The useful life period is typically where the reliability evaluation is conducted. Some papers include the wear out period in modeling the components using probability distributions [40]. It is also common in the literature that the power system components down times and up times assumed to follow an exponential distribution function. Many components in power systems fail in purely random fashion, and the failure rate is assumed to be the same at any time during the component's useful life. Constant failure rate leads to the exponential distribution modeling where the failure rate is constant with time [30, 41].

Distribution system components in this research are assumed to be *repairable* components with a *time to repair* or to *restore* service. Most components in power systems are repairable or replaceable. If a component is repaired, it is assumed that it will perform its function as new component with the same failure rate. The time it takes for each component to fail is called the mean time to failure (MTTF), or simply T_f. Similarly, the time to restore service or to repair the faulty component is called the mean time to repair (MTTR), or simply T_r. Note that both T_f and T_r are the *average* values over a long period of time and over many cycles of operate/fail-repair/operate/fail-repair/…and it is assumed that the component has only two states: either *up* or *down*. The time it takes for a component to fail and to be repaired is called the mean time between failures (MTBF), or simply the mean cycle time, T_{fr} where,

$$\text{MTBF} = \text{MTTF} + \text{MTTR}$$

$$T_{fr} = T_f + T_r \tag{2.1}$$

The mean time to failure, T_f, and mean time of repair, T_r, and 'one average cycle' of time to fail and repair' are shown in Fig. 2.1.

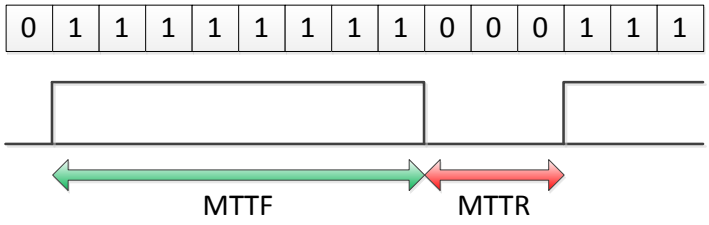

Fig. 2.1 Depiction of a 'cycle' of mean time to failure and mean time to repair

The reciprocal of the mean cycle time is defined as the mean *failure frequency* and is denoted as *f*,

$$f = \frac{1}{MTBF} = \frac{1}{MTTF + MTTR} \tag{2.2}$$

Note that MTBF, MTTF, and MTTR have the units of time, generally hours, and *f* has the units of 'per hour'. The probability of a component to be in the operational state is called the *availability*, denoted as A, and the probability to be in the failure state is called the *unavailability*, denoted as U. A and U will be used in this report as the notation for availability and unavailability. The availability and unavailability are related to MTTF and MTTR as follows:

$$A = \frac{MTTF}{MTBF} = \frac{MTTF}{MTTF + MTTR} \tag{2.3}$$

$$U = \frac{MTTR}{MTBF} = \frac{MTTR}{MTTF + MTTR}. \tag{2.4}$$

The frequency and duration of interruptions for a component over one year are defined as average interruption frequency (AIF) and average interruption duration (AID) [22]. The AIF for a component is defined as a number of failures over one year and can be expressed as:

$$AIF_i = 8760f = \frac{8760}{MTTF + MTTR} \tag{2.5}$$

where *i* is the bus or feeder number. Similarly, the AID is the duration in hours for all interruptions in one year and expressed as:

$$AID_i = 8760U_i = (MTTR)(AIF_i). \tag{2.6}$$

The failure duration (FD) can also be defined as the average duration of a single failure. Another important load index is the energy not supplied (ENS) during interruptions. The FD and ENS can be calculated as follows:

$$FD_i = \frac{AID_i}{AIF_i} \tag{2.7}$$

$$ENS_i = AID_i P_{avg}^i \tag{2.8}$$

Where P_{avg}^i is the annual average power for bus *i*. For two components connected in a series, the system will perform its designed function if both components are working (i.e., they are both up). If there is a failure in any one of these two components, the receiving end will experience an interruption or outage (i.e., the load is down) [22]. The availability of this system can be expressed as:

$$A_{sys} = A_1 A_2 = \frac{T_{f1}}{T_{f1} + T_{r1}} \frac{T_{f2}}{T_{f2} + T_{r2}}. \tag{2.9}$$

Similarly, for a system of two parallel components, the load will experience an outage if both components fail at the same time. The two parallel components probability is:

$$A_{sys} = 1 - U_1 U_2 = 1 - \frac{T_{r1}}{T_{f1} + T_{r1}} \frac{T_{r2}}{T_{f2} + T_{r2}} \tag{2.10}$$

For two simple components in either series or parallel, T_f and T_r are related to the MTTF and the MTTR the entire system, namely T_f^{eq}, T_r^{eq} respectively. For two components in series, the frequency of failure for the equivalent system equal to:

$$f_s = f_1 + f_2$$

In power systems, consider the adjustment of the above equation to account for a practical assumption that a second component cannot fail when the first component has already failed. The equivalent frequency will then be:

$$f_s = f_1 A_2 + f_2 A_1. \tag{2.11}$$

After substituting all variables from (2.2) and (2.3):

$$f_s = \frac{T_{f1} + T_{f2}}{(T_{f1} + T_{r1})(T_{f2} + T_{r2})}. \tag{2.12}$$

To find the equivalent failure cycle period (T_{frs}):

$$T_{frs} = \frac{1}{f_s} = \frac{1}{f_1 A_2 + f_2 A_1} \tag{2.13}$$

Then, using (2.2) and (2.3), the equivalent time to fail and time to repair can be found as:

$$T_{fs} = A_s T_{frs} = \frac{T_{f1} T_{f2}}{T_{f1} + T_{f2}} \tag{2.14}$$

$$T_{rs} = U_s T_{frs} = \frac{(T_{f1} + T_{r1})(T_{f2} + T_{r2}) - T_{f1} T_{f2}}{T_{f1} + T_{f2}} \tag{2.15}$$

A similar procedure can be used to find the equivalent variables in two parallel components. For two parallel components, both components should fail at the same time to cause an outage or service interruption to the customer. The frequency of failures is then equal to:

$$f_p = f_1 U_2 + f_2 U_1 \tag{2.16}$$

The relationship is shown in Table 2.1 [34, 35]. The results in Table 2.1 assume that the power supply is 100% reliable, and outages of components are probabilistically independent. Further, the results in Table 2.1 show *approximate*

formulas for the case that $T_f >> T_r$. Note that in typical power distribution engineering, T_f is in the order of tens of thousands of hours, and T_r is in the order of a few hours. The exact formulas are also shown Table 2.1.

Table 2.1 Equivalent times of failure and repair of series and parallel components

		T_f^{eq}	T_r^{eq}
Approximate Formulas $T_r << T_f$	*Series*	$\frac{T_{f1}T_{f2}}{T_{f1}+T_{f2}}$	$\frac{T_{r1}T_{f2}+T_{r2}T_{f1}}{T_{f1}+T_{f2}}$
	Parallel	$\frac{T_{f1}T_{f2}}{T_{r1}+T_{r2}}$	$\frac{T_{r1}T_{r2}}{T_{r1}+T_{r2}}$
Exact formulas	*Series*	$\frac{T_{f1}T_{f2}}{T_{f1}+T_{f2}}$	$\frac{(T_{f1}+T_{r1})(T_{f2}+T_{r2})-T_{f1}T_{f2}}{T_{f1}+T_{f2}}$
	Parallel	$\frac{T_{r1}T_{f2}+T_{r2}T_{f1}+T_{f1}T_{f2}}{T_{r1}+T_{r2}}$	$\frac{T_{r1}T_{r2}}{T_{r1}+T_{r2}}$

It is possible to combine the results of Table 2.1, Eq. (2.5) and Eq. (2.6) to obtain the AID and AIF for a receiving end bus, fed by either two series components or two parallel components. This result gives the equivalent AID^{eq} and equivalent AIF^{eq} (as 'seen' at the receiving bus), as shown in Table 2.2. As in Table 2.1, the equivalent AID and AIF of two simple components in series or parallel assume that $T_f >> T_r$ and that the supply bus is 100% reliable. The results in Table 2.2 are simply obtained using the results of Table 2.1, followed by the definition of the equivalent AID and AIF at a power delivery bus being $T_r^{eq} AIF$ and $8760/(T_f^{eq}+T_r^{eq})$, respectively. Most of the indices depend on the interruption frequency or interruption duration. Billinton and Allan [41] show how repair time and failure rate may be used in the radial case to find reliability at distribution system buses.

Table 2.2 Equivalent AIF and AID as a function of the AID and AIF of each component

	Series	Parallel
AIF^{eq}	$AIF_1 + AIF_2$	$\frac{AID_1 AIF_2 + AID_2 AIF_1}{8760}$
AID^{eq}	$AID_1 + AID_2$	$\frac{AID_1 AID_2}{8760}$

SAIFI is the average interruptions frequency per customer and can be calculated by finding the interruption frequency of all buses divided by the number of customers connected in the system:

$$SAIFI = \frac{\sum_{i=1}^{B} AIF_i N_i}{N_T} \tag{2.17}$$

where N_i is the total number of customers connected to a given bus i, N_T is the total number of customers in the system, and B is the total number of buses. Similarly, SAIDI is simply the summation of the interruption duration of all buses, divided by the number of customers connected in the system:

$$SAIDI = \frac{\sum_{i=1}^{B} AID_i N_i}{N_T} \tag{2.18}$$

2.3 Markov Models for Distribution System Reliability Evaluation

In power systems, as in many practical systems, the system has different discrete states, and it operates in one state and can change its state at any time. The reliability of these systems can be analyzed using CTMC. The objective in the reliability evaluation of the power distribution system is to determine the availability, mean time to failure, interruption duration, and interruption

frequency of each load point in the system. The interruption occurs when the load is disconnected from the source. It is important to detect the system states where the link between the load and the source is disconnected. Then, each state can be identified as a working (normal operation) and not working (outage) state, which is then incorporated in the analysis of the Markov model to compute the steady state probability, mean time to failure, duration, and frequency.

The technique to solve the connectivity problems and to classify each state based on the continuous connection between the load and the source will be explained in the next chapter. Markov analysis used to find the steady state probability, mean time to failure, and failure frequency will be explained in this section.

In many applications, the majority of the components in the system have two possible states—up and down. The transition rate from state 1 (up) to state 2 (down) is called the failure rate (λ), and it is estimated by counting the number of failures divided by the total operation time in one year. The rate of transition from the down state to up state is called the repair rate (μ), and it is calculated by counting the number of repairs, divided by the total duration of all repairs. This model is called the binary model and is shown in Fig. 2.2.

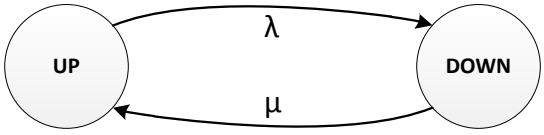

Fig. 2.2 Two states binary model

The number of states in the Markov model using the binary model is related to the number of lines and components included in the study. Let *n* be the number of components in the system; the total number of states will be 2^n. Each state denotes the status of the components as working (up) or not working (down). Each component status can be defined as follows:

i=1: if the component working (up)

i=0: if the components not working (down).

The general state space will be:

$$S= \{S_1, S_2, S_3,..., S_N\}$$

where $N=2^n$ and $S=i_1i_2i_3...i_n$. As an example, for two components system, the states can be defined as:

S_1= 11 (both working)

S_2= 10 (working, not working)

S_3= 01 (not working, working)

S_4= 00 (both not working).

The state transition diagram (STD) and the state transition matrix (STM) for the two components system are shown in Fig. 2.3.

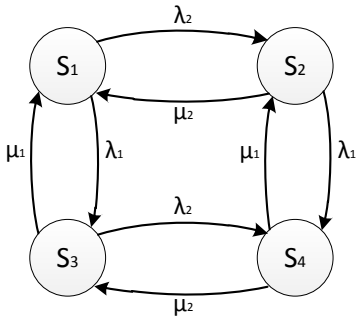

$$\sigma = \begin{bmatrix} 0 & \lambda_2 & \lambda_1 & 0 \\ \mu_2 & 0 & 0 & \lambda_1 \\ \mu_1 & 0 & 0 & \lambda_2 \\ 0 & \mu_1 & \mu_2 & 0 \end{bmatrix}.$$

Fig. 2.3 STD and STM for the two components system

2.3.1 Using Markov Models to Calculate Reliability

The time dependent probabilities can be found by solving the Markov differential equations [31]. The general format for the differential equations is:

$$\begin{bmatrix} -\sum_{j=2}^{n}\sigma_{1j} & \sigma_{21} & \cdots & \sigma_{n1} \\ \sigma_{12} & -\sum_{\substack{j=1 \\ j\neq 2}}^{n}\sigma_{2j} & \cdots & \sigma_{n2} \\ \vdots & \vdots & \cdots & \vdots \\ \sigma_{1n} & \sigma_{2n} & \cdots & -\sum_{j=1}^{n-1}\sigma_{nj} \end{bmatrix} \begin{bmatrix} P_1(t) \\ P_2(t) \\ \vdots \\ P_n(t) \end{bmatrix} = \begin{bmatrix} P_1'(t) \\ P_2'(t) \\ \vdots \\ P_n'(t) \end{bmatrix} \tag{2.19}$$

where Q is the coefficient matrix that can be formed from the transition rates matrix (σ-matrix). The long run (or steady state) probabilities can be found by solving the set of Markov differential equations (Kolmogorov equations) with the conditions that the sum of all probabilities equal to 1 and all time derivatives of the probabilities equal zero [31]. The derivatives can be replaced with a zero value and then solving the set of equations simultaneously:

$$Q\begin{bmatrix} P_1 \\ P_2 \\ \vdots \\ P_n \end{bmatrix} = 0 \tag{2.20}$$

$$\sum_{j=1}^{n} P_j = 1 \tag{2.21}$$

The matrix representation after substituting the last row of Q,P, and $\dot{P}$ with the summation of all the probabilities equal to one is:

$$\begin{bmatrix} -\sum_{j=2}^{n}\sigma_{1j} & \sigma_{21} & \dots & \sigma_{n1} \\ \sigma_{12} & -\sum_{\substack{j=1 \\ j\neq 2}}^{n}\sigma_{2j} & \dots & \sigma_{n2} \\ \vdots & \vdots & \dots & \vdots \\ 1 & 1 & \dots & 1 \end{bmatrix} \begin{bmatrix} P_1 \\ P_2 \\ \vdots \\ P_n \end{bmatrix} = \begin{bmatrix} 0 \\ 0 \\ \vdots \\ 1 \end{bmatrix}. \tag{2.22}$$

Equation (2.22) is solved to find the steady state probabilities for all the state. The states can be classified based on the system connection as up (working) or down (not working). Then, the steady state probabilities can be added together for each group to calculate the availability and unavailability of the system.

To find the expected average time to move from state *i* to state *j*, consider the state space in Fig. 2.3. The average time to travel from state 1 to state 4, where state 4 is assumed to be the only (down) state in the system, is calculated as follows:

$$E[T_{11}] = \frac{1}{\lambda_1 + \lambda_2} + \frac{\lambda_1}{\lambda_1 + \lambda_2} E[T_{01}] + \frac{\lambda_2}{\lambda_1 + \lambda_2} E[T_{10}] \tag{2.23}$$

$$E[T_{01}] = \frac{1}{\mu_1 + \lambda_2} + \frac{\mu_1}{\mu_1 + \lambda_2} E[T_{11}] + \frac{\lambda_2}{\mu_1 + \lambda_2} E[T_{00}] \tag{2.24}$$

$$E[T_{10}] = \frac{1}{\lambda_1 + \mu_2} + \frac{\mu_2}{\lambda_1 + \mu_2} E[T_{11}] + \frac{\lambda_1}{\lambda_1 + \mu_2} E[T_{00}] \tag{2.25}$$

$$E[T_{00}] = 0 \tag{2.26}$$

where $E[T_{11}]$ is the average expected time to move from state 1 to state 4. In general, $T_{(i_1,i_2,..,i_N)}$ denotes the first passage time to move from state $(i_1, i_2, .., i_N)$ to any down state in the state space.

The time or the number of steps the system takes before entering the absorbing state can be found by evaluating the fundamental matrix of the

absorbing Markov chains *N* [31]. The fundamental matrix *N* [31] can be found by solving:

$$N = [I - S]^{-1} \tag{2.27}$$

The matrix *N* is the average time that the system resides in each transient state or how many steps it takes before it enters one of the absorbing states. In the applications where the system or component is repairable, there is no absorbing states since the system can be repaired and maintains its operational state again. The failure states can be assigned as absorbing states to compute the average time or steps before entering any of the failure states. In this case, the average time the system operates before failing can be computed from matrix *N* after classifying all the failure states as absorbing states. This average time is called the mean time to failure (MTTF).

Besides finding the steady state probabilities of the system and the mean time to failure and repair, it is also useful to find the frequency of occurrence of the down states of the system. To find the expected time of residence for state *i*, all other states are considered as absorbing states. The expected frequency then can be written as:

$$f_i = P_i \sum_{j=2}^{n} \sigma_{ij}. \tag{2.28}$$

From (2.28), the expected frequency of any state is the probability of being in that state multiplied by the rates of departure from the same state.

2.3.2 Merging of States

In power systems, it is more beneficial to evaluate the expected number of outages and how long the system can run without the customer realizing service has been interrupted. The steady state probability of each state can be found by solving the limiting probabilities and the Markov coefficient matrix. Then, the availability and unavailability of the two system events (up and down) are computed by adding all the up and down states.

$$A = P_{up} = \sum_{i=1}^{u} P_i \qquad\qquad U = P_{down} = \sum_{i=1}^{d} P_i \tag{2.29}$$

where *u* and *d* are the number of up and down states, respectively.

The MTTF is the mean time the system takes to move from the up state (operational state) to the down state (failure state). In most of the application, the initial state of the system is in the normal operation state where all the components are up. What is important here is to compute the mean time to leave this state and enter one of the down states. In power systems, any down state can be an absorbing state since what is important in the reliability study of the power system is the frequency and duration of the outages seen by the customer and not the combination of component failures. The MTTF can be calculated for the system, assuming that the initial state is in the normal operation state and using the truncated matrix S_u and fundamental matrix N_{ud}.

The failure frequency is equivalent to the frequency of occurrence of all the down states. To merge all the down states into a single aggregate state, the

state frequencies are added together excluding any mutual occurrence between them. The merged frequency of two down states [31] is:

$$f_m = f_i + f_j - f_{ij} - f_{ji} \tag{2.30}$$

where f_{ij} is the frequency of occurrence from state *i* to state *j* and vice versa for f_{ji}.

To find the frequency of the merged down states, the transition matrix is modified to remove any mutual transition rates between any down states. Then, this modified transition matrix is used with the steady state probabilities for all states to compute the frequency of the merged down states. The frequency of each down state can be computed as:

$$f_i = P_i \sum_{j=2}^{n} \sigma'_{ij} \tag{2.31}$$

where *i* is the number of down states and σ'_{ij} is the transition rate from the down state *i* to the up state *j*. The system failure frequency can then be computed as:

$$f_{system} = \sum_{i=1}^{d} f_i. \tag{2.32}$$

2.3.3 Equivalent Series and Parallel Models

As the number of the states in the system becomes large, the reliability evaluation of the Markov model can become problematic and time consuming. It is possible, though, to reduce the number of states and the size of the Markov model matrices by combining the series and parallel components in the system [30, 31].

In the case where two components are connected in series, the MTTF is the reciprocal of the sum of the two components' failure rates. Therefore, the equivalent failure rate for two series component (λ_s) is:

$$\lambda_s = \lambda_1 + \lambda_2 \tag{2.33}$$

The equivalent repair rate μ_s for two series components can be expressed as:

$$\mu_s = \frac{(\lambda_1 + \lambda_2)(\mu_1\mu_2)}{\lambda_1\lambda_2 + \lambda_1\mu_2 + \lambda_2\mu_1} \tag{2.34}$$

For two parallel components connected in parallel with full redundancy, the system will fail if both components fail at the same time. The equivalent repair rate (μ_p) is:

$$\mu_p = \mu_1 + \mu_2 \tag{2.35}$$

and the equivalent failure rate (λ_p) is:

$$\lambda_p = \frac{(\lambda_1\lambda_2)(\mu_1 + \mu_2)}{\mu_1\mu_2 + \lambda_1\mu_2 + \lambda_2\mu_1} \tag{2.36}$$

Chapter 3

THE ENCODED MARKOV CUT SET ALGORITHM

3.1 Using Graph Theory in Reliability Evaluation

Distribution systems can be modeled with a unidirectional probabilistic graph whose vertices represent the nodes (or loads) and the edges represent the links (or lines). The nodes are assumed to be 100% reliable, or perfect, where the probability to work equal to one. However, the links are assumed imperfect with associated probability to fail for each component or area. Another important assumption is that all the components in the system are independent from each other in their failures. Without this assumption, the correlation of failure events makes the problem complicated and difficult to solve. The assumption of independent failures may not be accurate in actual power systems. A lightning strike or a storm may cause a simultaneous failure of several components.

For any distribution network, there are four line sets:

1. Tie set (TS);
2. Minimal tie set (MTS);
3. Cut set (CS); and
4. Minimal cut set (MCS).

A tie set is any set of lines that connects the source (input) and the load (output). The tie set can include additional lines Ω_L if the elements of Ω_L are removed from the set, resulting in the remaining lines connecting the input and output. Unlike the tie set, the *minimal* tie set is the minimum set of lines where if one line were removed from the set, the input-output connection would be broken. Fig. 3.1

explains the difference between the tie set and *minimal* tie set. In Fig. 3.1(a), the tie set includes lines 3, 4, 5, and 6. If line 6 is removed from the set, lines 3, 4, and 5 will link between the input and the output. On the other hand, in Fig. 3.1(b) the minimal tie set contains lines 3, 4, 5, and if one of these lines is removed, the link between the input and the output will be disconnected.

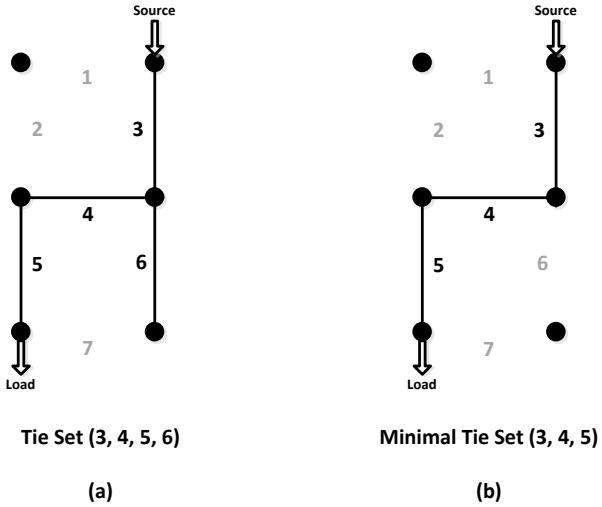

Fig. 3.1 Illustration of the difference between tie set and minimal tie set

On the other hand, Fig. 3.2(a) shows a network with a cut set where lines 4, 5, 7 are disconnected from the circuit and thus there is no path between the input and output. The cited lines form a cut set because if at least one element is reconnected, the output may still be disconnected from the input. On the other hand, in Fig. 3.2(b) lines 5, 7 are disconnected, and this set is called a *minimal* cut set because connecting one of these elements will link input and output.

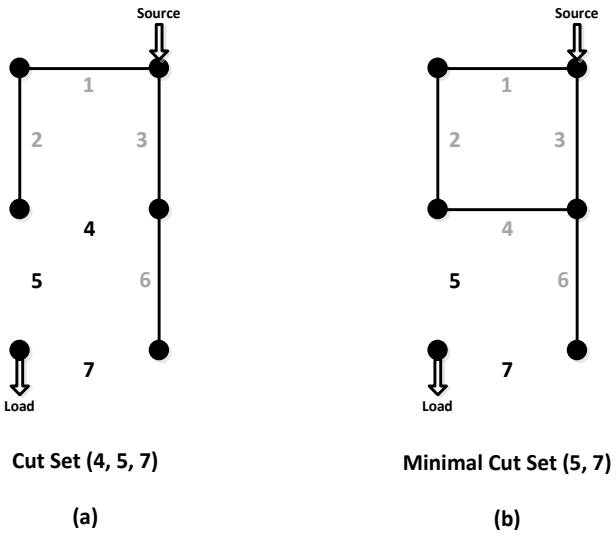

Fig. 3.2 Illustration of the difference between cut set and minimal cut set

The TS, MTS, CS, and MCS are useful in evaluating the reliability of small systems using Markov models. These sets are used to classify all the states as *up* or *down* states to then construct Markov matrices and compute the reliability of the system. The difficulty of the method lies in identifying the tie and cut sets, especially in large complex networked systems. Several methods are available in the literature for identifying the MCSs of complex networks (e.g., [42, 43]). For large systems, the number of combinations increases as the combinatorial of the number of system components, thereby making identification of the cut set components by inspection becomes difficult and time consuming. These reliability studies are generally off-line studies, but because of the combinatorial nature of the calculation, the calculation time is nonetheless an issue. Thus, it is important to find a better method to determine all the TSs and CSs for large and complex systems.

3.2 Distribution Network Reliability Using EMCS Algorithm

Different levels are proposed in this research to evaluate the reliability of networked systems using cut and tie sets, prime number encoding, Petri nets, and Markov models. The flow diagram for the proposed encoded Markov cut set (EMCS) algorithm levels is shown in Fig. 3.3 [44].

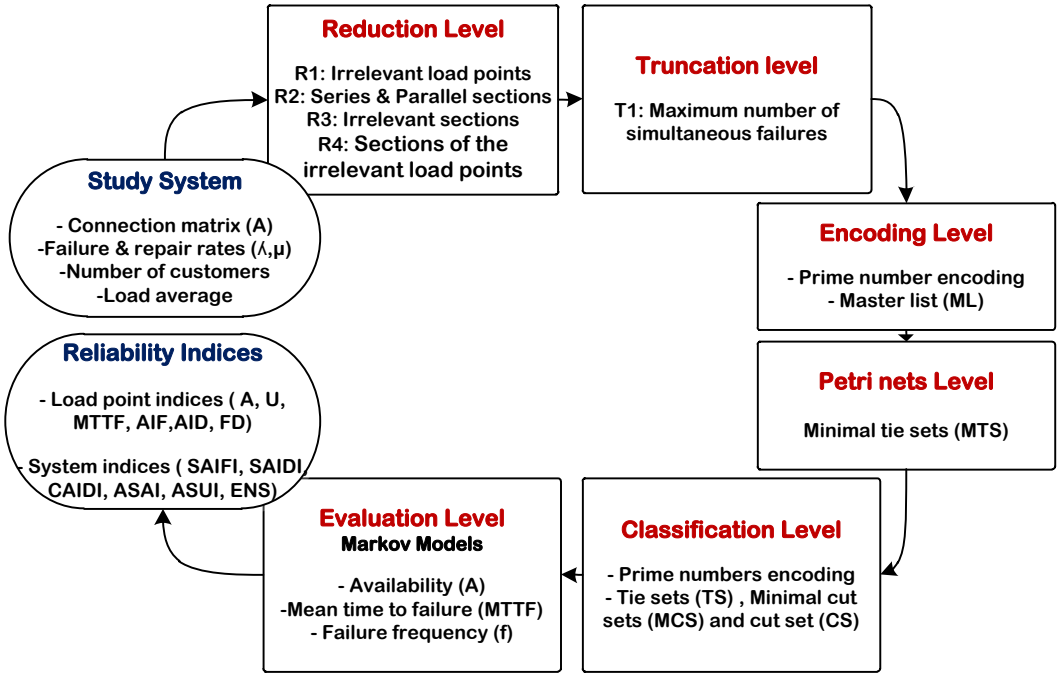

Fig. 3.3 Flow chart for the proposed EMCS algorithm

The proposed levels will be explained in details in Sections 3.3-3.7. They are briefly explained as follows:

- Reduction level: Different reduction techniques are proposed and applied to simplify the assessment and decrease the number of segments included in each load point reliability calculation. The goal behind reducing the number of segments or sections is to decrease the number of states and transition matrix size used in the Markov analysis. The accuracy of the

calculation should not be affected by all the reduction techniques used in this level.

- Truncation level: The Markov state space can be truncated according to the maximum allowed number of simultaneous failures in the system. The number and size of the truncated state space is specified based on the required accuracy level of the assessment.
- Encoding level: The number of states in any typical complex system is considered to be large with a relatively large number of components included in each state. Encoding all the components and then all the states will simplify and accelerate classifying the states and constructing Markov matrices. A master list (ML) with all encoded IDs and flags is created to be used later to categorize the state space.
- Petri nets level: In this level, the Petri nets concept is used to find the minimal tie sets (MTS). All the minimal tie sets can be found using this technique, which are then used to recognize the tie sets from the state population.
- Classification level: The unique factorization theorem and the encoded IDs for all MTS are used to find all tie sets (TS) in the state space. Then, the remaining states are classified as minimal cut sets (MCS) or cut sets (CS).
- Markov model level: After classifying all the states as MTS, TS, MCS, and CS, these sets are used to tag all the states as up or down states. Then,

Markov models are used to compute all the load and system reliability indices.

3.3 Reduction and Truncation Techniques

In evaluating the reliability of the networked system, the computational time is large and related directly to the size of the network. Therefore, researchers are trying to find simplified techniques for reducing the size of the network and expediting the computation time [45, 46]. In this thesis, to reduce the number of states in the system, different reduction methods are proposed and applied to the system's connection. The number of states is directly related to the number of components or sections in the system. The reduction methods reduce the number of sections and nodes in the system without affecting the accuracy of the reliability indices. This is due to the assumption that all the lines and transformers are protected with 100% reliable devices that can isolate faults instantaneously. Four different reduction levels (R1, R2, R3, and R4) and a truncation technique (T1) are used in this study as shown in the subsequent subsections.

3.3.1 Irrelevant Load Points

Each load point in the system is evaluated individually and independently. When the load point is assessed, all other load points have no influence on the reliability of the load point under study. Therefore, every other load point is considered irrelevant to the load point under study. In the connection matrix, all the load nodes—except the load node under study (e.g., node *x*)—are removed from the network, since they do not have any reliability value in the evaluation

process. This technique will reduce the number of nodes by *L-1* where *L* is the total number of loads in the system.

3.3.2 Series and Parallel Sections

In the second reduction stage, all the series and parallel sections or components in the system are merged. One node and one section are eliminated when two components are combined in series. The parallel combination will not affect the number of nodes in the system but will reduce the number of sections by one.

3.3.3 Irrelevant Sections

In the third reduction stage, the irrelevant sections are removed from the model. The irrelevant sections can be defined as sections that do not share any node with any possible path between the source and the load under study. The only point at which the irrelevant section is connected to any possible route is the 100% reliable source bus.

The method used to distinguish all the irrelevant sections from all the possible routes between the source and the load is as follows:

1. Let A^T be the connection matrix and M the input-output vector where $A^T = [a_{ij}]$ and $a_{ij} = 1$ if there is a line or component between i,j, and A^T and a_{ij} are equal to 0 otherwise, and vector M is a column vector where $m_i = 1$ for $i =$ *source or destination* and $m_i = 0$ otherwise.
2. Delete the input element from M vector and the associated row in the A^T matrix.

3. Multiply each column in A^T by *M*.
4. If the sum of the multiplication does not equal zero, update *M* by adding the column in A^T to *M*, then tag the column in A^T.
5. Repeat steps 3-4 until all the columns have been investigated.
6. Delete all untagged columns (sections).

3.3.4 Sections of the Irrelevant Load Points

The last reduction stage is applied when all the lines and components connecting between all possible routes and irrelevant loads are removed from the connection matrix. There is no effect from those load nodes and their associated segments since all the lines and transformers are assumed to be protected with 100% reliable devices that can isolate the faults instantaneously.

3.3.5 Maximum Simultaneous Failures

Assuming that each component in the system has two operational modes, either up or down, the total number of states in the system will be 2^n, where *n* is the number of components in the system. Since the state space can be extremely large with a large number of components, a simple and direct truncation method can be used to reduce the number of states. Truncation means deleting states having more than a pre-specified number of simultaneous failures. By definition, the maximum simultaneous failures in the system are set to be 3. In power systems, an occurrence of 3 simultaneous failures is considered rare, and the added failure rates from 4 or more simultaneous failures are very small and can be neglected.

All the reduction techniques are shown in Fig. 3.4. In Table 3.1, the effect of each reduction level on the number of nodes, sections, and states is listed.

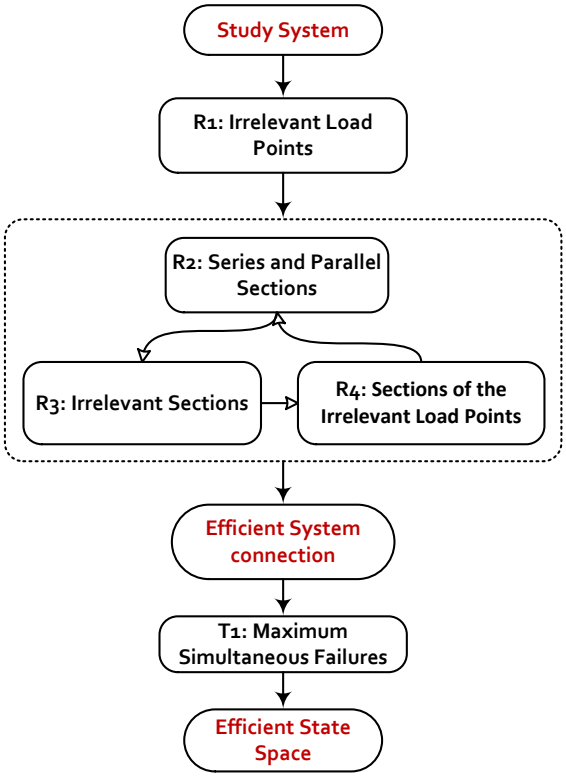

Fig. 3.4 Flow diagram for all reduction techniques

Table 3.1 The effect of each reduction technique

Reduction Technique		Nodes	Sections	States
R1	Irrelevant load points	Yes	No	No
R2	Series sections	Yes	Yes	Yes
	Parallel sections	No	Yes	Yes
R3	Irrelevant sections	Yes	Yes	Yes
R4	Sections of the irrelevant load points	No	Yes	Yes
T1	Maximum simultaneous failures	No	Yes	Yes

3.4 Prime Number Encoding Technique

In the application of prime number encoding to the evaluation of distribution network reliability, prime numbers are used to encode the sections of

the power distribution network [47]. A prime number encoding-decoding technique is used to classify the state space as minimal tie sets, tie sets, minimal cut sets, and cut sets. This technique makes finding and categorizing the states of the system more flexible. The prime numbers corresponding to each line in the 14 line system are shown in Table 3.2. The next step will be to assign an identification number (ID) to each possible line combination for all tie and cut sets. The IDs will be the product of the prime numbers for all lines in all the possible combinations.

Table 3.2 Prime numbers encoding for a general 14 line system

Line	1	2	3	4	5	6	7
Prime Number	2	3	5	7	11	13	17
Line	8	9	10	11	12	13	14
Prime Number	19	23	29	31	37	41	43

One limitation of this encoding system is that the large ID numbers can be as large as 10^{17} for only 14 lines in the combination. This is a large number and standardized software use could be problematic (e.g., on some computers and for some computational languages there is a lack of capability to store and perform precise operations large numbers. This is limited by both the software and the word length used). Dividing large numbers may result in rounded output, especially in the remainder. This imprecision can affect restoring the original line set and give incorrect results for the minimal cut sets. One way to avoid this encoding limitation is to modify the encoding technique so that one such modified encoding technique assigns the same prime sequence for each group of lines. For

the same 14 line system, lines 1 to 14 can be encoded as shown in Table 3.3. The ID for each line combination will now consist of two columns—one column for each set of lines (see Table 3.4).

Table 3.3 Modified prime numbers encoding for a general 14 line system

Line	1	2	3	4	5	6	7
Prime Number	2	3	5	7	11	13	17
Line	8	9	10	11	12	13	14
Prime Number	2	3	5	7	11	13	17

The indicated modified prime encoding will provide more accuracy and flexibility in the reliability calculations. The number of columns or the number of prime sets depends on the number of lines or components in the system. There is no apparent limitation to this technique.

Table 3.4 Prime numbers encoding and IDs for a general 14 line system

Possible Line Combinations	Prime Numbers Encoding	ID
1	2 , 0	[2 , 0]
:	:	:
8	0 , 2	[0 , 2]
:	:	:
1, 4	2 * 7 , 0	[14 , 0]
:	:	:
2, 5, 8	3 * 11 , 2	[33 , 2]
:	:	:
1, 2, 3 …… ,14	2 * 3 … *17, 2* 3….. * 17	[510510 , 510510]

One main advantage of using prime numbers to encode any possible combination or set is that the ID is *unique* for each set of lines. Each ID can be decoded easily to restore the line numbers by factorizing the ID and returning

each prime number to its corresponding component's number. Fig. 3.5 shows the block diagram for the encoding-decoding method.

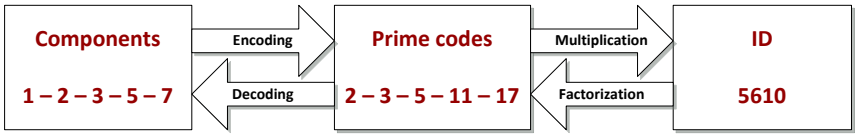

Fig. 3.5 Component encoding-decoding

3.5 Petri Nets and Minimal Tie Sets

3.5.1 Petri Nets

Since 1962 [48], Petri nets have been widely used in system reliability evaluation, fault tree analysis, distributed databases, and other applications. In the area of reliability evaluation, Petri nets have been used to determine simple tie sets, identification of *k*-trees, and in fault tree analysis. A Petri net is a directed graph with two types of nodes: *places* (circles) and *transitions* (bars). These nodes are linked by sets of *arcs*, and there can be more than one connection between the places and transitions. Places may contain a number of *tokens* to reflect the dynamic behavior of the system. Figure 3.6 shows the basic components of Petri nets [48].

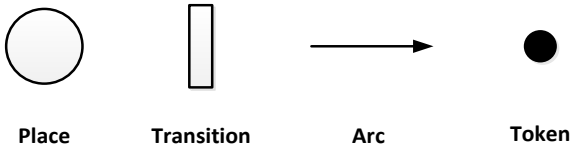

Fig. 3.6 Basic Petri net components

The static structure of the system is represented by the Petri net graph, in which the connections between different parts and components are modeled by

places, arcs, and transitions. The dynamic behavior of the modeled system is demonstrated by executing a Petri net model by "firing" the transitions [48]. As shown in Fig. 3.7, each transition can be fired *if and only if* the arc connecting a node to a transition holds at least the same number of tokens as the weight of the input arc [49].

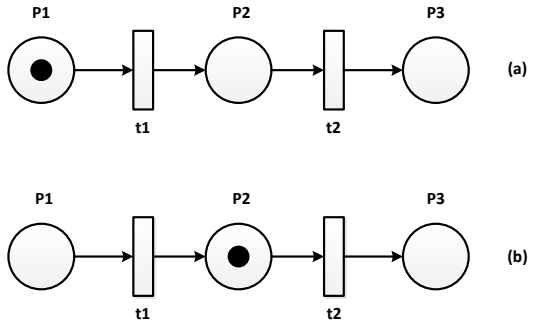

Fig. 3.7 Petri net model (a) initial Petri net (b) after t_1 is fired

3.5.2 Using Petri Nets to Find Minimal Tie Sets

To determine the MTS, it is necessary to find the transitions of the given graph by which a token at a destination node is reachable from a token at a source place. This can be done by solving the state space representation of Petri nets [50]:

$$A^T \sum = M \tag{3.1}$$

where A^T is the connection matrix of the Petri net (transition to place incident matrix), $A^T = [a_{ij}]$, and $a_{ij} = 1$ if there is a connection (arc) between i,j, and $a_{ij} =$ is equal to zero if there is no connection. Vector M is a column vector of the input-output (change in marking), where $m_i = 1$ for i = *source or destination* and $m_i = 0$

otherwise; and $\sum$ is a column vector for the firing count and its element $\sum_i = 0$ if the bus is not included in the path.

A flow chart for using a Petri net to evaluate the MTS is shown in Fig. 3.8, and the following steps summarize this procedure [49]:

1. Find the A^T matrix (connection matrix) and M matrix (input – output vector).
2. Compare all the columns A^T with M. If any column is equal to M, it is a success path of length one ($L=1$).
3. Increment the value of L by one.
4. Find all possible L combinations for A^T columns**.**
5. Add L columns for each combination using mod-2 addition. If the addition equals M, the indices corresponding to these columns represent a successful minimal path of length L.
6. Repeat steps 3 - 5 until L equals N-1, where N is the total number of columns in A^T.

3.6 Prime Number Classification Technique

The unique factorization theorem and the encoded IDs for all MTSs are used to catch all TSs in the state space. Then, the remaining states can be classified as MCSs or CSs.

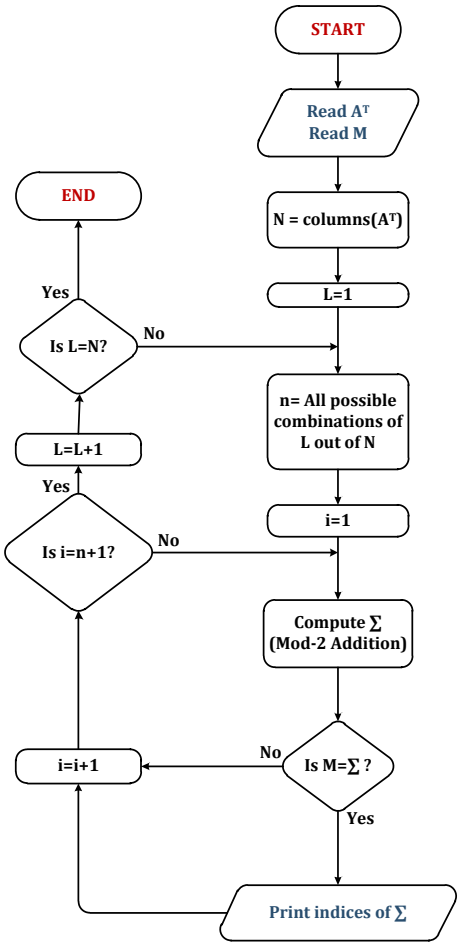

Fig. 3.8 Flow chart for Petri nets - minimal tie set method

To classify the states or the combinations of the system as MTSs or TSs, a master list (ML) is created with all possible combinations for all the lines in the system. After defining all the states in the ML, a flag and an ID are assigned to each state in the ML. The flag is used to identify each ID based on its status. In the first stage, the MTS flag is assigned the value +1. Then, a direct iterative method is used to identify the TSs using each MTS found in the first stage. The technique used to identify the TSs using prime number IDs is as follows in pseudocode:

If Remainder $\left(\frac{\mathrm{ID}_1}{\mathrm{ID}_2}\right) = 0$

Then components$(\mathrm{ID}_2) \subset$ components(ID_1)

ID_1 is a tie or cut set

where ID_2 is the MTS ID and ID_1 is each remaining ID with an unassigned status flag (*flag* = 0). If the components of ID_2 are a subset of the components of ID_1, the remainder of their division will be equal to 0, in which case ID_1 will be a TS with a flag equal to -1. The remaining IDs with unassigned flags will be CS or MCS; a similar concept can be used to separate them. Fig. 3.9 shows a flow chart for the TS identification technique.

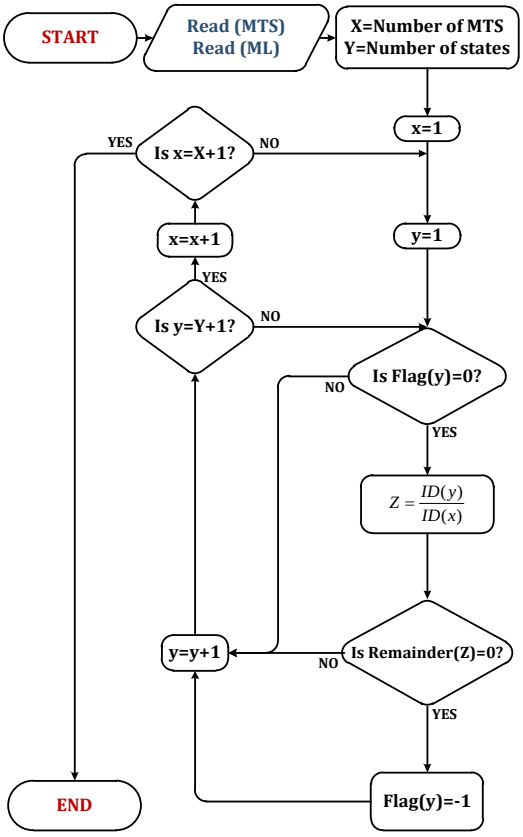

Fig. 3.9 Flow chart for the TS identification technique

To apply all these techniques explained in Sections 3.3–3.6, consider the system shown in Fig. 3.10. The two primary feeders and all the secondary feeders are assumed to be identical. In Fig. 3.10 (a), the lines are numbered based on their connections to the source; in Fig. 3.10(b), the lines are encoded using prime numbers in two groups, as shown in Table 3.4. To simplify the analysis, one load is specified in this network to classify all the states as seen by the load.

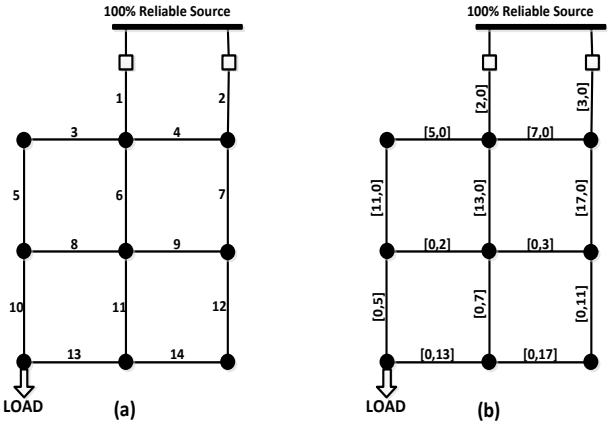

Fig. 3.10 Encoded secondary grid network under study

In Fig. 3.10, it is assumed that the maximum number of components that can form a cut set is 3. After applying all the reduction techniques, the number of states dropped from 16,384 to 4,096. This is due to the series combination for lines 3 and 5 and lines 12 and 14. The truncation technique reduces the states further from 4,096 to 299 states based on the predefined 3 maximum simultaneous failures in the system. Fig. 3.11 shows the system after combining the series components.

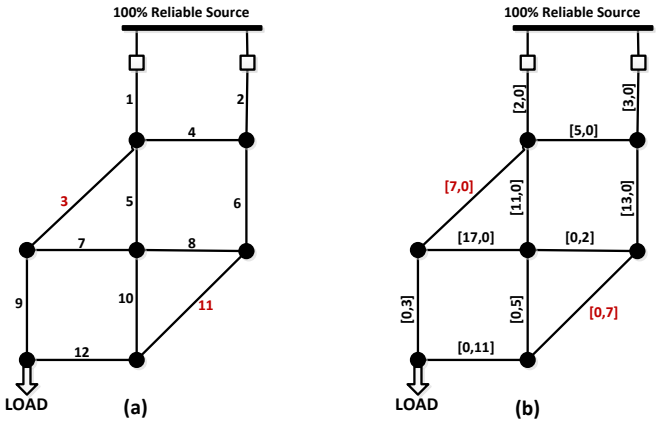

Fig. 3.11 Secondary grid network after applying all reduction methods

The total number of states, minimal cut, and tie sets for different maximum failures are shown in Table 3.5. As a result of applying the proposed techniques to the circuit in Fig.3.11, the MCSs of the system are depicted in Table 3.6.

Table 3.5 MTS, TS, MCS, and CS for different maximum failures

Maximum failures	Total states	MTS	TS	MCS	CS
1	15	0	15	0	0
2	79	0	77	2	0
3	299	0	273	6	20
4	794	0	640	12	142
5	1586	3	1040	19	524

Table 3.6 MCSs IDs, prime codes, and components

ID	MCS Prime codes	MCS Components
[85085,2310]	5-7-11-13-17, 2-3-5-7-11	1-2
[2805,2310]	3-5-11-17, 2-3-5-7-11	1-4-6
[714,2310]	2-3-7-17, 2-3-5-7-11	3-5-6
[6006,210]	2-3-7-11-13, 2-3-5-7	3-7-12
[510510,22]	2-3-5-7-11-13-17, 2-11	9-10-11
[510510,70]	2-3-5-7-11-13-17, 2-5-7	9-12

3.7 Using Markov Models to Calculate Load and System Reliability Indices

After classifying all the states as tie or cut sets, the Markov transition and coefficient matrices (σ and Q matrices) are formed using the transition rates between all the states. The tie and cut sets are used to classify the states as up or down states. Then, the availability of each state is computed, as explained in Section 2.3.

The next stage will be forming the truncated matrix *S* from the probability matrix *P*. Then, (2.27) is used to compute the fundamental matrix *N*, which is then used to calculate the MTTF for each up state.

In the third stage, the down states are merged together to remove any mutual occurrence between them. Then, the frequency of the merged down state is computed using the modified transition matrix (with the merged state) and the availabilities found in stage 1.

Subsequently, the availabilities, MTTF, and failure frequency are used to compute all the load point and system reliability indices. Fig. 3.12 shows the flow diagram that explains how to compute the availability, mean time to failure, and failure frequency for each load point using Markov model. Table. 3.7 details the main equations used to compute the load and system reliability indices.

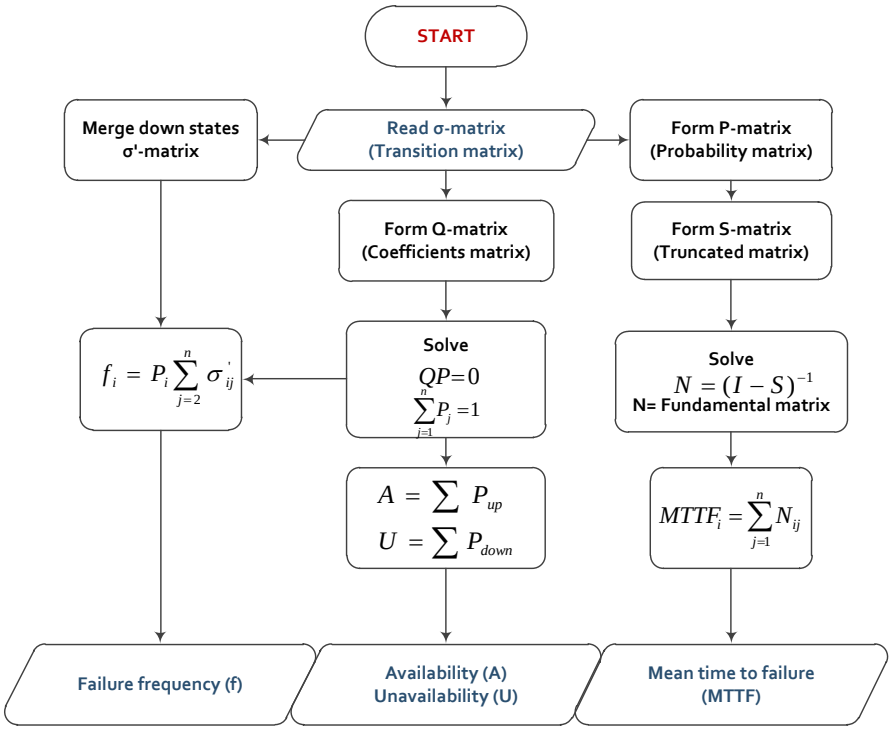

Fig. 3.12 Flow chart for computing A, MTTF, and *f* using Markov models

Table 3.7 Equations used to compute the load and system reliability indices

	Index	Unit	Equation
Load Point Indices	U	-	$U = 1 - A$
	MTTF	y	$MTTF\ (S1)$
	AIF	f/y	$AIF = f$
	AID	h/y	$AID = U \times 8760$
	FD	h/f	$FD = \frac{AID}{AIF}$
	ENS	MWh	$ENS = AID \times P_{avg}$
System Reliability Indices	SAIFI	f/c.y	$SAIFI = \frac{\sum_{i=1}^{B} AIF_i N_i}{N_T}$
	SAIDI	h/c.y	$SAIDI = \frac{\sum_{i=1}^{B} AID_i N_i}{N_T}$
	CAIDI	h/f	$CAIDI = \frac{SAIDI}{SAIFI}$
	ASAI	-	$ASAI = \frac{\sum_{i=1}^{B} 8760 N_i - \sum_{i=1}^{B} AID_i N_i}{\sum_{i=1}^{B} 8760 N_i}$
	ASUI	-	$ASUI = 1 - ASAI$
	ENS	MWh/y	$ENS = \sum_{i=1}^{B} AID_i P_{avgi}$

Chapter 4

RELIABILITY BOUNDS EVALUATION FOR POWER DISTRIBUTION SYSTEM

4.1 Minimal Cut Set Method: A General Approach

For networked distribution systems, there are two subsystems that can represent the connections of the original system. Each subsystem is comprised of series-parallel connections; the first set is the minimal tie set (MTS), and the other is the minimal cut set (MCS). The MTS and MCS are explained in Section 3.1. Fig. 4.1 explains a complex system and its two minimal sets.

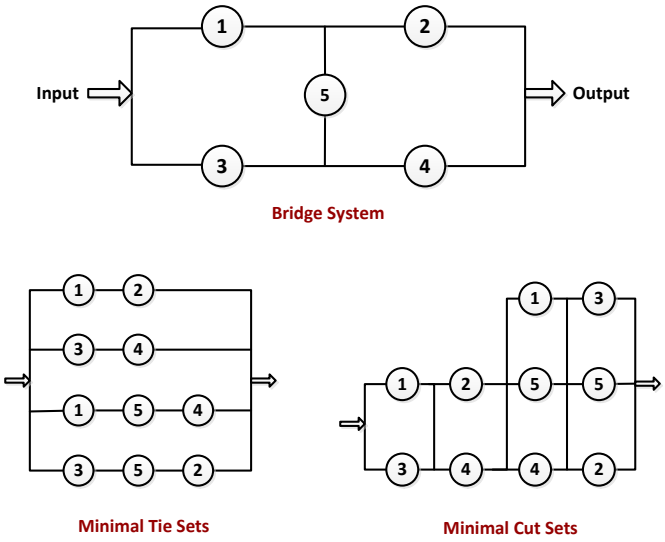

Fig. 4.1 Simple illustration for minimal tie - cut sets

To calculate the reliability of the distribution network using the MCS method, the reliability of each set is computed by calculating the failure probability of all components in parallel. Then, the reliability of the system can be found by evaluating the equivalent MCSs connected in series. The direct series

and parallel equivalent equations cannot be used to calculate the reliability of the system using the MCS. This is due to the possible correlation between any two sets, since components may be repeated and appear in more than one set. The only way to avoid this restriction is to solve the MCS subsystem using the basic union and intersection probability calculations to block the effect of the dependent cut sets [51, 52]. The U and AIF of the system will be:

$$\begin{gathered} U = U(C_1 \cup C_2 \cup C_3 \ldots . \cup C_m) \\ U = \{U(C_1) + \cdots + U(C_m)\} - \{U(C_1 \cap C_2) \ldots . + U(C_i \cap C_j)\} \ldots \ldots \\ \ldots . (-1)^{m-1} U(C_1 \cap C_2 \ldots . \cap C_m) \end{gathered} \tag{4.1}$$

$$\begin{gathered} AIF = AIF(C_1 \cup C_2 \cup C_3 \ldots . \cup C_m) \\ AIF = \{AIF(C_1) + \cdots + AIF(C_m)\} - \{AIF(C_1 \cap C_2) \ldots + AIF(C_i \cap C_j)\} .. \\ \ldots (-1)^{m-1} AIF(C_1 \cap C_2 \ldots . \cap C_m) \end{gathered} \tag{4.2}$$

where C_i is the ith minimal cut set ($i \neq j$), and m is the total number of minimal cut sets. The solution using (4.1) and (4.2) will be complicated and time consuming. To overcome the complexity of using this method, particularly in large complex systems, an approximate calculation of the upper and lower bounds for the U and AIF can be applied.

The successive addition for the odd and even terms in (4.1) and (4.2) will gradually converge the upper and lower bounds of the unavailability and average failure frequency [51, 52]. For highly reliable components, the first odd and even terms can give a small margin between the upper and lower bounds. This will simplify the computation and provide acceptable results with minimal errors.

The upper bounds for the U and AIF are:

$$U_u = \sum_{i=1}^{m} U(C_i) \tag{4.3}$$

$$AIF_u = \sum_{i=1}^{m} AIF(C_i) \tag{4.4}$$

and the lower bounds are:

$$U_l = \sum_{i=1}^{m} U(C_i) - \sum_{i=1}^{n} U(C_i \cap C_j) \tag{4.5}$$

$$AIF_l = \sum_{i=1}^{m} AIF(C_i) - \sum_{i=1}^{n} AIF(C_i \cap C_j) \tag{4.6}$$

To calculate the upper and lower bounds of the system for the A, AID, FD, and ENS, use [53]:

$$A_u = 1 - U_l \qquad A_l = 1 - U_u \tag{4.7, 4.8}$$

$$AID_u = 8760U_u \qquad AID_l = 8760U_l \tag{4.9, 4.10}$$

$$FD_u = \frac{AID_u}{AIF_l} \qquad FD_l = \frac{AID_l}{AIF_u} \tag{4.11, 4.12}$$

$$ENS_u = AID_u\, P_{avg} \qquad ENS_l = AID_l\, P_{avg} \tag{4.13, 4.14}$$

The upper and lower bounds of SAIFI can be calculated by finding the interruption frequency of all buses, divided by the number of customers connected in the system:

$$SAIFI_u = \frac{\sum_{i=1}^{B} AIF_{ui} N_i}{N_T} \tag{4.15}$$

$$SAIFI_l = \frac{\sum_{i=1}^{B} AIF_{li} N_i}{N_T} \tag{4.16}$$

A similar idea can be applied for SAIDI, which is simply the summation of the interruption duration of all buses, divided by the number of customers connected in the system:

$$SAIDI_u = \frac{\sum_{i=1}^{B} AID_{ui} N_i}{N_T} \tag{4.17}$$

$$SAIDI_l = \frac{\sum_{i=1}^{B} AID_{li} N_i}{N_T} \tag{4.18}$$

Other system indices include customer average interruption duration index (CAIDI), Average system availability index (ASAI), average system unavailability index (ASUI), and ENS:

$$CAIDI_u = \frac{SAIDI_u}{SAIFI_l} \qquad CAIDI_l = \frac{SAIDI_l}{SAIFI_u} \tag{4.19, 4.20}$$

$$ASAI_u = \frac{\sum_{i=1}^{B}(8760N_i - AID_{li}N_i)}{8760N_T} \qquad ASAI_l = \frac{\sum_{i=1}^{B}(8760N_i - AID_{ui}N_i)}{8760N_T} \tag{4.21, 4.22}$$

$$ASUI_u = 1 - ASAI_l \qquad ASUI_l = 1 - ASAI_u \tag{4.23, 4.24}$$

$$ENS_u = \sum_{i=1}^{B} AID_{ui}\, P_{avg} \qquad ENS_l = \sum_{i=1}^{B} AID_{li}\, P_{avg} \tag{4.25, 4.26}$$

4.2 Roy Billinton Test System (RBTS)

In this study, the Roy Billinton test system (RBTS) is used to evaluate the reliability under different scenarios. The RBTS has been referenced for many reliability studies and evaluation techniques in the literature. A description of the RBTS and system data can be found in [41, 54]. The advantage of the RBTS is the availability of the practical reliability data for all components. Another advantage is the manageable size of this system, which makes it easier to

perform hand calculations to verify any reliability model or technique used to evaluate the reliability indices.

The RBTS has 5 loads busbars (Bus 2-Bus 6) with different connections and characteristics for each subsystem. The single line diagram for the RBTS system is shown in Fig. 4.2.

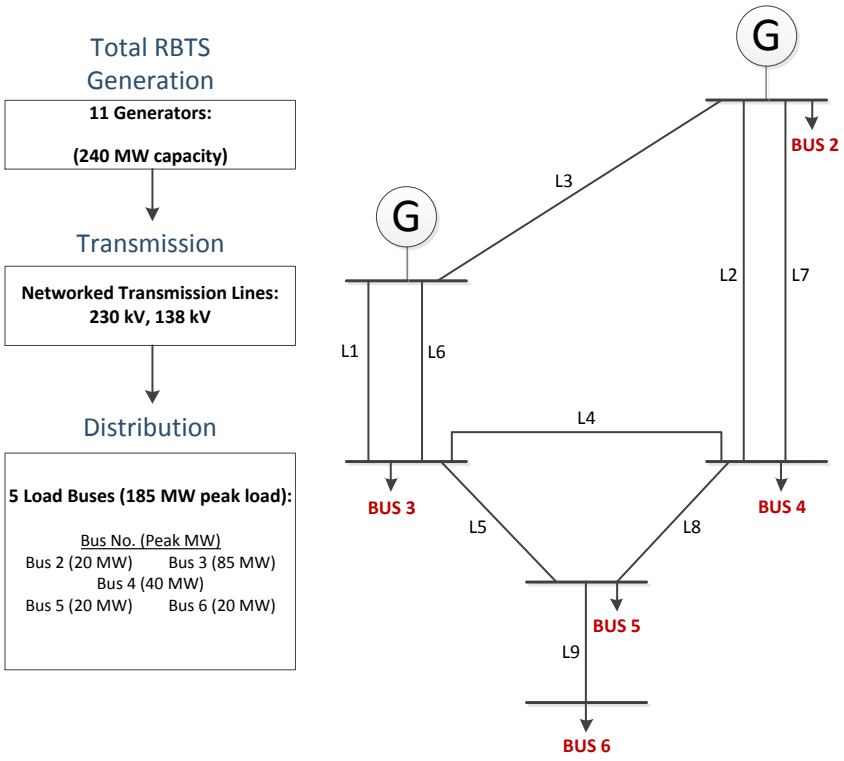

Fig. 4.2 Single line diagram for RBTS

The following comments are related to the RBTS under study in this report:

- All feeders and transformers are assumed to be equipped with interruption devices to isolate any sustained failure. It is assumed that all interruption devices in the system are 100% reliable (fuses, disconnects, and breakers) and capable of isolating the faulted segment instantaneously. The switching time is considered to be zero or less

than 5 minutes where the event is considered as momentary interruption based on the IEEE standard 1366 [55].

- The normally open tie switches are also considered 100% reliable with zero switching time.
- Transformers connected for residential, commercial, and governmental users are considered utility property. Therefore, the transformers are included in the single line diagrams and in the reliability evaluation. On the other hand, the small industrial customers are connected to the high voltage side, and the transformers in this case are customer property. These transformers are not shown in the single line diagram and not included in the calculation.
- The main feeders in the system can be either overhead lines or underground cables.
- It is assumed that adequate capacity is installed in the system for the normal operation and all failure scenarios. All the lines and components are within the capacity limits.
- The initial state of the test systems is assumed to be in normal operation mode, where all the components and lines in the system work properly.
- The average load given for each load point is the average load seen at each load point based on the average consumption over a year.

4.3 Using Prime Number Encoding and Petri Nets in Reliability Bounds Evaluation

The general flow diagram for all proposed techniques used in the reliability bounds evaluation is shown in Fig. 4.3 [53]. After applying the prime number encoding and Petri nets techniques to classify all the states in the system, the classified MCSs are used to calculate the reliability bounds, which were explained in Section 4.1.

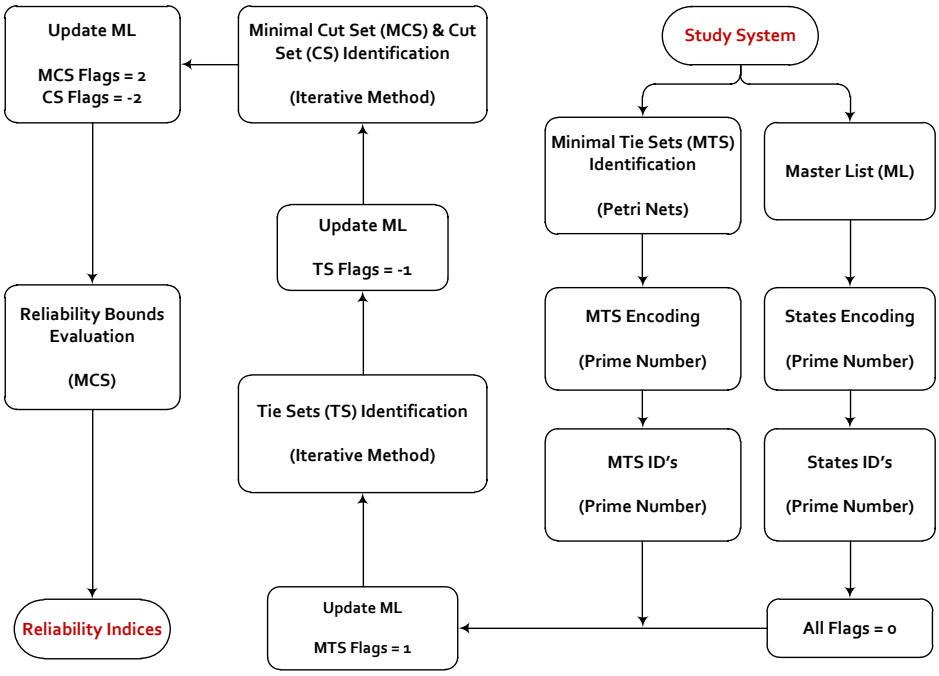

Fig. 4.3 Flow chart for evaluating the reliability bounds

To apply all the prime number encoding and Petri nets techniques, consider the system shown in Fig. 4.4. The system under study is the 11 kV side of the Bus 2 of RBTS [54]. The reliability data for RBTS Bus 2 can be found in Appendix B.

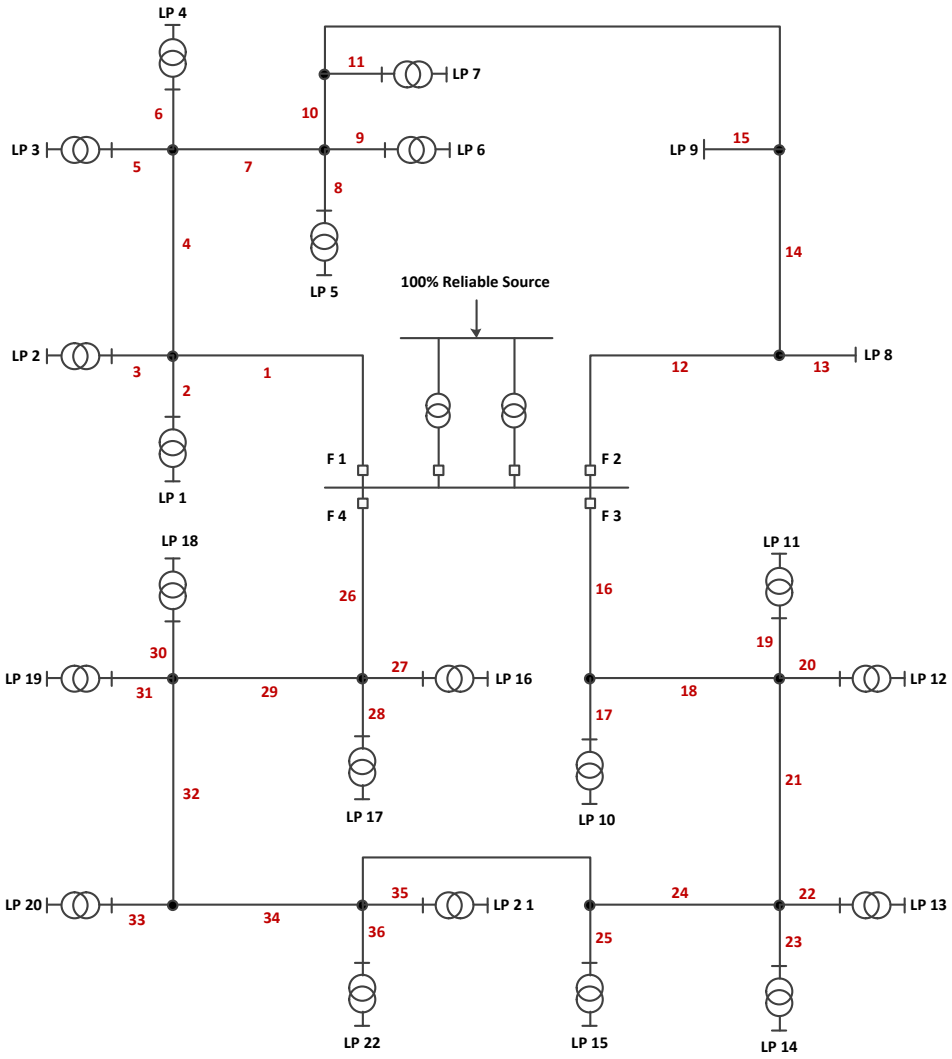

Fig. 4.4 Single line diagram for RBTS Bus 2

In Fig. 4.4, it is assumed that the maximum number of components that can form a cut set is 3. This may be a reasonable assumption, since in power distribution systems, the occurrence of 4 failures at the same time is considered to be rare, and the effect of 4 components in parallel in a state diagram is insignificant. If this assumption is relaxed, the complexity of the solution increases, but is still calculable by a similar procedure.

As a result of applying the algorithm to the circuit in Fig. 4.4, the total numbers of the MTSs and MCSs for all load points are shown in Fig. 4.5. The blocks that represent the sets for LP 1 are shown in Fig. 4.6, where each set is represented by a parallel connection of its components.

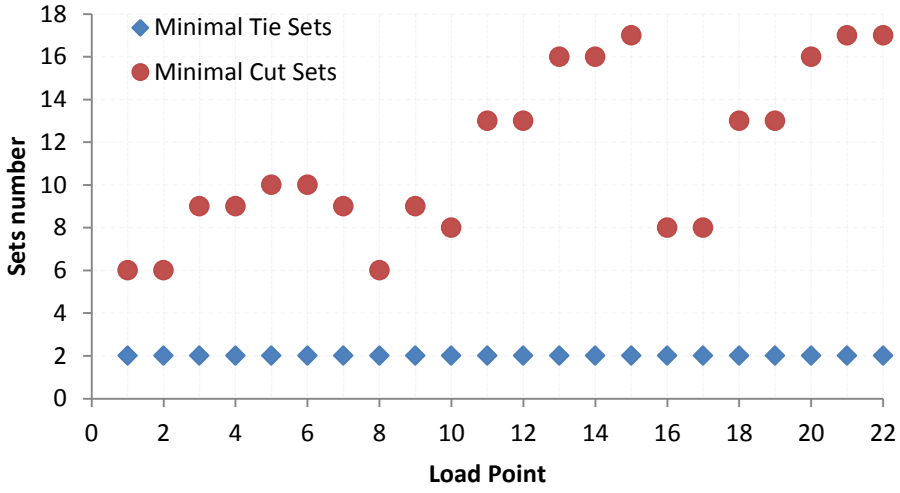

Fig. 4.5 Total number of the MTS and MCS for RBTS Bus 2

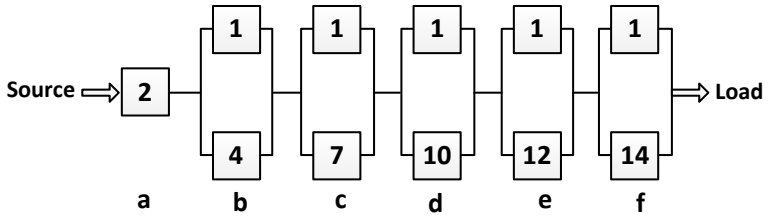

Fig. 4.6 Block diagram for the minimal cut sets for LP 1 – RBTS Bus 2

The calculation of the upper and lower bounds of the load indices for LP 1 is shown in Table 4.1. The difference between the upper and lower bounds for all the load indices is insignificant and can be ignored. The upper bound equations ((4.3) and (4.4)) can be used as approximations for the reliability calculation when

the availability of the system components is very high. The upper and lower bounds for the system indices are also shown in Table 4.2.

Table 4.1 Reliability load indices for LP 1 – RBTS Bus 2

Load Index	Upper Bound	Lower Bound
A	0.999635396	0.999635396
U	0.000364604	0.000364604
AIF (f/y)	0.054012479	0.054012473
AID (h/y)	3.193933055	3.193933042
FD (h/f)	59.13324941	59.13324293
ENS (MWh/y)	1.708754184	1.708754177

Table 4.2 Reliability system indices for RBTS Bus 2

System Index	Upper Bound	Lower Bound
SAIFI (f/c.y)	0.060950419	0.060950407
SAIDI (h/c.y)	3.225517233	3.225517207
CAIDI (h/y)	52.94270576	52.94269517
ASAI	0.99963179	0.99963179
ASUI	0.00036821	0.00036821
ENS (MWh/y)	18.04666543	18.04666524

In Fig. 4.7, the effect of higher component failures and repair rates is demonstrated. The failure rate used in this case is equal to 20 f/y for all components, and the time to repair is 20 h. As shown in Fig. 4.7 and Table 4.3, the difference between the upper and lower bounds is significant, and any approximation will introduce a considerable error for load and system indices.

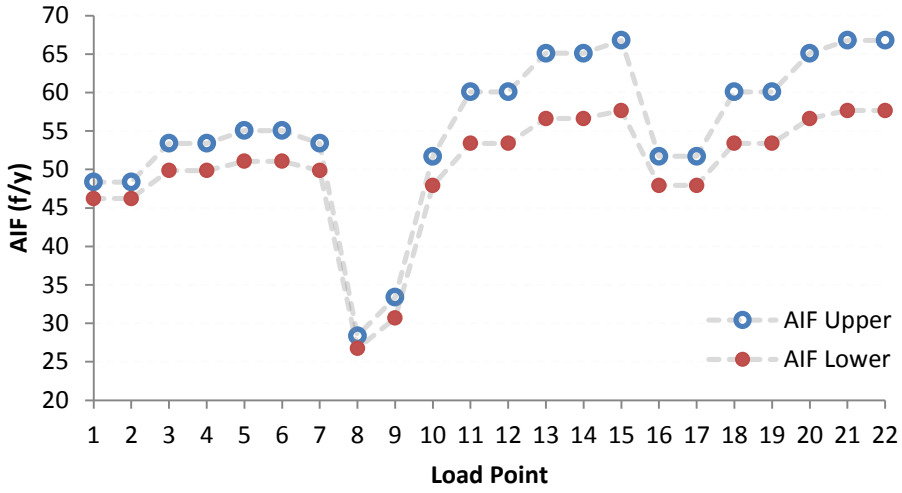

Fig. 4.7 Upper and lower load indices bounds for RBTS Bus 2 (λ=20 f/y, MTTR=20 h)

Table 4.3 Reliability system indices for RBTS Bus 2 (λ=20 f/y, MTTR=20 h)

System Index	Upper Bound	Lower Bound
SAIFI (f/c.y)	54.90934	50.21773
SAIDI (h/c.y)	896.9959	865.788
CAIDI (h/y)	17.86268	15.80304
ASAI	0.901166	0.897603
ASUI	0.102397	0.098834
ENS (MWh/y)	5545.148	5307.479

Chapter 5

RELIABILITY ASSESSMENT USING EMCS ALGORITHM

5.1 Using the EMCS Algorithm to Evaluate the Reliability

The reliability indices help the utilities evaluate their networks and improve these reliability indices for better service. The system and load point reliability indices are useful tools for assessing past and future reliability performance. They are also useful in predicting the severity of component failures in future operations of the power system. A reliability evaluation study quantifies reliability based on component reliability data and can be used to identify the problematic components in the system that can impact reliability. It can also help predict the reliability performance of the system after any expansion and quantify the impact of adding new components to the system. The number and locations of new components needed to improve reliability indices to certain limits can be identified and studied.

To evaluate the reliability of the secondary grid network, the EMCS method is used as explained in Chapter 3. MATLAB was used to evaluate the distribution system reliability using EMCS algorithm. A sample MATLAB code for the EMCS algorithm can be found in Appendix C. The general flow diagram for evaluating the reliability of a grid network using the EMCS algorithm is shown in Fig. 5.1.

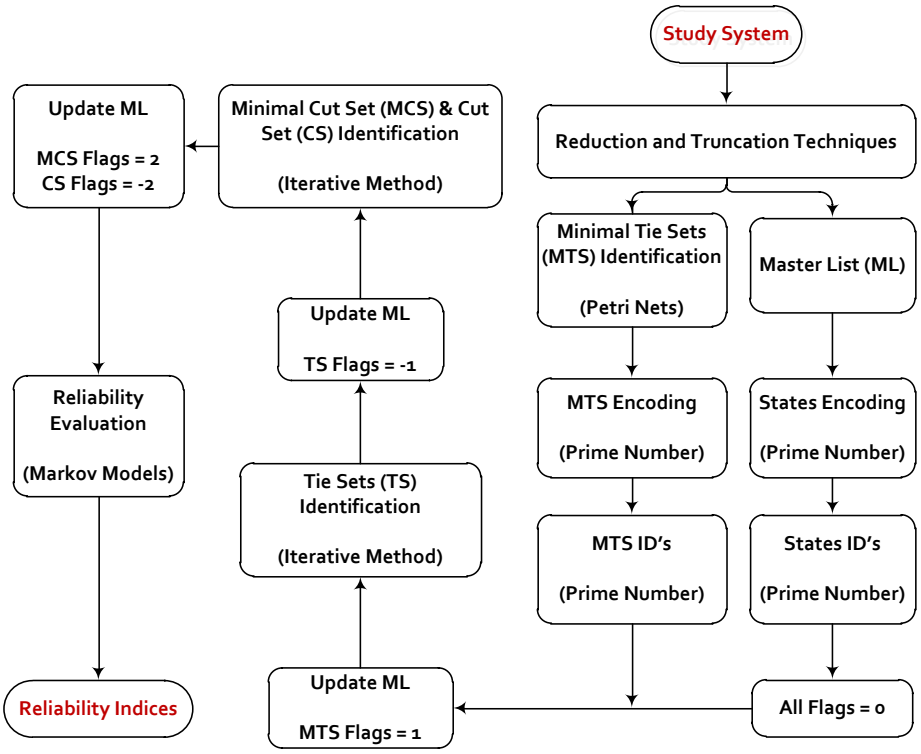

Fig. 5.1 Flow chart for EMCS algorithm

5.2 RBTS Bus 4 Study System

The system under study is the RBTS Bus 4 [54]. The single line diagram for the system is shown in Fig. 5.2. The number of components and customers in this system are shown in Table 5.1.

Table 5.1 Number of components and customers for RBTS Bus 4

	11 kV subsystem	33 kV subsystem	Total
Feeders	67	4	71
Transformers	29	6	35
Busbars	3	3	6
Total number of components	99	13	112
Main feeders	7	-	7
Load points	38	-	38
Customers	4779	-	4779

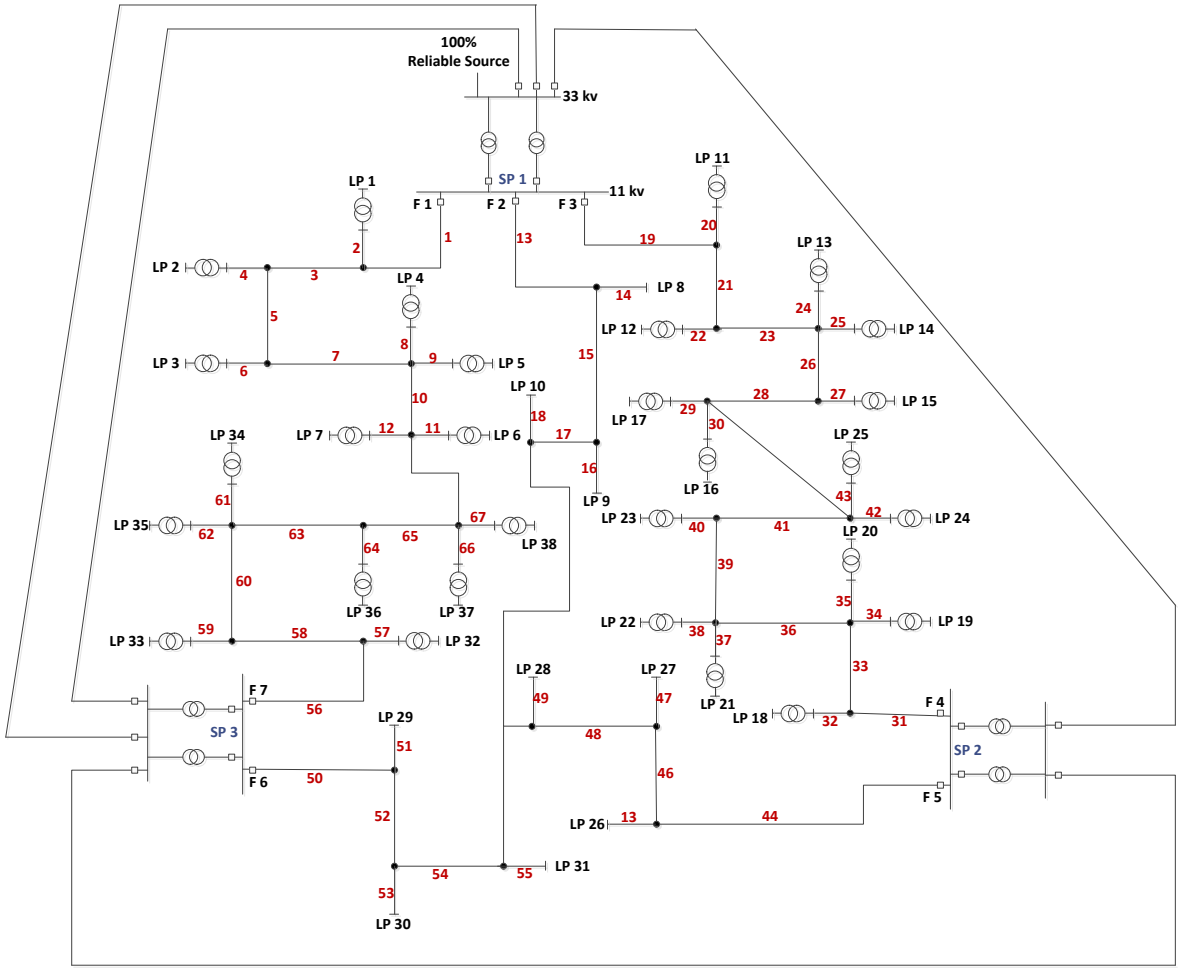

Fig. 5.2 Single line diagram for RBTS Bus 4

The reliability data for RBTS Bus 4 can be found in Appendix B [54]. In this study, overhead lines are used to analyze the system, and underground cables are used as a possible approach to improve the reliability of the system. The 11 kV and 33 kV subsystems are both included in this study.

The faulted 11/0.415 kV transformers are repaired and returned to service with listed repair rate and time. Replacing the transformer after failure is considered an optional technique to reduce the outage time and improve the outage duration experienced by the customer (whether they are residential, commercial, or small industrial users). The 33/11 kV transformers are only replaced when they fail.

5.3 RBTS Bus 4 Reliability Analysis

The reliability study performed on the RBTS Bus 4 and different load and system indices were calculated. The study takes into account the failures on the 11 kV and 33 kV feeders and transformers. All interruption devices and tie switches are considered 100% reliable and to operate successfully when they are needed.

The first stage of analysis applies the reduction techniques explained in Section 3.3. These techniques will lessen the number of components and states of the system. Reducing the number of states will reduce the size of all reliability matrices and expedite the computation process. As shown in Fig. 5.3 for LP 1, the number of nodes for the base case system is 98 nodes. In this case, there is no reduction method applied to the system. After applying all the reduction methods (R1-R4), the number of nodes decreases from 98 to only 9 nodes. The reduction levels (R2-R4) are repeated twice for the maximum reduction outcome.

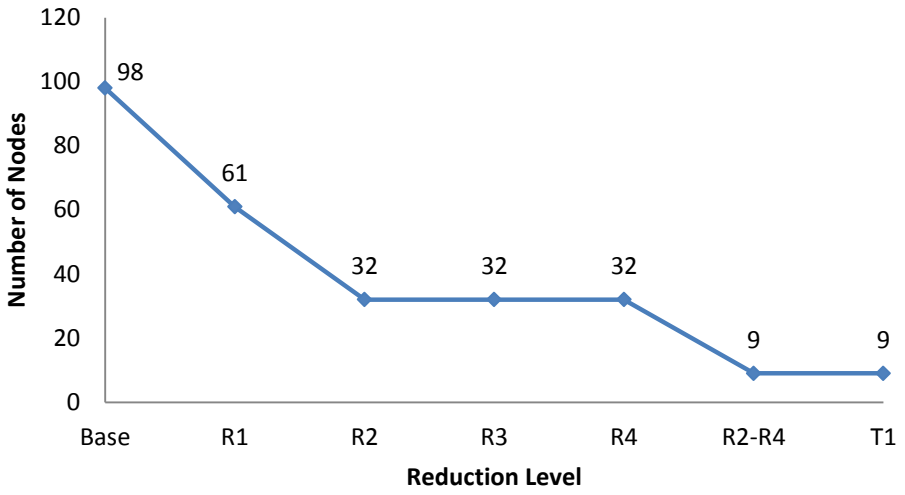

Fig. 5.3 Number of nodes after each reduction level for LP 1 – RBTS Bus 4

The number of components for LP 1 is shown in Fig. 5.4. The components and states are not affected by the first reduction method (R1) since only irrelevant load nodes are removed in this stage. In the second reduction method (R2), the components and states are reduced after combining all the series and parallel components. In the third method (R3), the components and states are also removed if they do not share any common node with all components of the possible input-output routes. The last reduction stage (R4) removes the components of the irrelevant loads deleted in R1. The number of components at the end of reduction process reduced from 106 components to only 13 equivalent components.

After the reduction level 4, the truncation level reduces the number of states according to the specified number of simultaneous failures in the system. The number is usually two or three failures, depending on the system and the failure reliability data of its components. For this system, the maximum number

of failures is three. The number of states reduced after applying all reduction techniques from 8.11×10^{31} to only 378 states, which is shown for LP 1 in Fig. 5.5.

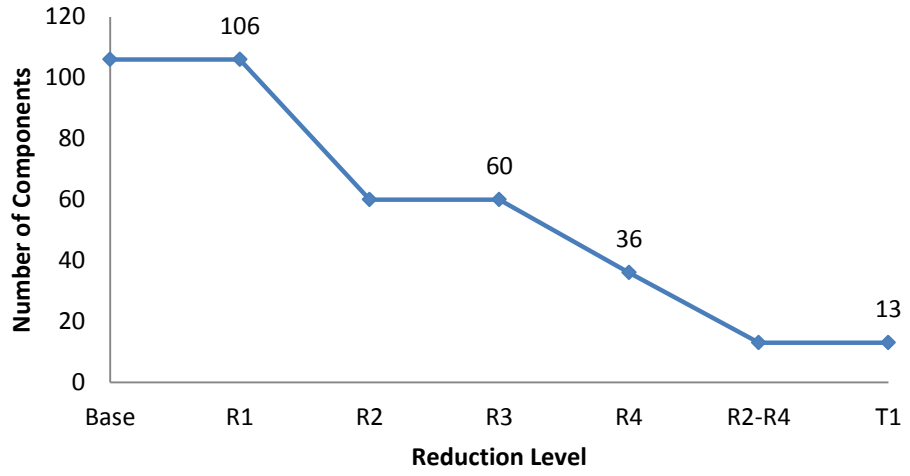

Fig. 5.4 Number of components after each reduction level for LP 1 – RBTS Bus 4

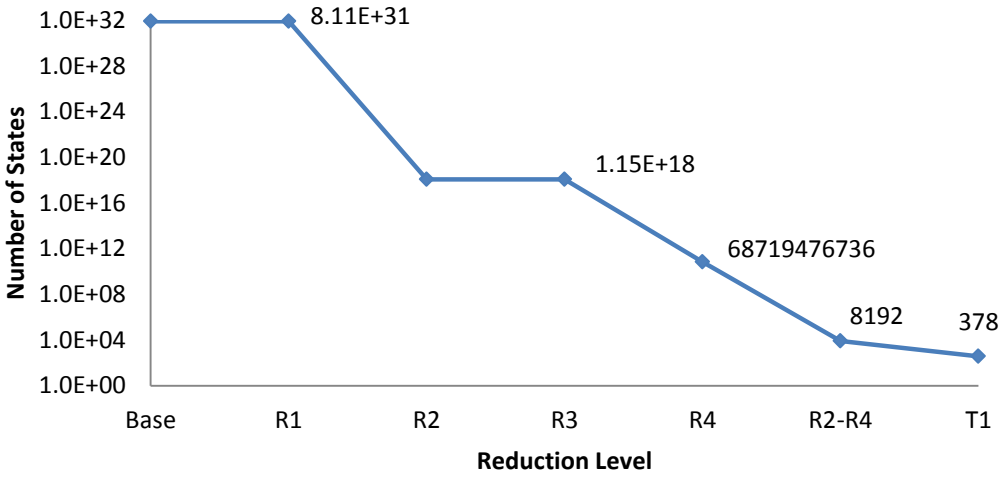

Fig. 5.5 Number of states after each reduction level for LP 1 – RBTS Bus 4

After reducing the number of components and states of the system, Petri nets and prime number encoding were used to create the master list and determine the minimal tie, tie, minimal cut, and cut sets. Table 5.2 shows the new equivalents sections with their original sections from Fig. 5.2.

Table 5.2 Equivalent sections and their original sections for LP 1 – RBTS Bus 4

Equivalent section	Original sections
1	1
2	2, 78
3	3, 5, 7, 10, 56, 58, 60, 63, 65
4	13, 15, 17
5	19, 21, 23, 26, 28, 31, 33, 36, 39, 41
6	44, 46, 48
7	50, 52, 54
8	68, 69
9	70
10	71
11	72, 73
12	74, 75
13	76, 77
Deleted sections	4, 6, 8, 9, 11, 12, 14, 16, 18, 20, 22, 24, 25, 27, 29, 30, 32, 34, 35, 37, 38, 40, 42, 43, 45, 47, 49, 51, 53, 55, 57, 59, 61, 62, 64, 66, 67, 79-106

Moreover, all states are encoded using the prime number encoding technique explained in Section 3.4. Because the reduced model has only 13 sections, with the maximum number of section in each group assumed to be 5, each ID for each state will consist of three groups, as shown in Table. 5.3. The combination in Table 5.4 represents the system when it is normally operating with no sections in fault. The prime numbers used for each group are also listed, and the ID is the multiplication of all the prime numbers in each group. The next step is finding the tie and cut sets using Petri net and prime number encoding techniques. The different numbers of minimal tie sets, tie sets, minimal cut sets, and cut sets are listed in Table 5.6 for each maximum number of failures.

Table 5.3 States prime encoding for LP 1 – RBTS Bus 4

	Group 1					Group 2					Group 3		
Section	1	2	3	4	5	6	7	8	9	10	11	12	13
Prime number	2	3	5	7	11	2	3	5	7	11	2	3	5
ID	2310					2310					30		

Table 5.4 Different sets count for each maximum failures for LP 1 – RBTS Bus 4

Max. failures	MTS	TS	MCS	CS	Total states
1	0	13	1	0	14
2	0	78	2	12	92
3	0	285	5	88	378
4	0	702	12	379	1093
5	3	1222	21	1134	2380

In Tables 5.5 and 5.6, all the minimal tie and minimal cut sets are listed for load 1. Although all the minimal tie sets are computed, they are not presented in the state space. This is because the maximum number of failures allowed is 3, which then removed the minimal tie sets states from the state space. At the end of the reduction process, the minimal tie sets IDs will not be able to locate their states in the state space.

After classifying all the states as tie or cut sets, the availability, MTTF, and failure frequency can be found using the Markov models explained in Section 3.7. The transition matrices used for various maximum numbers of failures are shown in Fig. 5.6. The size and the number of nonzero elements in the transition matrix can affect the capability and computation speed of evaluating the reliability of using Markov models. After computing availability, MTTF, and failure frequency using Markov models, the load point and system reliability

indices can be calculated. All the load point reliability indices are listed in Table 5.7.

Table 5.5 Minimal tie sets for LP 1 – RBTS Bus 4

Tie set level	ID			Sections												
3	6	1	2	1	2	-	-	-	-	-	-	-	-	11	-	-
4	15	5	5	-	2	3	-	-	-	-	8	-	-	-	-	13
5	66	7	3	1	2	-	-	5	-	-	-	9	-	-	12	-
	105	3	2	-	2	3	4	-	-	7	-	-	-	11	-	-
	15	77	5	-	2	3	-	-	-	-	-	9	10	-	-	13
6	42	14	3	1	2	-	4	-	6	-	-	9	-	-	12	-
	42	15	5	1	2	-	4	-	-	7	8	-	-	-	-	13
	66	55	3	1	2	-	-	5	-	-	8	-	10	-	12	-
	165	6	2	-	2	3	-	5	6	7	-	-	-	11	-	-
	15	42	3	-	2	3	-	-	6	7	-	9	-	-	12	-
7	42	110	3	1	2	-	4	-	6	-	8	-	10	-	12	-
	42	231	5	1	2	-	4	-	-	7	-	9	10	-	-	13
	66	30	5	1	2	-	-	5	6	7	8	-	-	-	-	13
	1155	21	3	-	2	3	4	5	-	7	-	9	-	-	12	-
	165	11	30	-	2	3	-	5	-	-	-	-	10	11	12	13
	15	330	3	-	2	3	-	-	6	7	8	-	10	-	12	-
8	66	462	5	1	2	-	-	5	6	7	-	9	10	-	-	13
	1155	165	3	-	2	3	4	5	-	7	8	-	10	-	12	-
	105	22	30	-	2	3	4	-	6	-	-	-	10	11	12	13

Table 5.6 Minimal cut sets for LP 1 – RBTS Bus 4

Cut set level	ID			Sections												
1	770	2310	30	-	2	-	-	-	-	-	-	-	-	-	-	-
2	231	2310	30	1	-	3	-	-	-	-	-	-	-	-	-	-
3	1155	770	6	1	-	-	-	-	-	7	-	-	-	-	-	13
	2310	66	15	-	-	-	-	-	-	-	8	9	-	11	-	-
	2310	2310	1	-	-	-	-	-	-	-	-	-	-	11	12	13

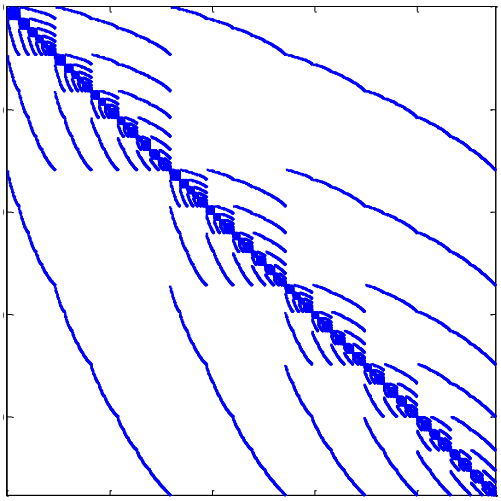

Max. number of failures = 5
Number of nonzero elements = 20644

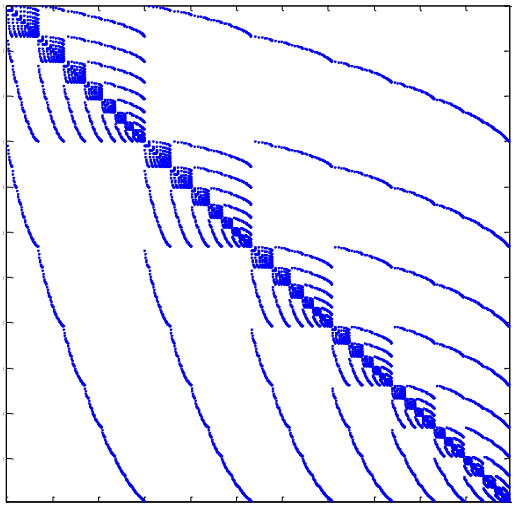

Max. number of failures = 4
Number of nonzero elements = 7774

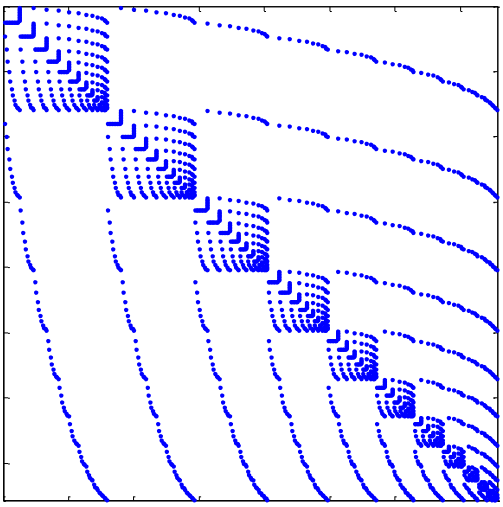

Max. number of failures = 3
Number of nonzero elements = 2054

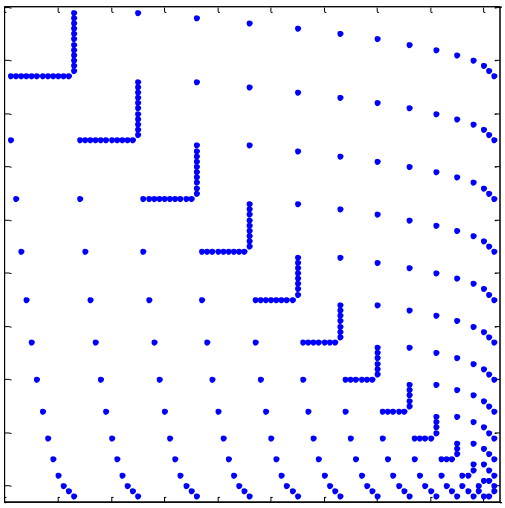

Max. number of failures = 2
Number of nonzero elements = 338

Fig. 5.6 Transition matrix for various maximum failures for LP 1 – RBTS Bus 4

(Nonzero entries denoted by "**.**")

Table 5.7 Load points reliability indices for all load points – RBTS Bus 4

Load Points	A	U	MTT (y)	AIF (f/y)	AID (h/y)	FD (h/f)	ENS (MWh)
1	0.999635	0.000365	18.5076	0.0540	3.1940	59.1431	1.7407
2	0.999630	0.000370	15.6737	0.0638	3.2427	50.8511	1.7673
3	0.999635	0.000365	18.4972	0.0540	3.1940	59.1091	1.7408
4	0.999628	0.000372	14.9101	0.0670	3.2590	48.6148	1.7762
5	0.999630	0.000370	15.6694	0.0638	3.2428	50.8361	1.6214
6	0.999628	0.000372	14.9099	0.0670	3.2590	48.6138	1.3525
7	0.999630	0.000370	15.6693	0.0638	3.2428	50.8350	1.3458
8	0.999978	0.000022	25.6368	0.0390	0.1950	4.9997	0.1950
9	0.999972	0.000028	20.5108	0.0488	0.2438	4.9998	0.3656
10	0.999970	0.000030	19.2310	0.0520	0.2600	5.0000	0.2600
11	0.999628	0.000372	14.9178	0.0670	3.2589	48.6416	1.7761
12	0.999630	0.000370	15.6745	0.0638	3.2427	50.8540	1.7673
13	0.999630	0.000370	15.6712	0.0638	3.2428	50.8428	1.7673
14	0.999635	0.000365	18.4979	0.0540	3.1940	59.1114	1.5970
15	0.999630	0.000370	15.6694	0.0638	3.2428	50.8362	1.6214
16	0.999635	0.000365	18.4947	0.0540	3.1941	59.0997	1.3255
17	0.999630	0.000370	15.6690	0.0638	3.2428	50.8343	1.3458
18	0.999630	0.000370	15.6799	0.0638	3.2427	50.8645	1.7673
19	0.999635	0.000365	18.5028	0.0540	3.1940	59.1214	1.7407
20	0.999630	0.000370	15.6749	0.0638	3.2427	50.8500	1.7673
21	0.999630	0.000370	15.6715	0.0638	3.2428	50.8402	1.7673
22	0.999635	0.000365	18.4980	0.0540	3.1940	59.1079	1.5970
23	0.999630	0.000370	15.6695	0.0638	3.2428	50.8351	1.6214
24	0.999630	0.000370	15.6690	0.0638	3.2428	50.8343	1.3458
25	0.999635	0.000365	18.4947	0.0540	3.1941	59.0997	1.3255
26	0.999972	0.000028	20.5108	0.0488	0.2438	4.9997	0.2438
27	0.999970	0.000030	19.2291	0.0520	0.2600	4.9998	0.2600
28	0.999978	0.000022	25.6412	0.0390	0.1950	5.0000	0.1950
29	0.999978	0.000022	25.6374	0.0390	0.1950	4.9996	0.1950
30	0.999972	0.000028	20.5105	0.0488	0.2438	4.9997	0.2438
31	0.999978	0.000022	25.6412	0.0390	0.1950	5.0000	0.2925
32	0.999628	0.000372	14.9200	0.0670	3.2589	48.6417	1.7761
33	0.999628	0.000372	14.9164	0.0670	3.2590	48.6314	1.7761
34	0.999635	0.000365	18.4997	0.0540	3.1940	59.1127	1.7407
35	0.999628	0.000372	14.9131	0.0670	3.2590	48.6218	1.7762
36	0.999635	0.000365	18.4965	0.0540	3.1941	59.1038	1.5970
37	0.999628	0.000372	14.9099	0.0670	3.2590	48.6138	1.6295
38	0.999635	0.000365	18.4951	0.0540	3.1941	59.1006	1.3255

In Fig. 5.7, the availability and unavailability for all load points in the system are shown. The availability for LP 8–LP 10 and LP 26–LP 31 are higher due to the absence of transformers in these loads connections. The transformers at these loads are considered customer property and will not be included in the reliability evaluation.

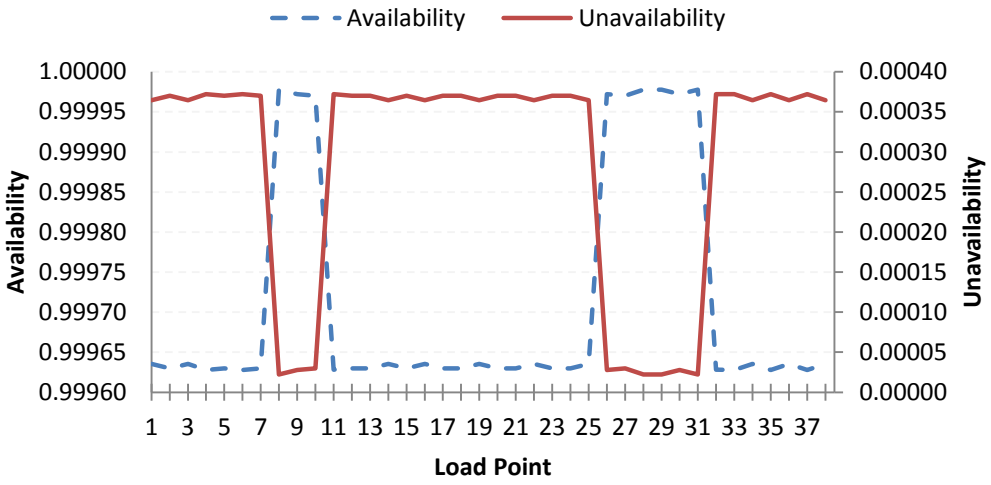

Fig. 5.7 Availability and unavailability for all load points – RBTS Bus 4

The AID and FD are shown in Fig. 5.8. The reduction in duration value at loads 8–10 and 26–31 is due to the absence of transformers. The customers at these load points are small industrial plants connected directly to the 11 kV side.

After computing the load points' reliability indices, the system reliability indices are calculated. The system reliability indices are shown in Table 5.8.

Table 5.8 System reliability indices – RBTS Bus 4

SAIFI (f/c.y)	SAIDI (h/c.y)	CAIDI (h/f)	ASAI	ASUI	ENS (MWh/y)
0.061551	3.226127	52.414085	0.999632	0.000368	49.349240

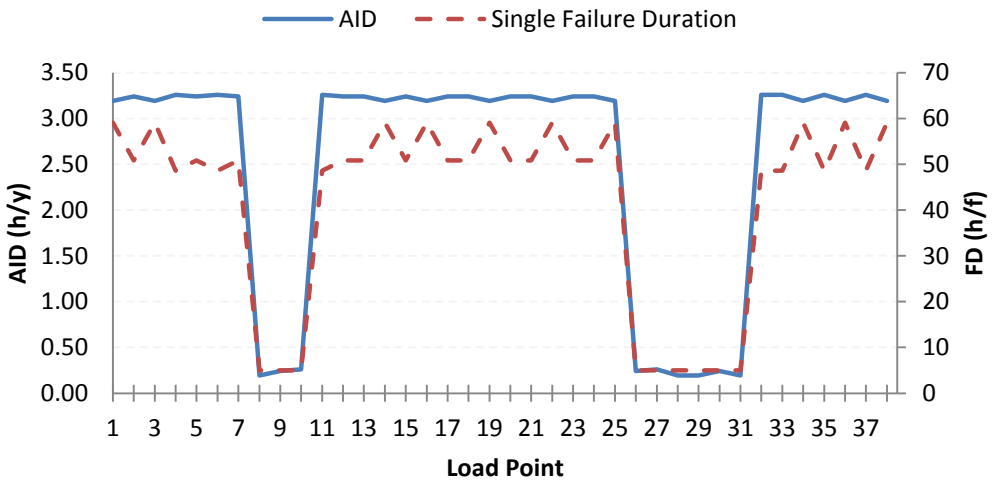

Fig. 5.8 AID and FD for all load points – RBTS Bus 4

Table 5.9 shows the system reliability calculation with different values of maximum simultaneous failures. In Table 5.2, the number of states and the percentage of change are also shown for each case.

Table 5.9 System indices and percentage of change for each maximum failure – RBTS Bus 4

Max. failures	States number		SAIFI (f/y)	SAIDI (h/y)	CAIDI (h/f)
1	14	Index	0.0614	3.2207	52.4532
		Percentage of change (%)	-	-	-
2	92	Index	0.062	3.226	52.414
		Percentage of change (%)	0.241	0.166	0.074
3	378	Index	0.061	3.226	52.414
		Percentage of change (%)	0.0002	0.0001	0.0001
4	1093	Index	0.061	3.2261	52.414
		Percentage of change (%)	0	0	0
5	2380	Index	0.061	3.226	52.414
		Percentage of change (%)	0	0	0

After reducing the number components and states, the prime number encoding was used to determine the minimal tie sets. Then, the prime number

encoding technique was used to create the master list and to categorize the tie sets, cut, and minimal cut sets. The load points and system reliability indices could then be computed using the Markov models explained in Chapter 2. The computation time for each maximum number of simultaneous failures is shown in Figs. 5.9. The computation time for applying all reduction and truncation techniques and creating the master list for all states is nearly the same for all maximum failures. The time to find the MCS and CS as well as evaluate the reliability indices using Markov models increases as the number of maximum failures increases.

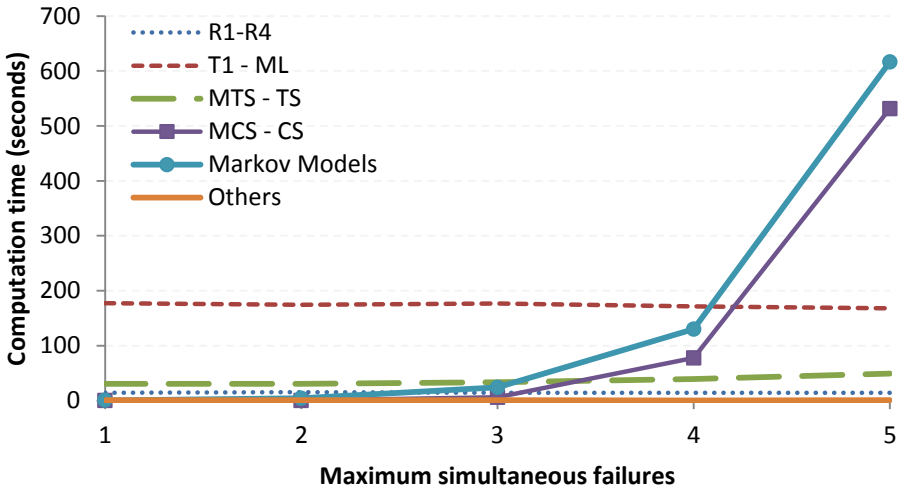

Fig. 5.9 Computation time in seconds for each maximum number of failures – RBTS Bus 4

The reliability indices also help the utilities evaluate their networks and improve these reliability indices for providing better service. These indices can be improved by reducing the main influencing factors [18] including:

- Outage duration

- Outage frequency
- Number of customers interrupted.

The system reliability indices are calculated to measure the effect the improvement of each component would have on these indices. In Fig. 5.10, the SAIDI is computed for each component with a 50% reduction in repair time. The percentage of change in SAIDI is also shown for each component. The most significant impact to SAIDI occurs when the repair time for the transformers decreased. The repair time can be improved by reducing the response time of the maintenance crew to repair the transformers by managing the location of the crews, the spare parts inventory, and travel time to the faulted site.

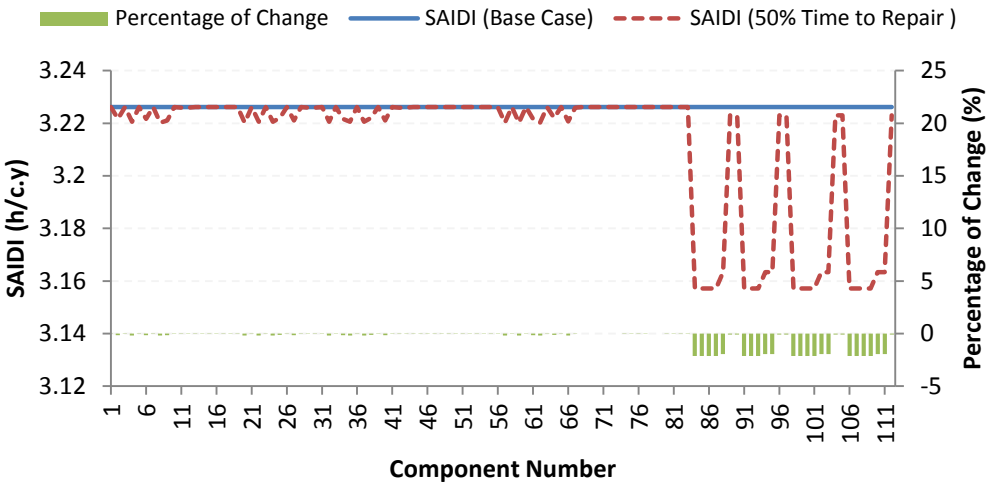

Fig. 5.10 SAIDI for repair time improvement by 50% – RBTS Bus 4

The effect of improving each component failure rate is demonstrated in Fig. 5.11. The SAIFI is improved even more when the lines connected to the high-density load points are improved. This will decrease the average failures seen by the customers. The customers will experience shorter interruption

duration due to the increase in MTTF at each load point. The lines can be improved by enhancing the component's quality and reducing failure rate. This can be achieved by monitoring and increasing the preventive maintenance and replacing the components when they reach their expected lifetime. Additionally, it may also be helpful to isolate the overhead lines to protect them from tree or animal contact.

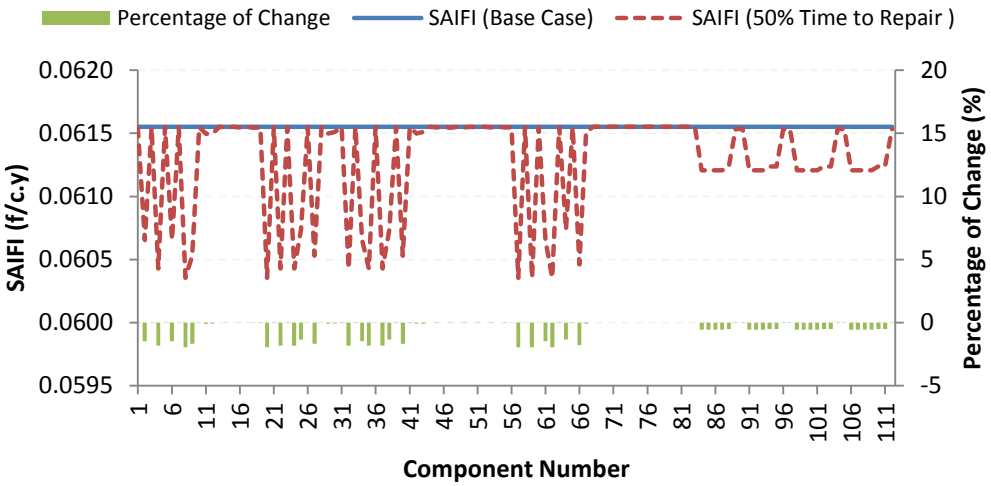

Fig. 5.11 SAIFI for failure rate improvement by 50% – RBTS Bus 4

To study the complete system change with the change in each component's repair time, the reliability index (*RI*) is proposed where 4 different system indices are combined and weighted to form this *RI*:

$$RI = w_1 SAIFI_{pu} + w_2 SAIDI_{pu} + w_3 ASUI_{pu} + w_4 ENS_{pu} \tag{5.1}$$

$$\sum_{i=1}^{n} w_i = 1 \tag{5.2}$$

where w_i is the weight for each i index and n is the number of system indices included in the RI. The $SAIFI_{pu}$, $SAIDI_{pu}$, $ASUI_{pu}$, and ENS_{pu} are the system indices per unit. The weights for all indices used in *RI* are equal to 0.25.

The *RI* is shown in Fig. 5.12. Based on the system indices and weights used in this index, the greatest improvement occurs when the failure rate of the transformers connected to the higher customer density load points are improved.

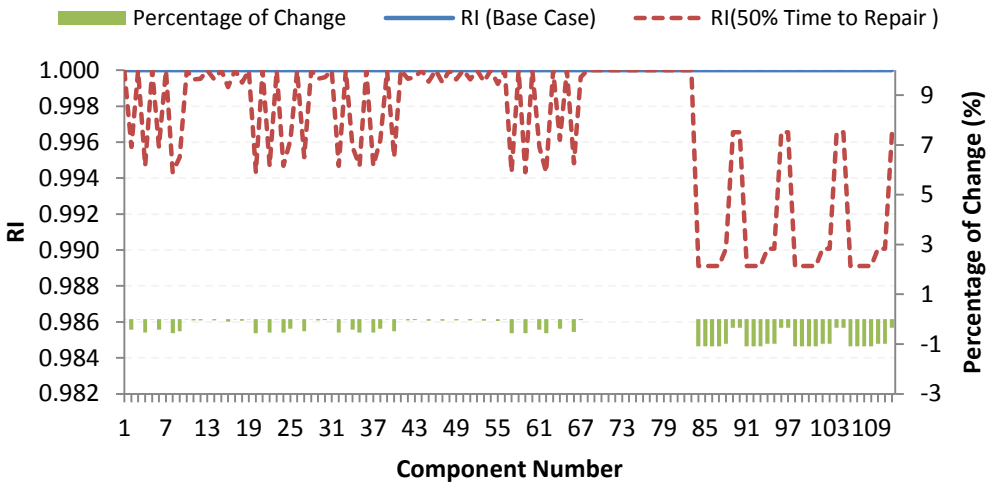

Fig. 5.12 *RI* for failure rate improvement by 50% – RBTS Bus 4

Four different cases are demonstrated in Table 5.10 to study the effect of replacing the overhead lines with underground cables along with the effect of replacing the 11/0.415 kV transformers during their failures. Underground cables have a smaller failure rate but longer repair time. Replacing the transformer during the fault instead of repairing it will lessen the outage time and will not affect the failure rate of the transformer.

Table 5.10 Different cases for the main feeders and transformers – RBTS Bus 4

	11 kV Feeders			11/0.415 kV Transformers		
	Feeder type	Failure rate (f/y.km)	Repair time (h)	Transformer restoration method	Failure rate (f/y)	Restoration time (h)
Case 1	Overhead lines	0.065	5	Repair	0.015	200
Case 2	Overhead lines	0.065	5	Replace	0.015	10
Case 3	Underground cables	0.04	30	Repair	0.015	200
Case 4	Underground cables	0.04	30	Replace	0.015	10

The availability for different cases in Table 5.10 is shown in Fig. 5.13. Replacing transformers decreases outage duration at each load point, which can lead to better availability. The availability for Case 2 is better than for Case 4 because the overhead lines require less repair time than underground cables do.

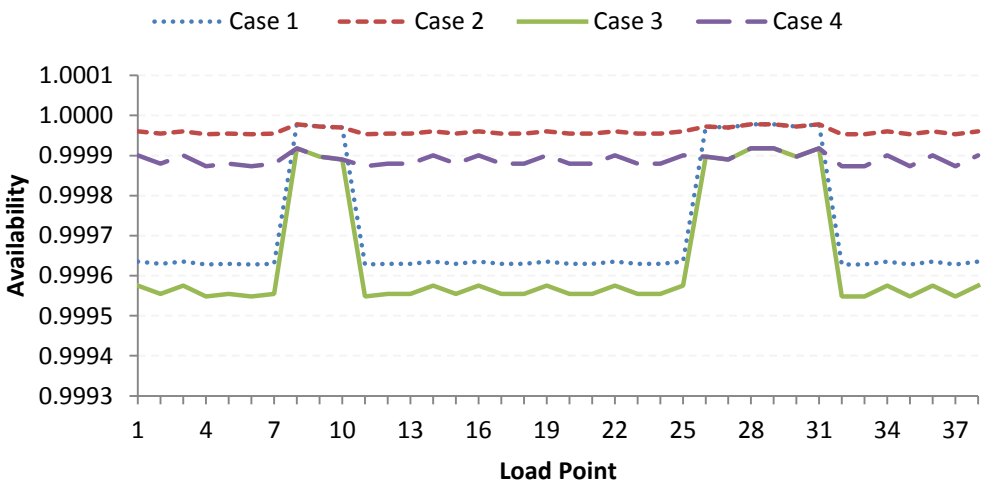

Fig. 5.13 Availability for different cases in Table 5.10 – RBTS Bus 4

Repairing or replacing the transformers has no effect on the MTTF and will only change the repair time. The failure rate for the transformers will remain the same. Because Cases 3 and 4 have higher MTTF due to lower failure rates of

the underground cables, this can lead (as shown in Fig. 5.14) to a lower failure frequency.

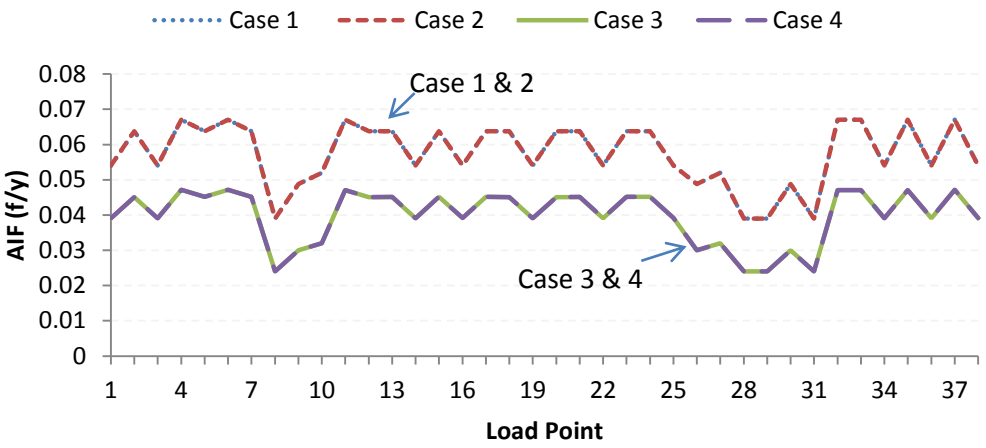

Fig. 5.14 AIF for different cases in Table 5.10 – RBTS Bus 4

Replacing any transformer will take less time than repairing it, and this will improve the AID in Cases 2 and 4, as shown in Fig. 5.15. This is also the reason for the improvement in ENS shown in Fig. 5.16. LP 8–LP 10 and LP 26–LP 31 are not affected by the transformer restoration method because there are no transformers included in the reliability evaluation at these load points.

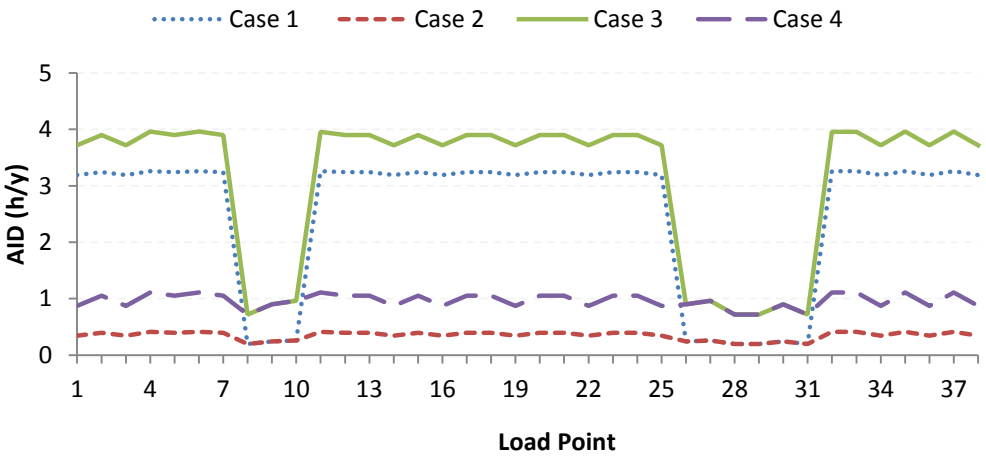

Fig. 5.15 AID for different cases in Table 5.10 – RBTS Bus 4

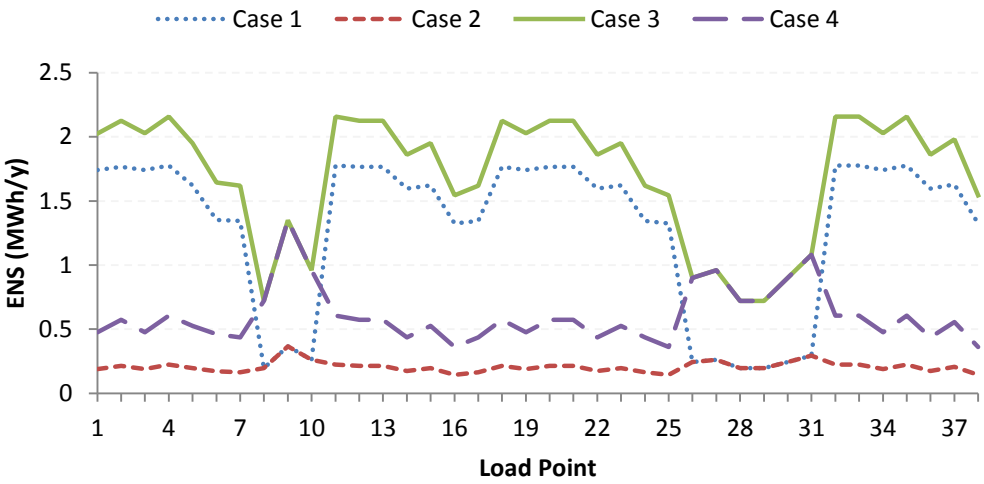

Fig. 5.16 ENS for different cases in Table 5.10 – RBTS Bus 4

In Table 5.11 and Fig. 5.17, the system reliability indices are calculated for all Cases. It is shown that SAIDI, CAIDI, and ENS are improved when the transformers are replaced during the outages. The SAIFI is improved when the underground cables are used in the system because they have a smaller failure rate.

Table 5.11 System reliability indices for the cases in Table 5.10 – RBTS Bus 4

	SAIFI (f/c.y)	SAIDI (h/c.y)	CAIDI (h/f)	ASAI	ASUI	ENS (MWh/y)
Case 1	0.06155	3.22613	52.41409	0.99963	0.00037	49.34924
Case 2	0.06157	0.38259	6.21387	0.99996	0.00004	7.81227
Case 3	0.04371	3.85404	88.17209	0.99956	0.00044	64.50936
Case 4	0.04372	1.01071	23.11531	0.99988	0.00012	22.97536

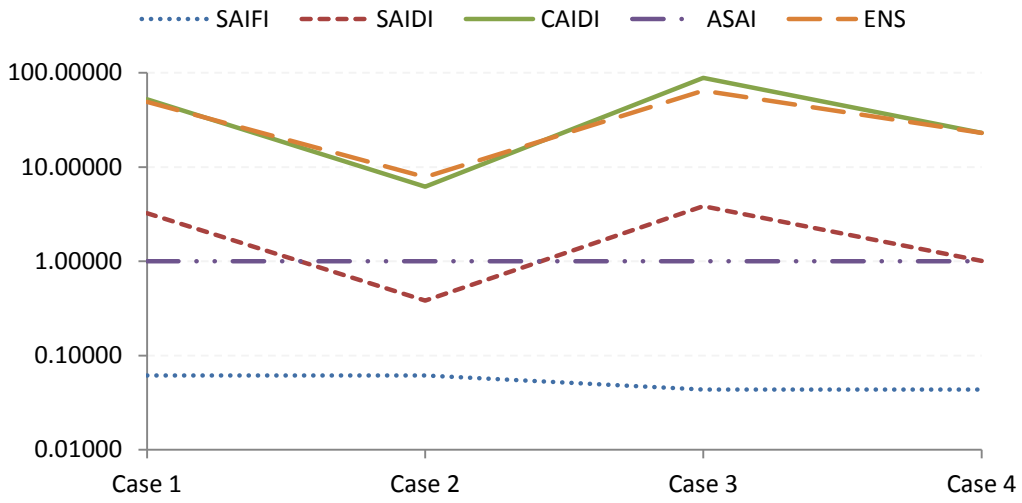

Fig. 5.17 System reliability indices for different cases in Table 5.11– RBTS Bus 4

Chapter 6

DISTRIBUTED RESOURCES RELIABILITY INTEGRATION

6.1 Distributed Resources Applications in Distribution Systems

DG is defined as a small scale generation unit that is installed in the distribution system and typically connected at substations, on distribution feeders, or at the customer load level [56–58]. DG differs fundamentally from the traditional model of central generation as it can be located near end-users within an industrial area, inside a building, or in a community. Different types of DGs have been developed due to the increasing interest in the DG in recent years [59].

DG units vary in size, fuel type, and efficiency, and they can be associated with two technologies, conventional energy technology and renewable energy technology. Technologies that utilize conventional energy resources include reciprocating engines, combustion turbines, micro-turbines, and fuel cells. Conversely, renewable energy resources are based on different forms of natural resources such as heat and light from the sun, the force of the wind, and the combustion value of organic matter [59–62]. A few examples of renewable DGs include photovoltaic cells, wind turbines, and biomass. The most promising renewable energies in the United States are wind and solar. The advantages and disadvantages of wind energy and photovoltaic are listed in Table 6.1.

The main difference between the renewable and conventional resources is that the output of the renewable resources depends on variable inputs such as wind or solar energy. The power produced from renewable resources may fluctuate more, making it difficult forecast. In the case in which a DG is

connected to the local load to supply the load during interruptions, the demand and supply may not match, especially if the DG is renewable. In this case, the DG is either disconnected due to the activation of the frequency or voltage protection devices or the system will shed some loads and only supply critical loads. The emphasis of this research is the design phase and not the operational aspects of the distribution system. If the DG is incapable of supplying the full load demand, the DG will be disconnected from the local load.

Table 6.1 Advantages and disadvantages for several renewable energies

	Advantages	Disadvantages
Wind Energy	• Short time to design and install • Low emission • Different modular size	• Wind is highly variable • Limited resource sites • Audible and visual noise • Low availability during high demand periods
Photovoltaic	• Flexible in term of size and site • Simple operation • No moving parts and noise • Low maintenance • Short time for design and installation • No emissions	• High capital cost • Large area required • Low efficiency • Low availability during high demand periods • Low capacity factor

There are many potential applications for DG technologies. They can be classified as backup DGs or base load DGs. The DG can be used as a backup generator to replace the normal source when it fails to supply the load, thereby allowing the customer's facility to continue to operate satisfactorily during the power outages. Most backup generators are diesel engines because of their low cost, fuel availability, and quick start time.

A backup DG is connected to the local load, and a manual or automatic switch is installed on the feeder side of the DG local load. During faults on the main feeder or its laterals, the circuit breaker on the substation side will trip to clear the fault, causing the whole feeder to be interrupted. Then, the DG switch can be closed and the DG unit can start supplying its local load.

A base load DG is used by some customers to provide a portion or all of their electricity needs in parallel with the electric power system. It can also be used as an independent standalone source of power. The technologies used for these applications include renewable DGs such as wind, photovoltaic, fuel cells, and combined heat and power (CHP).

6.2 Reliability Evaluation of Distribution System Including DG

The main direct contribution of DG to reliability is on the customer side rather than on the utility or system side. The base level of reliability is always provided by the utility, and the DG's role is to boost the level of reliability by supplying the local load during interruptions (assuming that the DG is properly sized to serve at least the critical loads). The duration of interruptions at the load bus are expected to be fewer when a standby DG is connected. Different factors should be considered when evaluating the reliability impact of the DG on the local load, such as fuel availability, power output, unit's failure rate, repair time, and starting time. Many papers have discussed the technologies of DG units and their economical, environmental, and operational benefits [63–66].

The presence of the DG in the distribution system may improve system reliability as a result of supplying loads in islanded operation. The islanded

operation implies that the load is disconnected from the substation and supplied from the DG until the utility restores the power from the main supply. The DG may not be able to supply the demand completely during the islanded mode. This is due to the availability and the capacity of the DG, especially when it depends on renewable resources. The DG also requires protection at the point of common coupling (PCC) between the utility grid and the DG facility to prevent any unintentional islanding. Generally, the DG cannot be islanded during interruptions with the external loads to the DG facility. This creates quality and safety problems to the utility in the maintenance and restoration processes. In most of the cases, load shedding is required in the local facility and only the critical loads are restored using the DG.

Analyzing the reliability of future distribution systems, including the DG, is different than analyzing the generation and transmission systems with large scale central units. The main difference is in the interaction between the generation units, the lines and components network, and the load points. In the future distribution system, higher penetration of the DG will be connected to the local load or at different points of the main feeder. The DG has a smaller capacity to load ratio than do the central generation units. This ratio can limit the availability of the DG to supply the demand during the interruptions since the probability of the load demand to be greater than the DG power output is high.

As shown in Fig. 6.1, during normal operation, the load is connected to the utility supply via the components and the feeders in the distribution network. If the distribution system connection fails to supply power to the load, the load is

supplied from the DG in an islanded operation. If the DG is a conventional backup unit, the DG is operated and connected to the load only during emergencies. If the DG unit is a renewable base load unit, it is continuously operated in parallel with the utility supply. But it has to be disconnected and reconnected again during interruptions.

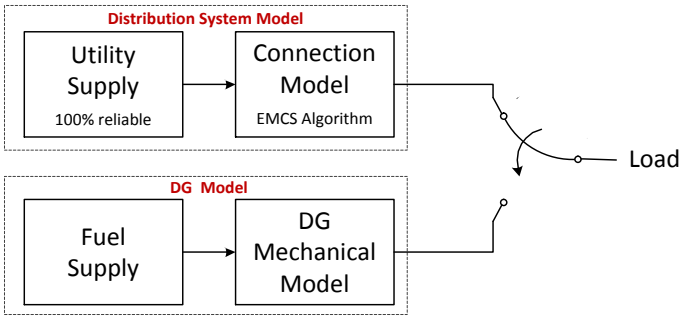

Fig. 6.1 Distribution connection system and DG system reliability models

The networked distribution system reliability analysis was covered in Chapters 3-5. The DG modeling, DG system adequacy analysis, and integrating the reliability of the DGs in future distribution systems will be covered in this chapter. The integration of the DG in the reliability evaluation of future distribution systems consists of three main phases: DG unit reliability modeling, DG islanded system adequacy assessment, and DG islanded system reliability integration. These three phases are shown in Fig. 6.2 and will be explained in Sections 6.3–6.5.

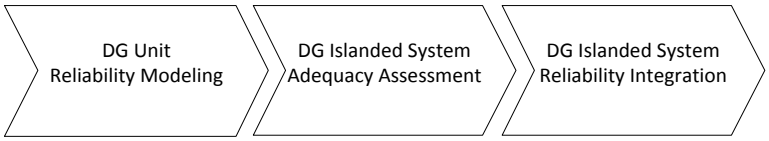

Fig. 6.2 The integration of the DG in the reliability evaluation

The reliability model of the DG unit is a logical and mathematical representation of the impact of different failure modes of the DG and fuel supply availability on the DG power output. The difference between the DG model of conventional and renewable units, from the reliability point of view, is that conventional units generate the rated power if they are operational, On the other hand, the output power of the renewable units is related to the primary energy source such as wind speed or solar radiation intensity, even if the unit is in a working state. In the DG islanded system, the DG may not be able to supply the local load due to the insufficiency of the generated power to match the demand or internal failure in the unit.

To integrate the DG islanded system's reliability into the distribution system reliability model, all the components (e.g., switches or protection devices) or failure modes that are related to the operation of the DG during interruptions should be incorporated into the DG reliability model. Then, a complete reliability model is proposed to evaluate the reliability of the distribution system including DG, compare different designs and different DG technologies from the reliability point of view, and optimize the size, number, and location of the DG units in the system.

6.3 DG Unit Reliability Modeling

In general, the DG unit reliability model consists of two main models: the fuel supply and the mechanical models. The fuel supply model represents the availability of the fuel supply to the unit during the study period. The mechanical

model represents the ability of the unit to operate successfully when it is needed without any failures.

6.3.1 Reliability Model for Conventional DG

In this research, the conventional DG unit is used as a backup generator that runs only during outages to supply the load and boost its reliability. The total operation cost of the DG is less than the expected outage cost of the load, but most likely higher than the main supply electricity price.

The fuel supply for the conventional generators (gas, diesel) is non-intermittent and assumed to be 100 % reliable. The mechanical model can be demonstrated by the two states model (up and down), where the up state represents the normal operation of the DG unit and the down state represents the failure of the unit to operate successfully. The conventional DG is assumed to have either full or zero capacity output. Fig. 6.3 shows the reliability model for the conventional DG.

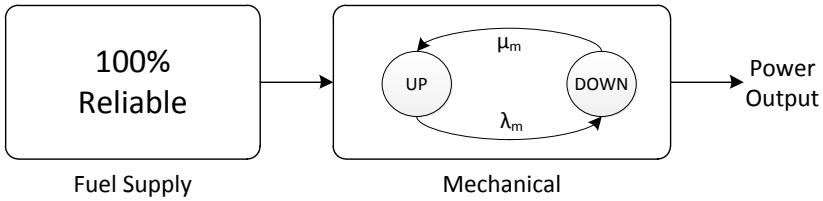

Fig. 6.3 Conventional DG reliability model

As shown in Fig. 6.4, the transition from the up state to the down state is known as the mechanical failure rate (λ_m), and the transition from the down state to the up state is the mechanical repair rate (μ_m). The transition from one state to

another is assumed to be exponentially distributed and the availability and unavailability of the DG conventional unit are given by:

$$A_{DG} = \frac{\mu_m}{\mu_m + \lambda_m} = \frac{MTTF_m}{MTTF_m + MTTR_m} \tag{6.1}$$

$$U_{DG} = \frac{\lambda_m}{\mu_m + \lambda_m} = \frac{MTTR_m}{MTTF_m + MTTR_m} \tag{6.2}$$

The unit unavailability is also known as forced outage rate (FOR). Based on this model, the DG is available with power output (P_{DG}) equal to its nominal power output only when there is no failure in the mechanical structure of the DG. The power output probability for the conventional DG is shown in Table 6.2, called the capacity probability table (CPT).

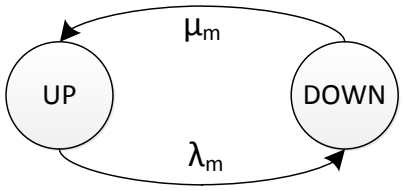

Fig. 6.4 Conventional DG mechanical model

Table 6.2 CPT for conventional DG unit

State		Power Output	Probability
1	Up	P_{DG}	A_{DG}
0	Down	0	$1 - A_{DG}$

6.3.2 Reliability Model for Renewable DG

The renewable DG is a time varying output source in which the output changes as the source availability changes. Because the primary energy source for

the renewable DG is intermittent, the power output characteristics of the wind and solar units are quite different from conventional units. The power output of these units depends on the stochastic nature and chronological variability of the natural primary source on top of the mechanical availability of the DG unit.

The solar and wind energy units are used as base load units and operated during the normal system operation to lower the electricity price. The cost of running these units is less than the price of electricity. These units can also be used as backup units if the DG power output is adequate enough to supply the load during the time of the outage. The renewable DG power and the load do not follow the same trend, and the emergency power demand is likely to be higher than the DG power output. In this case, the DG units would be disconnected from the islanded system.

In general, wind and solar unit modeling depends on the available historical data for each site. The historical wind speed for each site is used to predict the hourly data using a time series model such as auto-regressive and moving average model (ARMA) [67, 68]. The power output for each unit can be calculated based on the wind speed (or solar radiation) and by using the manufacturer's specifications and parameters such as cut-in wind speed, cut-out wind speed, rated wind speed, and rated power output of the wind turbine [69]. Likewise, photovoltaic (PV) power output is related to the locational insolation, and the temperature of the PV cells. The mechanical model of the renewable DG is similar to the conventional DG's mechanical model of the two states. The availability and unavailability of the mechanical unit are given in (6.1) and (6.2).

The objective of this research is not to evaluate the site's reliability but to study the influence of the DGs on the reliability study. The power output of actual wind and solar units is used in this research to study the impact of these units on the load and system reliability performance. The primary energy source (solar or wind) is intermittent, and Figs. 6.5 and 6.6 show the typical daily power output of the wind and solar units. Fig. 6.5 shows the average summer and winter PV power output for a site in Florida [70], and Fig. 6.6 shows the wind power output for different months of the year and the average output for a site in California [71]. The PV power output is more predictable than the wind power output since the wind speed is highly intermittent.

To model the renewable DG unit for the adequacy assessment, the annual per unit power output data for the renewable DG unit is used in the evaluation process. The first step is to arrange the per unit hourly DG power output in descending order, as shown in Fig. 6.7.

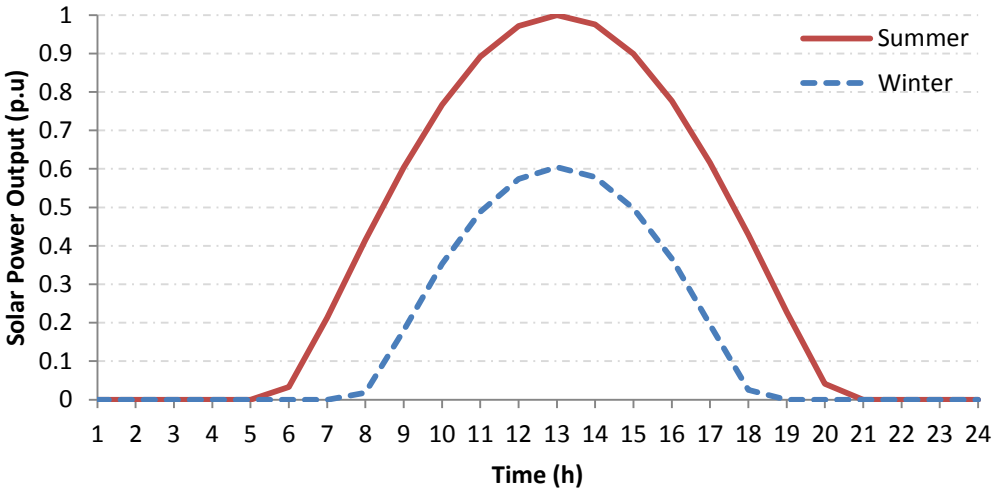

Fig. 6.5 PV power output average for the summer and winter

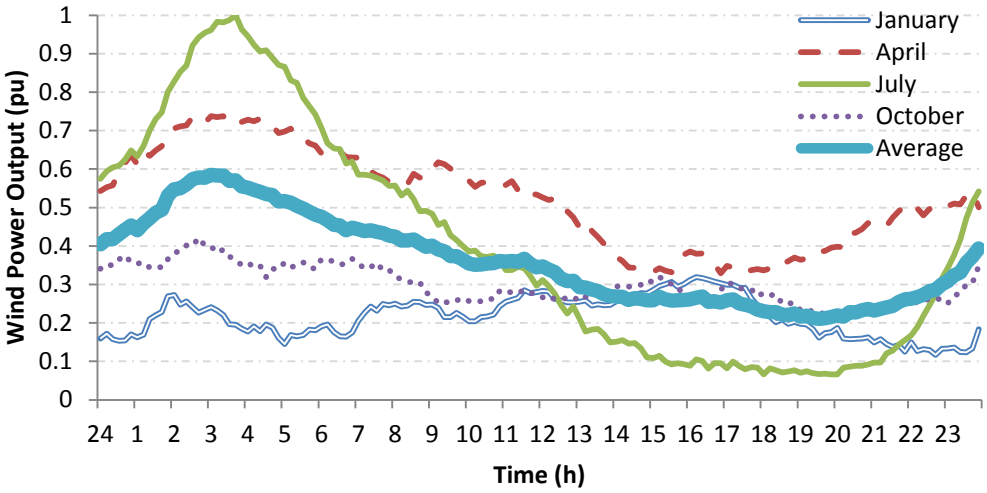

Fig. 6.6 Wind power output for different months in the year

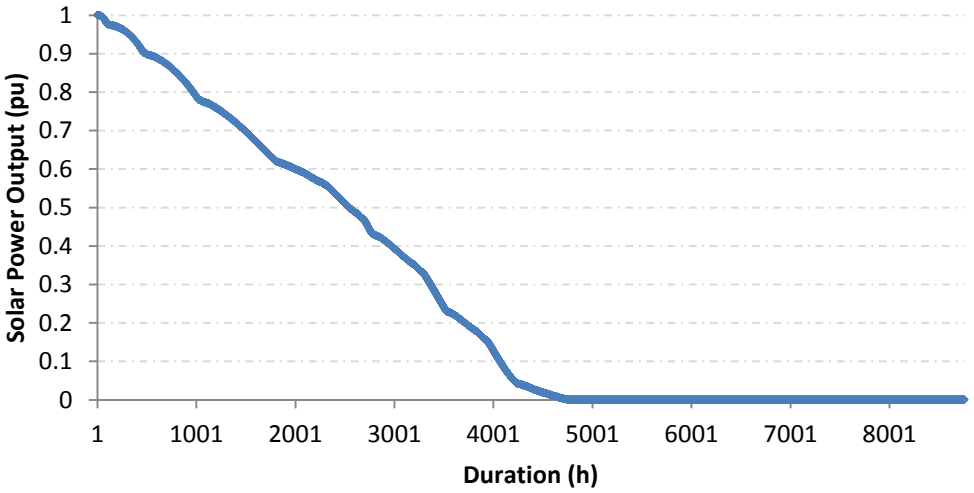

Fig. 6.7 Annual power output (in per unit) in descending order for the solar DG

All the hourly power outputs are classified based on the predefined number of segments (n). The total level count will be $n+1$, as shown in Fig. 6.8, where $n=10$ if the zero power output is considered as an independent level.

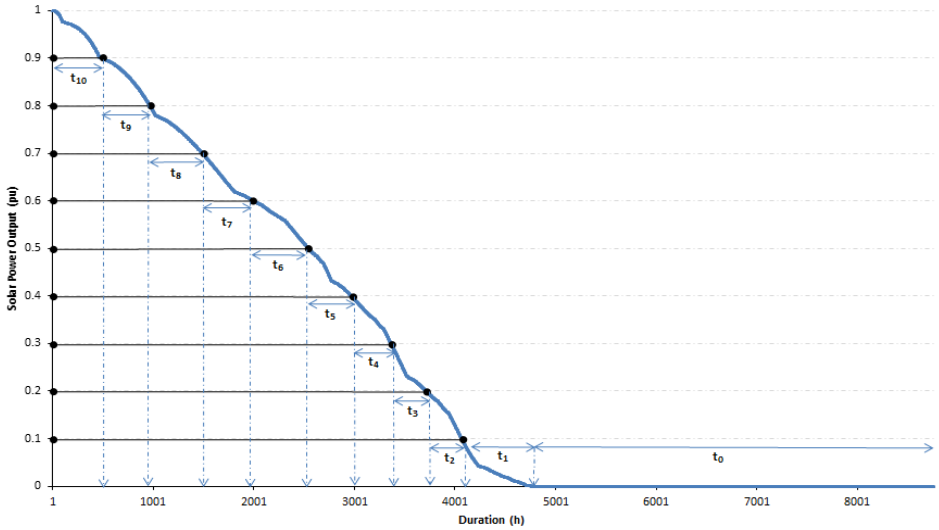

Fig. 6.8 Power output segments for the solar DG

The power output probability (or capacity probability) of the renewable DG units is related to the availability of the unit and the availability of the primary source, as shown in Table 6.3 (CPT). The DG power output will be zero if the primary energy source is completely absent or if the mechanical part of the unit is down [25]. The probability of each power output segment is calculated by dividing the annual time of each segment by the total annual hours (8760 h). The process of calculating the capacity probability for the renewable DG is briefly described as follows:

1- Arrange the hourly wind or solar power output curve in descending order.

2- Define the power output levels as segments of the rated power.

3- For each segment, measure the total time that the power output falls within the segment.

4- Divide the total time of each segment by the total number of hours in one year to calculate the probability of each segment.

5- Using the probability of each segment and the mechanical availability of the unit, calculate the capacity probability for each level.

Table 6.3 explains how the probability of each power segment is calculated. Fig. 6.9 shows the probability of each segment of the solar unit shown in Fig. 6.8, assuming that the unit is operating successfully. The capacity outage table (COT) can be created by using the probability of each level in the CPT. The COT shows outage capacity levels and the probability of their existence. For multiple units, the recursive algorithm is used to construct the COT by calculating the cumulative probability for all units in the system [41].

Table 6.3 CPT for renewable DG unit

States		Power Output	Capacity Outage	Probability
0	Down	0	100%	$A_{DG}\frac{t_0}{D}+U_{DG}$
1	Up (Derated)	ΔP_{DG}	$100\left(1-\frac{1}{N}\right)\%$	$A_{DG}\frac{t_1}{D}$
:	:	:	:	:
N	Up	$N\Delta P_{DG}$	0%	$A_{DG}\frac{t_N}{D}$

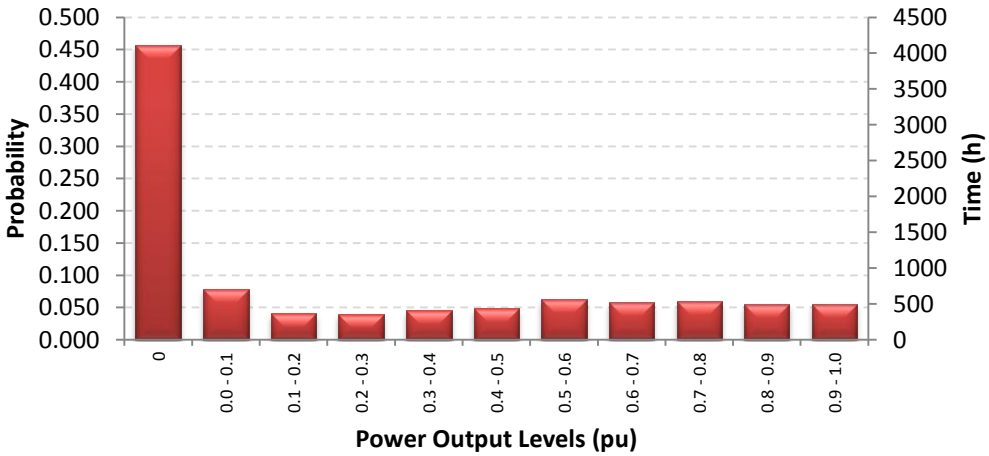

Fig. 6.9 Probability and time for each power output state for the solar DG

6.4 Adequacy Assessment of the DG Islanded System

6.4.1 Load Modeling

The load model is usually represented by either the daily peak load variation curve (DPLVC) or the load duration curve (LDC). The DPLVC is constructed by arranging the peak load data in descending order, and the LDC is formed by arranging the hourly load data in descending order. The LDC is more realistic and is used in this research to include any hourly and seasonal variation in the demand.

The chronological load models for different customer sectors used in this research are described and illustrated in [72, 73]. This load model simulates the hourly load behavior for seven different load sectors based on the type of the customer, the time of day, the day of the week, and the week of the year. The per unit hourly load can be determined using the following equation [74]:

$$L(t) = P_w P_d P_h(t) \tag{6.3}$$

where P_w is the percentage of weekly load in terms of the annual peak load, P_d is the percentage of the daily load in terms of the weekly peak load, and P_h is the percentage of the hourly load in terms of the daily peak. All the parameters are given in Appendix D.

In this research, residential, commercial, and industrial sectors were studied. Their daily load profiles for 24 hours and the weekly profiles are shown in Fig. 6.10 and 6.11, respectively.

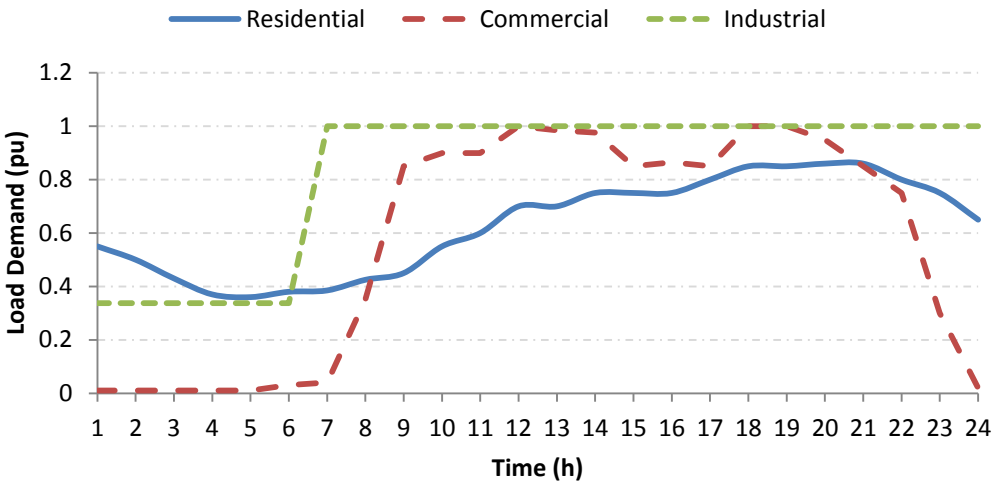

Fig. 6.10 Daily load profiles for the residential, commercial, and industrial customers

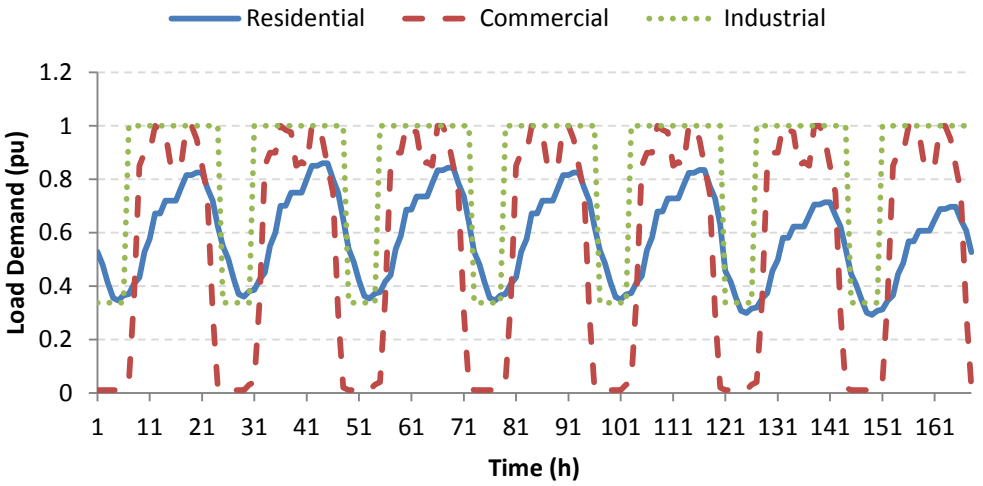

Fig. 6.11 Weekly load profiles for the residential, commercial, and industrial customers

The annual load duration curve can be developed using (6.3). As an example, the annual load curve for the residential load is shown in Fig. 6.12. The

demand probability table (DPT) of the load can be calculated in a similar fashion to how the CPT for renewable DGs was calculated.

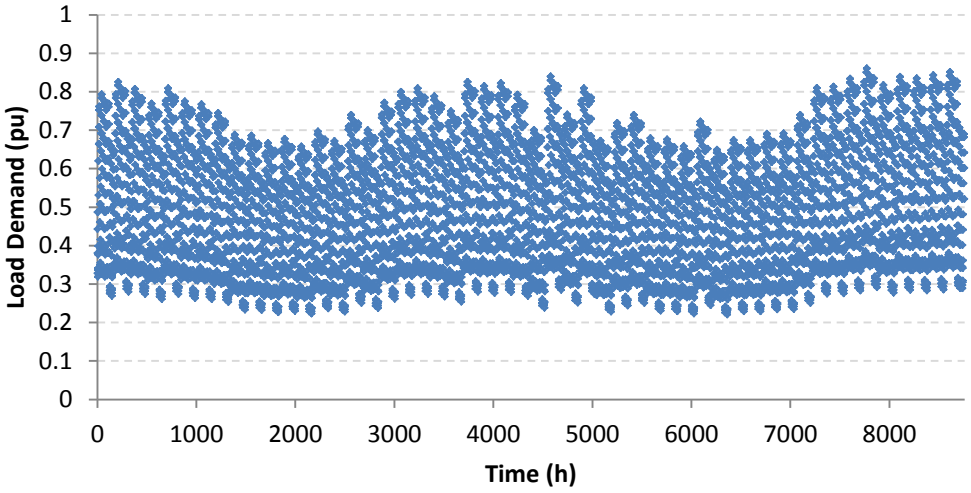

Fig. 6.12 Annual load curve for the residential customer

6.4.2 DG Islanded System Adequacy Assessment

The adequacy of the DG is commonly evaluated by convolving the time varying power output of the DG with the load duration curve to calculate the probability that the DG will supply the load demand. This adequacy analysis can be used to study the impact of the DG on the load and system reliability improvement during interruptions.

The reduction on reliability indices is related to the islanded probability, frequency, and duration as seen by each load. During interruptions, if the total DG available capacity is greater than the load demand, the DG will supply the load. If the load is greater than the generated power, the DG will be disconnected or the DG can supply a curtailed load (e.g., critical components). The annual per unit

power output for different DG units and the annual per unit load demand for different customer sectors are shown in Figs. 6.13 and 6.14, respectively.

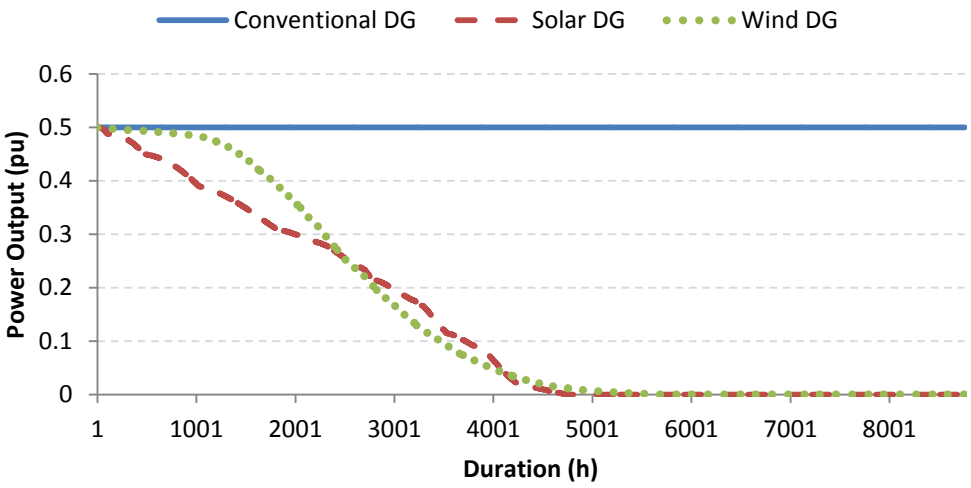

Fig. 6.13 Annual per unit power output for different DG technologies

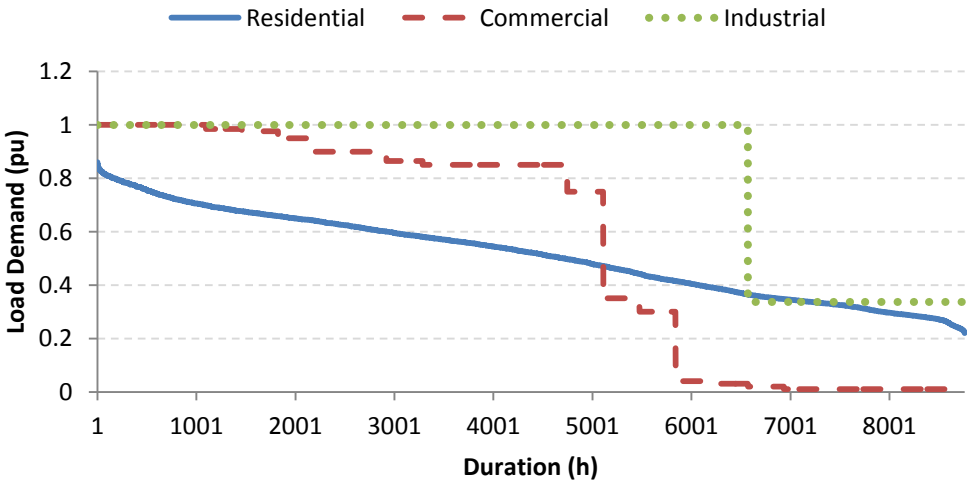

Fig. 6.14 Annual per unit load demand for different customers sectors

The most common indices used for adequacy assessment are: the loss of load expectation (LOLE), and the loss of load probability (LOLP). The LOLE is the expected number of hours per year during which the generated power is

insufficient to supply the demand. If the time used in calculating LOLE is per unit, this index is called LOLP.

The LOLP and LOLE for conventional and renewable DG are given by:

$$LOLP = P(Load > DG\ Capacity)$$

$$LOLP = \sum_{i=1}^{n} P_i \sum_{j=1}^{m} P(C_j < L_i) \tag{6.4}$$

$$LOLE = LOLP \times 8760\ \ h/y \tag{6.5}$$

where *n* and *m* are the total number of levels in DPT and CPT, respectively, P_i is the probability of the load level i, C_j is the DG capacity of the level j, and $P(C_j < L_i)$ is the probability that the capacity state j is less than load level i.

The adequacy indices are calculated by convolving the CPT of the DG with the DPT. Each power output or load segment is represented by the mean of all the data points in the segment. For each DG capacity level, the percentage of time for which the average demand is higher than the average generated power is used to calculate the LOLP.

The following steps summarize the procedure for evaluating the adequacy of the DG in supplying the load demand:

1- For both the DG and the load under study, the CPT and DPT are generated and the mean is computed for each segment to be used in the adequacy assessment.

2- For each DG power output segment in the CPT, the DPT is used to find the total time (or probability) for which the average load demand exceeds the average generated power for each segment.

3- The probability of each DG power output level is multiplied by the total time (or probability) found in step 2.

4- The cumulative sum of all the products in step 3 yields the LOLE (or LOLP).

Table 6.4 shows the CPT with the average generated power for each segment for three DG types: conventional, solar, and wind. The DG is assumed 100% reliable and the number of states (n) is 10 (excluding the zero power output level). The rated capacity ratio (RCR) for the conventional, solar, and wind DG is 0.5. As explained in (6.6), the rated capacity ratio is the ratio between the nameplate capacity of the DG and the annual peak demand.

$$RCR_{pu} = \frac{DG\ nameplate\ capacity}{Annual\ peak\ demand} \tag{6.6}$$

Table 6.5 demonstrates the DPT for the three types of customers (residential, commercial, and industrial). The residential annual peak demand occurs during a short period of time in the summer and winter and can be neglected from the DPT.

The LOLP for the three DG types (conventional, solar, and wind) and the three customers sectors (residential, commercial, and industrial) are shown in Table 6.6. The DG unit is assumed to be 100% reliable when it is needed. The smallest LOLP occurs when the residential customer installs a conventional DG to supply the local load. The largest LOLP occurs when a solar DG is used to supply the industrial load during interruptions.

Table 6.4 CPT for the conventional, solar, and wind DG (*n*=10)

State	Segment	Conventional DG (RCR=0.5)			Solar DG (RCR=0.5)			Wind DG (RCR=0.5)		
		Duration (h)	Average Power Output	Probability	Duration (h)	Average Power Output	Probability	Duration (h)	Average Power Output	Probability
0	0	0	0	0	4003	0.000	0.457	3068	0.000	0.350
1	0.0 - 0.1	0	0	0	1046	0.038	0.119	2226	0.028	0.254
2	0.1 - 0.2	0	0	0	743	0.151	0.085	662	0.146	0.076
3	0.2 - 0.3	0	0	0	973	0.255	0.111	510	0.247	0.058
4	0.3 - 0.4	0	0	0	1027	0.349	0.117	532	0.353	0.061
5	0.4 - 0.5	8760	0.5	1	968	0.455	0.111	1762	0.475	0.201
6	0.5 - 0.6	0	0	0	0	0.000	0.000	0	0.000	0.000
7	0.6 - 0.7	0	0	0	0	0.000	0.000	0	0.000	0.000
8	0.7 - 0.8	0	0	0	0	0.000	0.000	0	0.000	0.000
9	0.8 - 0.9	0	0	0	0	0.000	0.000	0	0.000	0.000
10	0.9 - 1	0	0	0	0	0.000	0.000	0	0.000	0.000

Table 6.5 DPT for the residential, commercial, industrial sectors (*n*=10)

State	Segment	Residential Customer			Commercial Customer			Industrial Customer		
		Duration (h)	Average Power Output	Probability	Duration (h)	Average Power Output	Probability	Duration (h)	Average Power Output	Probability
0	0	0	0.000	0.000	0	0.000	0.000	0	0.000	0.000
1	0.0 - 0.1	0	0.000	0.000	2920	0.017	0.333	0	0.000	0.000
2	0.1 - 0.2	0	0.000	0.000	0	0.000	0.000	0	0.000	0.000
3	0.2 - 0.3	837	0.276	0.096	365	0.300	0.042	0	0.000	0.000
4	0.3 - 0.4	1857	0.348	0.212	365	0.350	0.042	2190	0.337	0.250
5	0.4 - 0.5	1357	0.449	0.155	0	0.000	0.000	0	0.000	0.000
6	0.5 - 0.6	1793	0.553	0.205	0	0.000	0.000	0	0.000	0.000
7	0.6 - 0.7	1838	0.650	0.210	0	0.000	0.000	0	0.000	0.000
8	0.7 - 0.8	916	0.744	0.105	365	0.750	0.042	0	0.000	0.000
9	0.8 - 0.9	162	0.818	0.018	2555	0.866	0.292	0	0.000	0.000
10	0.9 - 1	0	0.000	0.000	2190	0.985	0.250	6570	1.000	0.750

Table 6.6 LOLP for the different DG units and customers in Tables 6.3 and 6.4

n=1000	Conventional (RCR=0.5)	Solar (RCR=0.5)	Wind (RCR=0.5)
Residential	0.5376	0.9128	0.8883
Commercial	0.5833	0.8049	0.7616
Industrial	0.7500	0.9431	0.9345

Fig. 6.15 demonstrates the impact of the RCR value on the LOLP of the residential, commercial, and industrial sites if a conventional DG is connected. In Fig. 6.16, the impact of the solar RCR on the LOLP is shown for different customers.

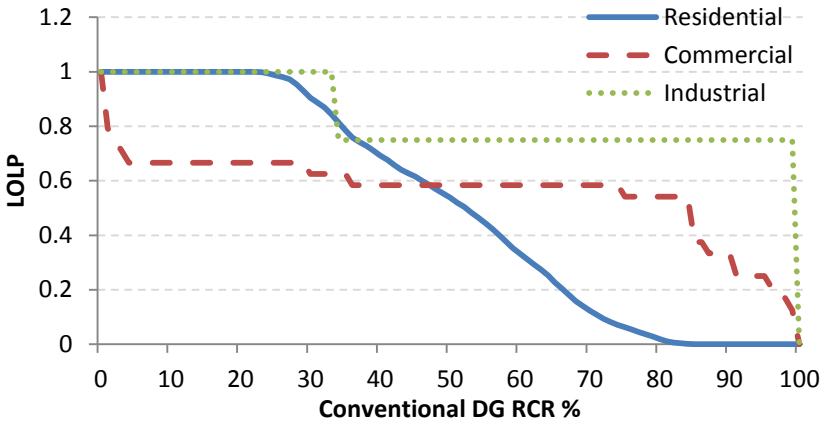

Fig. 6.15 LOLP for different conventional DG RCR and different load sectors

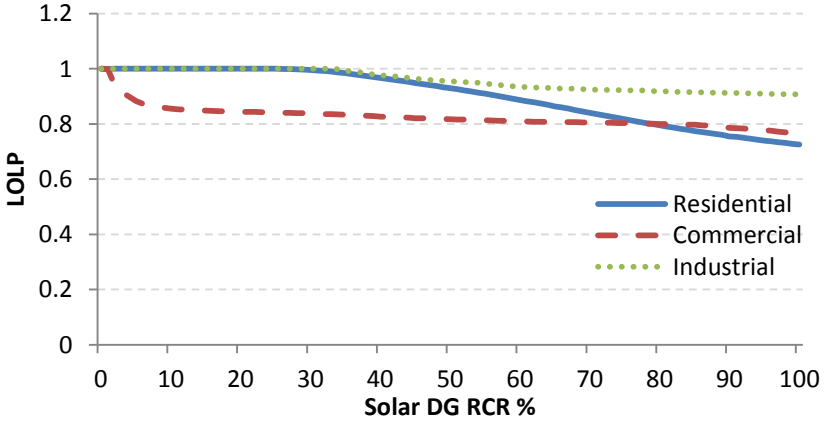

Fig. 6.16 LOLP for different solar DG RCR and different load sectors

6.5 DG Islanded System Reliability Integration

To evaluate the reliability of a networked distribution system including the DG, the DG and load models need to be integrated with the distribution system and its components. The load will receive the base load supply from the utility supply and the distribution connections. If the distribution system fails to supply the demand, the load will be disconnected from the distribution system and connected to the DG islanded system. The DG system model consists of the adequacy of the DG output power to supply the demand during the interruption, the DG mechanical operation, and the successful starting and switching the DG.

Successful DG starting and switching to disconnect the utility supply and connect the DG can be modeled as the probability to start and switch the DG when needed (P_{SS}) with a repair rate equal to (μ_{SS}). The starting and switching probability can be calculated as follows:

$$P_{ss} = \frac{Number\ of\ successful\ operations}{Total\ number\ of\ attempted\ operations}. \tag{5.7}$$

For the distribution system model in Fig. 6.17, the conditions under which the load experiences an interruption are:

- When the distribution connection system fails and the DG fails to start;
- When the distribution connection system fails and the switches fail to isolate the DG with the load;
- When the distribution connection system fails and the DG fails because of an internal mechanical failure; or

- When the distribution connection system fails and the DG power output is not adequate to supply the full demand.

When the DG is assumed to be 100% reliable and the probability to start and switch equal to one, the system can be modeled with the four states Markov model. Table 6.7 demonstrates the states and the status of each state, and Fig. 6.17 shows the state transition diagram (STD) and the state transition matrix (STM) for the distribution system model.

Table 6.7 Distribution system model states (DG is 100% reliable and P_{SS}=1)

State		DG Adequacy	Main Supply	Load Status
1	11	1	1	U
2	01	0	1	U
3	10	1	0	U
4	00	0	0	D

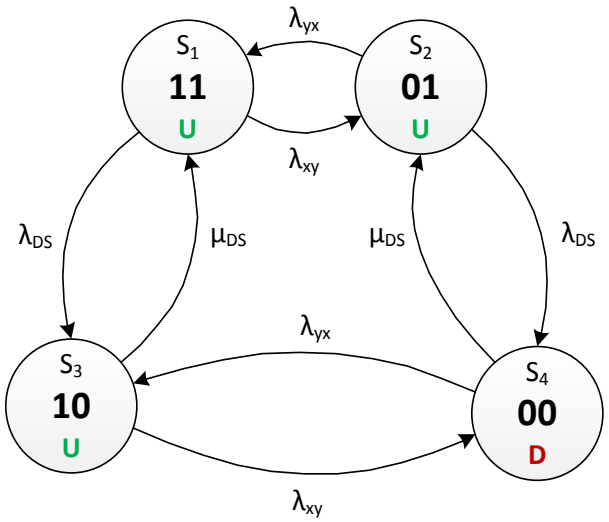

$$\sigma = \begin{bmatrix} 0 & \lambda_{xy} & \lambda_{DS} & 0 \\ \lambda_{yx} & 0 & 0 & \lambda_{DS} \\ \mu_{DS} & 0 & 0 & \lambda_{xy} \\ 0 & \mu_{DS} & \lambda_{yx} & 0 \end{bmatrix}$$

Fig. 6.17 STD and STM for the distribution system model (DG is 100% reliable and P_{SS}=1)

This model is suitable for both the conventional and renewable DG units in which the system will experience an outage only when the distribution connection system fails and the generated DG power is not adequate to fully supply the demand. The transition rate (λ_{DS}) is the failure rate of the distribution connection system from the EMCS analysis, and the repair rate (μ_{DS}) is the equivalent repair rate for each load to repair the fault in the system connection or its components.

As shown in Fig. 6.18, the transition (λ_{xy}) is the transition to move from a working state (x), where the DG power capacity is greater than the demand to a failing state (y), and where the load demand is greater than the generated DG power. Similarly, the transition (λ_{yx}) represents the transition of changing the states from the failing state (y) to the working state (x).

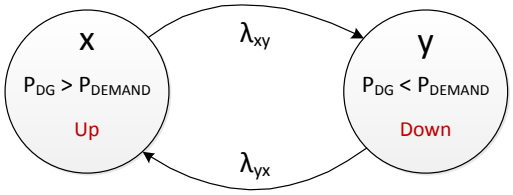

Fig. 6.18 Two states representation of the DG adequacy model

In general, the transition (λ_{xy}) can be computed as follows:

$$\lambda_{xy} = \frac{Number\ of\ observed\ transitions\ from\ x\ to\ y}{Total\ time\ spent\ in\ x} = \frac{N_{xy}}{D_x} \qquad (6.8)$$

For each load demand level (i), the transition (λ_{xy}^{i}) is calculated by counting the number of transitions from state x (where the DG power capacity is greater than the load demand) to state y (where the DG power capacity is less than the load demand). This number is then divided by the total time spent in state x.

The total transition rate (λ_{xy}) is calculated by multiplying each transition rate (λ_{xy}^{i}) for each load demand level (i) by the probability to stay in the level (i) as explained in (6.9) and (6.10),

$$\lambda_{xy} = \lambda_{xy}^{1} P_1 + \lambda_{xy}^{2} P_2 + \cdots + \lambda_{xy}^{n} P_n \tag{6.9}$$

$$\lambda_{xy} = \sum_{i=1}^{n} \lambda_{xy}^{i} P_i = \sum_{i=1}^{n} \frac{N_{xy}^{i}}{D_x^{i}} P_i. \tag{6.10}$$

The transition (λ_{yx}) is calculated using a similar method, as shown in (6.11) and (6.12),

$$\lambda_{yx} = \lambda_{yx}^{1} P_1 + \lambda_{yx}^{2} P_2 + \cdots + \lambda_{yx}^{n} P_n \tag{6.11}$$

$$\lambda_{yx} = \sum_{i=1}^{n} \lambda_{yx}^{i} P_i = \sum_{i=1}^{n} \frac{N_{yx}^{i}}{D_y^{i}} P_i. \tag{6.12}$$

The mean times to move from state *x* to state *y* or from state *y* to *x* are the reciprocals of λ_{xy} and λ_{yx} respectively. In Table 6.8, the transition rates (λ_{xy} and λ_{yx}) are calculated for the different combinations of the DG units and load customers.

Table 6.8 Adequacy transition rates and the mean time for each state

	DG (RCR=0.5)	$\boldsymbol{\lambda_{xy}}$	T_{xy}	$\boldsymbol{\lambda_{yx}}$	T_{xy}
Residential	Conventional	800.1	10.9	686.4	12.8
	Solar	1314.4	6.7	476.5	18.4
	Wind	929.8	9.4	374.6	23.4
Commercial	Conventional	876.0	10.0	625.7	14.0
	Solar	3025.0	2.9	388.9	22.5
	Wind	2099.8	4.2	445.5	19.7
Industrial	Conventional	1460.0	6.0	485.3	18.1
	Solar	6815.6	1.3	159.5	54.9
	Wind	6574.8	1.3	131.7	66.5

To integrate the DG mechanical failure into the model shown in Fig. 6.17, the model is modified to include the DG failure states. As shown in Table 6.9, the system has 8 states and it is down when the distribution main supply and the DG adequacy state are down or when the main supply and the DG mechanical part are in a state of failure.

Table 6.9 Distribution system model states (DG is not 100% reliable and P_{SS}=1)

State		DG failure	DG Adequacy	Main Supply	Load Status
1	111	1	1	1	U
2	101	1	0	1	U
3	011	0	1	1	U
4	001	0	0	1	U
5	110	1	1	0	U
6	100	1	0	0	D
7	010	0	1	0	D
8	000	0	0	0	D

Fig. 6.19 shows the STD and STM for the distribution system when the DG can fail due to a mechanical failure and P_{ss} is equal to one. The model shown in Fig. 6.19 is for the renewable DG units, where the DG is used as a base load unit to supply the load. This DG unit can fail mechanically at any time during the normal operation (the transitions from state 1 to 3 and from state 2 to 4). The only difference between the renewable and conventional DGs in the distribution system model is the DG failure during normal operation. In the conventional DG, there is no DG mechanical failure during normal system operation; the DG is used as a backup generator that operates only during outages. Therefore, there is no transition from state 1 to 3 or from state 2 to 4 when the conventional DG unit is considered in the analysis.

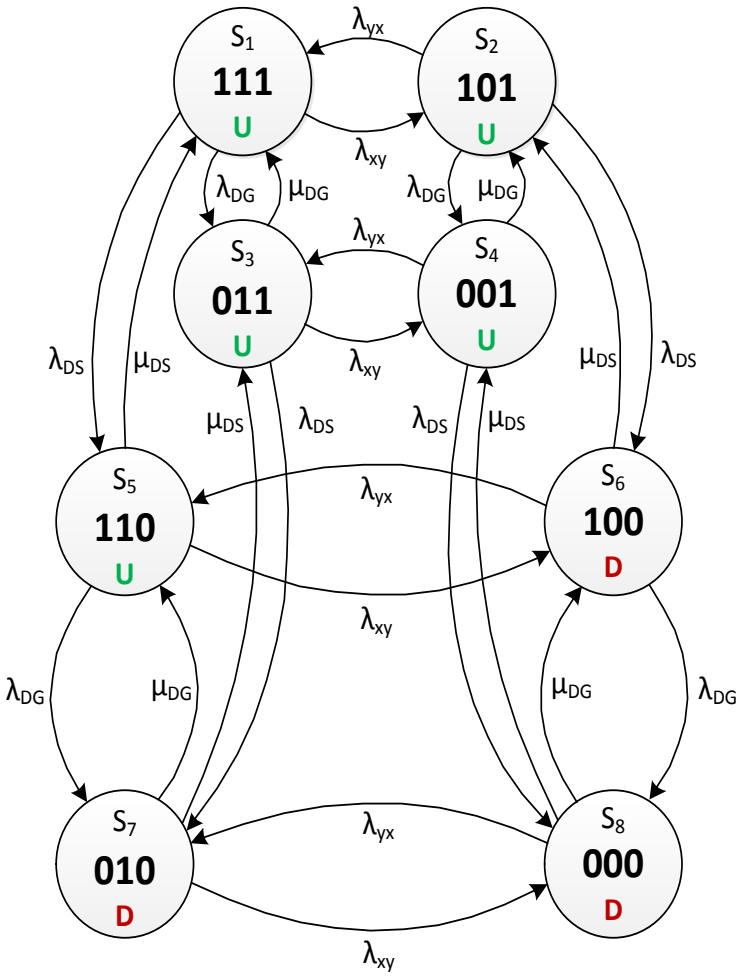

$$\sigma = \begin{bmatrix} 0 & \lambda_{xy} & \lambda_{DG} & 0 & \lambda_{DS} & 0 & 0 & 0 \\ \lambda_{yx} & 0 & 0 & \lambda_{DG} & 0 & \lambda_{DS} & 0 & 0 \\ \mu_{DG} & 0 & 0 & \lambda_{xy} & 0 & 0 & \lambda_{DS} & 0 \\ 0 & \mu_{DG} & \lambda_{yx} & 0 & 0 & 0 & 0 & \lambda_{DS} \\ \mu_{DS} & 0 & 0 & 0 & 0 & \lambda_{xy} & \lambda_{DG} & 0 \\ 0 & \mu_{DS} & 0 & 0 & \lambda_{yx} & 0 & 0 & \lambda_{DG} \\ 0 & 0 & \mu_{DS} & 0 & \mu_{DG} & 0 & 0 & \lambda_{xy} \\ 0 & 0 & 0 & \mu_{DS} & 0 & \mu_{DG} & \lambda_{yx} & 0 \end{bmatrix}$$

Fig. 6.19 STD and the STM for the distribution system model including renewable DG (DG is not 100% reliable and P_{SS}=1)

The last stage for the complete system model includes the probability of starting and switching the DG to the model as shown in Table 6.10. Some states in Table 6.10 (states 11–16) are considered unrealistic states and are removed from the state space.

In Fig. 6.20, the STD and STM are shown for the completed system model including the renewable DG. The system model including conventional DG will be similar to the model in Fig. 6.20, except that the transition from state 1 to 3 and state 2 to 4 will be zero.

Table 6.10 Distribution system model states (DG is not 100% reliable and $P_{SS} \neq 1$)

State		Starting/Switching	DG failure	DG Supply	Main Supply	Load Status
1	1111	1	1	1	1	U
2	1101	1	1	0	1	U
3	0011	0	0	1	1	U
4	0001	0	0	0	1	U
5	1110	1	1	1	0	U
6	1100	1	1	0	0	D
7	0010	0	0	1	0	D
8	0000	0	0	0	0	D
9	0110	0	1	1	0	D
10	0100	0	1	0	0	D
11	1011	1	0	1	1	X
12	1010	1	0	1	0	X
13	1001	1	0	0	1	X
14	1000	1	0	0	0	X
15	0111	0	1	1	1	X
16	0101	0	1	0	1	X

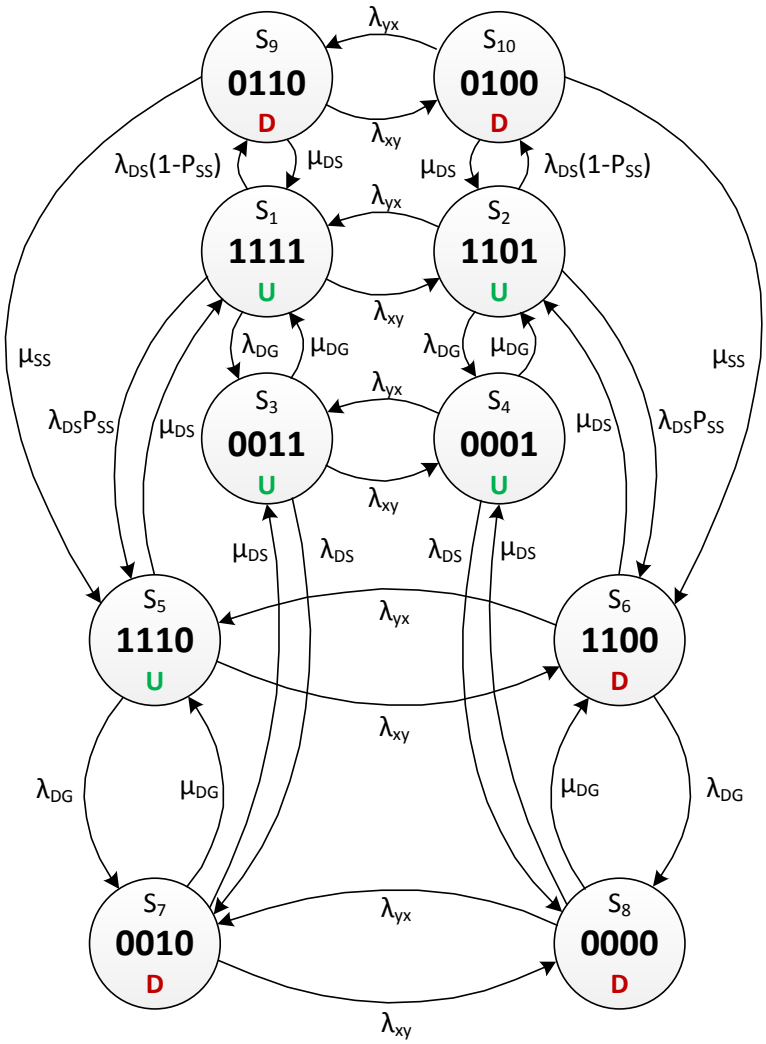

$$\sigma = \begin{bmatrix} 0 & \lambda_{xy} & \lambda_{DG} & 0 & \lambda_{DS}P_{SS} & 0 & 0 & 0 & \lambda_{DS}(1-P_{SS}) & 0 \\ \lambda_{yx} & 0 & 0 & \lambda_{DG} & 0 & \lambda_{DS}P_{SS} & 0 & 0 & 0 & \lambda_{DS}(1-P_{SS}) \\ \mu_{DG} & 0 & 0 & \lambda_{xy} & 0 & 0 & \lambda_{DS} & 0 & 0 & 0 \\ 0 & \mu_{DG} & \lambda_{yx} & 0 & 0 & 0 & 0 & \lambda_{DS} & 0 & 0 \\ \mu_{DS} & 0 & 0 & 0 & 0 & \lambda_{xy} & \lambda_{DG} & 0 & 0 & 0 \\ 0 & \mu_{DS} & 0 & 0 & \lambda_{yx} & 0 & 0 & \lambda_{DG} & 0 & 0 \\ 0 & 0 & \mu_{DS} & 0 & \mu_{DG} & 0 & 0 & \lambda_{xy} & 0 & 0 \\ 0 & 0 & 0 & \mu_{DS} & 0 & \mu_{DG} & \lambda_{yx} & 0 & 0 & 0 \\ \mu_{DS} & 0 & 0 & 0 & \mu_{SS} & 0 & 0 & 0 & 0 & \lambda_{xy} \\ 0 & \mu_{DS} & 0 & 0 & 0 & \mu_{SS} & 0 & 0 & \lambda_{yx} & 0 \end{bmatrix}$$

Fig. 6.20 STD and the STM for the distribution system model including renewable DG (DG is not 100% reliable and $P_{SS}\neq 1$)

6.6 Future Distribution System Reliability Analysis Including DG

The Bus 4 of the RBTS (shown in Fig. 5.2) is used to evaluate the reliability of the networked distribution system including DG. All the load points and their customer types and reliability data can be found in Appendix B. The small industrial users are assumed to have the same load model as the industrial load demonstrated in Section 6.3. The DG is connected at the load points (LP 1– LP 38), and the load duration curve at each load point is the aggregated load demand for all the customers connected to that bus. If the DG connected at load bus (x) cannot supply the full aggregated load demand, the DG will be disconnected from all customers connected to bus (x). The general flow diagram for the complete reliability analysis including DG is shown in Fig. 6.21.

The A, AIF, and AID for LP 1 are calculated using Markov model analysis. Different cases included in Table 6.20 where Case 0 is the original case without DG, Case 1 is the case where the DG is assumed to be 100 % reliable, and P_{SS} is unity (Fig. 6.17). Case 2 is the case where the DG can fail when it is needed and P_{SS} is unity (Fig. 6.19). Finally, Case 3 is the case where the DG can fail and the P_{SS} is not unity (Fig. 6.20). The RCR is considered to be 0.5 for all types of DGs and the distribution system failure rate and repair rate from the EMCS analysis are equal to 0.054 f/y and 148.11 r/y, respectively. The DG failure rate is considered to be 4 f/y for the conventional DG and 2 f/y for the solar and wind DG. The repair time is assumed to be 48 h. The probability to start and switch DG is assumed to be 0.95 with repair time equals to 12 h. To study the effect of different types of customers and DG units, the customers at LP 1 can be

either residential, commercial, or industrial and the DG type can be conventional, solar, or wind. The load reliability indices for LP 1 are shown in Table 6.11.

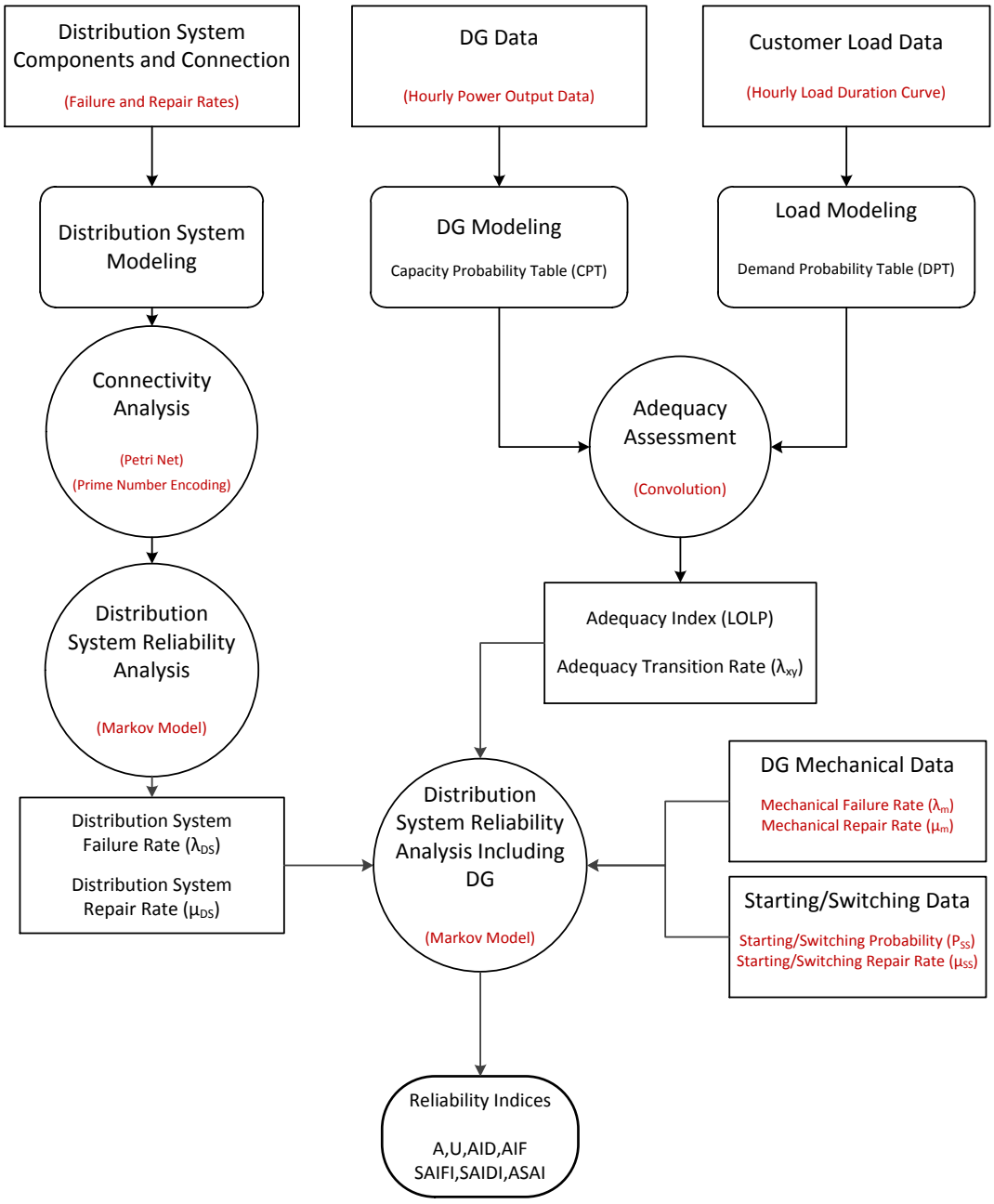

Fig, 6.21 Flow chart for the distribution system reliability analysis including DG

Table 6.11 Load reliability indices for LP 1 – RBTS Bus 4

		Residential			Commercial			Industrial		
		A	AIF (f/y)	AID (h/y)	A	AIF (f/y)	AID (h/y)	A	AIF (f/y)	AID (h/y)
Case 0 - No DG		0.999635	0.0540	3.1941	0.999635	0.0540	3.1940	0.999635	0.0540	3.1940
Case 1	Conventional	0.999804	0.1638	1.7191	0.999787	0.1646	1.8632	0.999726	0.1733	2.3971
	Solar	0.999732	0.1671	2.3442	0.999677	0.1735	2.8301	0.999644	0.1096	3.1209
	Wind	0.999740	0.1359	2.2767	0.999699	0.1786	2.6349	0.999643	0.1000	3.1312
Case 2	Conventional	0.999802	0.1628	1.7367	0.999785	0.1636	1.8791	0.999725	0.1721	2.4067
	Solar	0.999731	0.1661	2.3534	0.999676	0.1723	2.8341	0.999644	0.1090	3.1217
	Wind	0.999739	0.1352	2.2866	0.999699	0.1773	2.6410	0.999642	0.0995	3.1319
Case 3	Conventional	0.999800	0.1629	1.7490	0.999784	0.1636	1.8902	0.999725	0.1717	2.4133
	Solar	0.999731	0.1658	2.3604	0.999676	0.1715	2.8371	0.999644	0.1086	3.1223
	Wind	0.999738	0.1351	2.2942	0.999698	0.1767	2.6456	0.999642	0.0992	3.1324

Fig. 6.22 shows the AIF and AID percentage change from the original case when different DG units connected at LP 1 were the customers sector can be residential, commercial, or industrial. The AIF increases for all the DG types because of the increased frequency of changing the DG adequacy states. This change is due to the fluctuating weather conditions (or the load demand) during interruptions. On the other hand, the AID improves (decreases) and the maximum improvement for all the customer types occurs when the conventional type DG is connected.

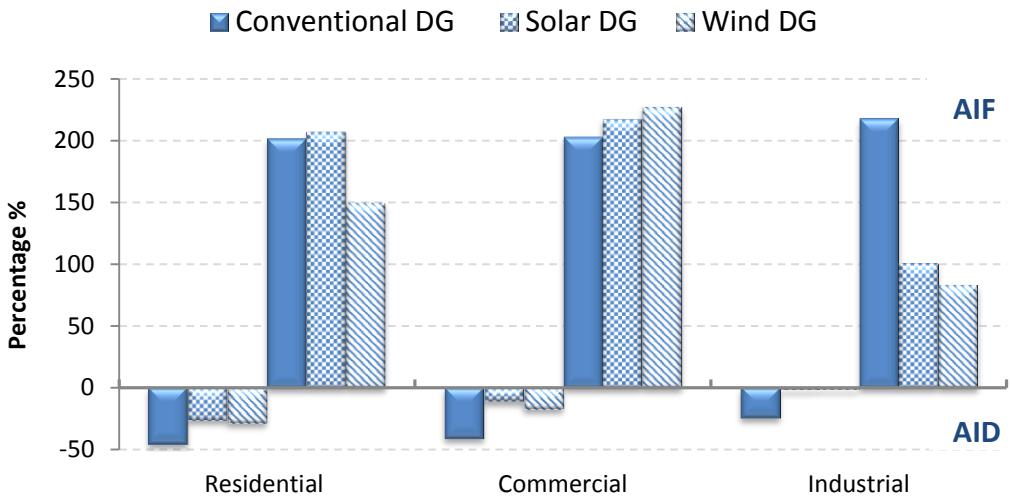

Fig. 6.22 AIF and AID percentage change when DG is connected at LP 1– RBTS Bus 4

In Table 6.12, the system reliability indices (SAIFI and SAIDI) are calculated when different types of loads and DGs are connected to LP 1. Fig. 6.23 shows that the maximum SAIFI increase of 9% occurs when the load is commercial and wind DG is installed at the load site. The lowest SAIFI increase of 3.4% occurs when the load is industrial and the DG is wind turbine. On the

other hand, SAIDI decreases by almost 2% when the conventional DG is connected at the residential load.

Table 6.12 System reliability indices – RBTS Bus 4

DG	Residential		Commercial		Industrial	
	SAIFI (f/c.y)	SAIDI (h/c.y)	SAIFI (f/c.y)	SAIDI (h/c.y)	SAIFI (f/c.y)	SAIDI (h/c.y)
No DG	0.0620	3.2261	0.0616	3.2261	0.0616	3.2261
Conventional	0.0670	3.1596	0.0666	3.1661	0.0670	3.1902
Solar	0.0667	3.1878	0.0670	3.2097	0.0641	3.2228
Wind	0.0653	3.1847	0.0672	3.2009	0.0636	3.2233

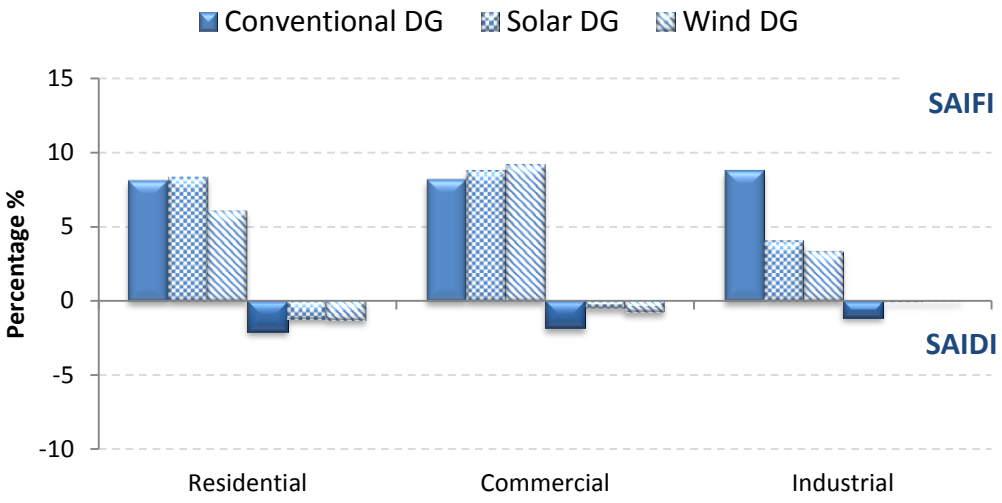

Fig. 6.23 SAIFI and SAIDI percentage change when DG is connected at LP 1– RBTS Bus 4

In Figs. 6.24 and 6.25, the reliability indices are calculated to study the effect of installing different DG units at each load point in the system. As shown in Fig. 6.24, SAIFI is improved when the DG unit is connected at the industrial sites. With the absence of the transformers in the calculation of the reliability at these sites, failure rates and repair times are decreased. Similarly, in Fig. 6.25, the

most improvement in SAIDI occurs when the DG units connected to the industrial sites.

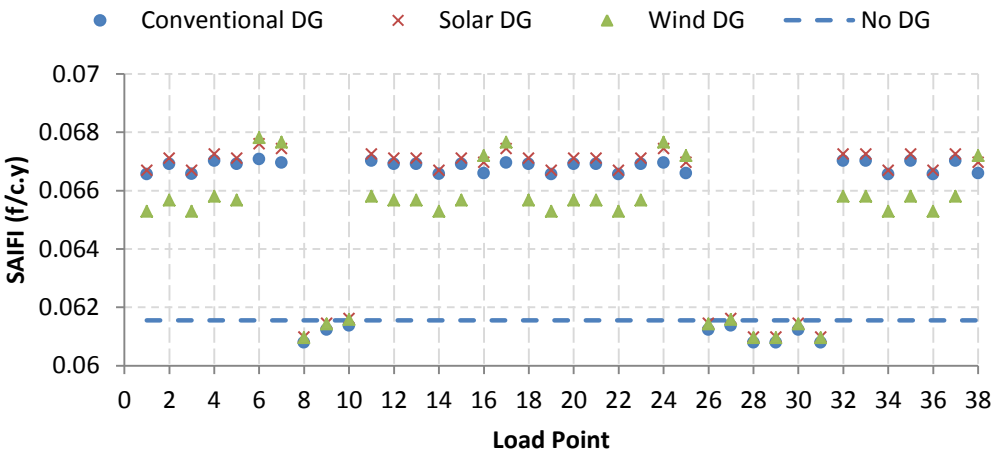

Fig. 6.24 SAIFI when DG unit is connected at each load point – RBTS Bus 4

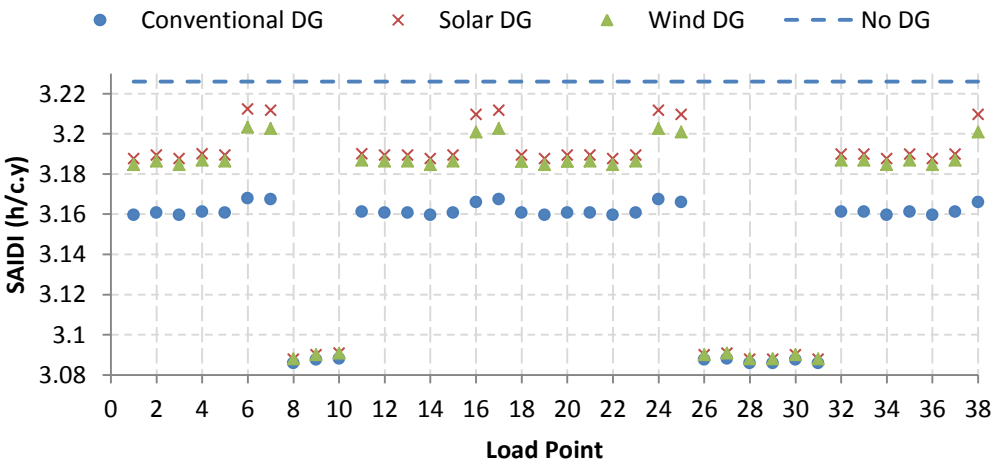

Fig. 6.25 SAIDI when DG unit is connected at each load point – RBTS Bus 4

In Figs. 6.26 and 6.27, the total RCR percentage of the DG in the system is varied and the system reliability indices are calculated. For each percentage level in Figs 6.26 and 6.27, one DG with RCR=0.5 is added by order to each load point in the system. The maximum system percentage is 50 % since the RCR for each DG is equal to 0.5.

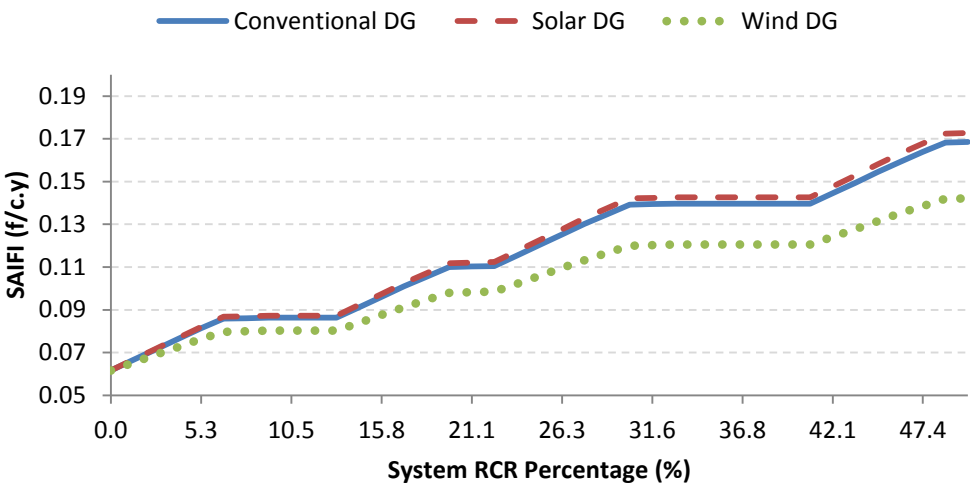

Fig. 6.26 SAIFI for different system RCR percentage levels – RBTS Bus 4

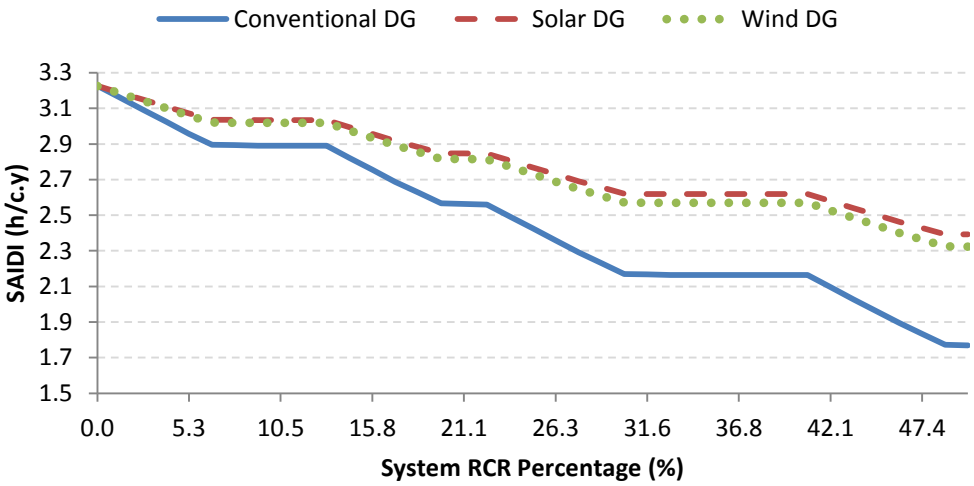

Fig. 6.27 SAIDI for different system RCR percentage levels – RBTS Bus 4

Chapter 7

CONCLUSIONS, CONTRIBUTIONS, AND FUTURE WORK

7.1 Conclusions and Contributions

The research work discussed in this report is concerned with the evaluation of the reliability of future networked distribution systems. The following main conclusions and contributions are presented in this thesis:

- An innovative analytical reliability analysis method has been developed and illustrated for a distribution system. The algorithm is termed the EMCS (encoded Markov cut set) algorithm.
- The reliability calculation is done in the design phase and is off-line; however, because of the combinatorial nature of the calculation, the calculation time is an important factor. Two concepts are used to automate the reliability calculation: Petri nets and prime number encoding, the main components of the EMCS algorithm. Petri nets and prime number encoding offer a consistent way to calculate system and load reliability. The Petri nets concept is used to identify the minimal tie sets of the networked distribution system. Prime number encoding is used to classify each remaining set in the state space as a tie set, cut set, or minimal cut set. Finally, the cut and tie sets are used to calculate the load and system reliability indices using Markov models.
- The size of the state space and the transition matrix used in the Markov models are proportional to the number of components in the system.

Different reduction and truncation techniques are used in this research to reduce the state space in each load point reliability computation. The proposed techniques reduced the number of states and transition matrix size without affecting computation accuracy.

- The advantage of using prime number encoding is the added flexibility and the speed to identify, locate, and extract the tie and cut sets from the set population.
- The method shown is algorithmic and does not introduce bias into the calculation of reliability; therefore, the method appears suitable for the evaluation of alternate designs of future distribution networks. The computation time improves when using the proposed algorithm. This is compared to a previous study [75] in which different Monte Carlo simulation techniques were used to evaluate the reliability of the RBTS. The reduction in computation time permits the analysis of a wider range of operating strategies and larger systems.
- The stochastic nature of the renewable DG power output and load demand is integrated successfully into the EMCS algorithm. This will make the EMCS capable of evaluating the networked distribution system including the renewable DGs. An adequacy transition rate is extracted from the DG annual power output data and the load duration curve that will be used in the Markov model analysis. The capacity probability table for the DG and demand probability table are computed and utilized in the DG adequacy assessment and distribution system model integration.

- The annual DG power output data for the conventional, solar, and wind DGs are used to generate the capacity probability table (CPT) in which the aggregated time, the probability, and the arithmetic average for each power output state are computed and used to assess DG adequacy. Similarly, the load duration curves for the residential, commercial, and industrial customers are used to generate the demand probability table (DPT). Different rated capacity ratios (RCRs) for different DG units and load sectors can be used to assess the impact of each DG unit and customer type on the reliability indices.
- The reliability evaluation of the networked distribution system is modified to account for the DG failure and repair rates, as well as the probability of starting and switching the DG islanding mode.
- For a single customer with DG, if the DG size supports the demand load and can be started successfully in a short time, the local load can experience shorter sustained interruption duration and may experience only momentary interruptions. The presence of the DG at the customer side may improve the load reliability indices as a result of supplying the load in the islanding mode operation. The system reliability indices might not be affected if the penetration of the DG in the system is very low.
- The DG may not be able to supply the load demand completely during interruptions. This is due to the availability and the rating capacity ratio (RCR) of the DG, especially if the DG is based on the intermittent renewable resources.

- The DG operating in islanding mode during outages can improve the interruption duration but can also lead to an increase in the interruption frequency. A renewable DG may perhaps increase the probability of experiencing inadequate power production due to the low capacity factor for the renewable based DG.
- The EMCS algorithm proposed in this research contributes to the reliability analysis of the future distribution systems including the conventional and renewable DGs. Case studies showed that the proposed algorithm can be a useful tool for distribution network planning and reconfiguration as it predicts the reliability performance of the system after any expansion and quantifies the impact of adding new components or DGs to the system.

7.2 Future Work

The following are recommendations for future work:

- Practical experience is needed including the application of these methods for real systems.
- An efficient approach needs to be developed to design (i.e., system planning) a distribution system to optimize the reliability indices under given constraints. The number and locations of new components needed to improve the reliability indices to specified values can then be identified and studied.

- Interruption devices should also be modeled and integrated into the proposed algorithm. Different failure modes for each interruption device in a distribution system should also be considered.
- Based on the future vision of the distribution intelligent network (microgrid), the DG is connected on the local load but allowed to supply other loads on the feeder. Alternatively, the DG is connected on the main feeder where it can supply group of loads during the interruption and restore the service to the customers as fast as possible. Evaluating the distribution system with smart restoration capability is a challenging issue, and the protection devices, switching time, restoration ranking techniques should be included in the study.
- The distribution system feeders and components are assumed to have sufficient capacity in this research. Including the capacity limits for the feeders in the system will require conducting a power flow study to validate the system states and make sure that the capacity of the system's feeders are not violated.
- An approach to classify and categorized the down states is another area of research. The down states can be classified based on the outage cost of each state, the time to repair, or frequency of occurrence of each state.
- The time correlation between the renewable DG power output and the load demand should be considered in the analysis. The influence of the time of the day can affect the adequacy of the DG to supply the load.

REFERENCES

[1] D. L. Beeman, R. H. Kaufmann, "The fundamentals of industrial distribution systems," *Transactions of the American Institute of Electrical Engineers*, Issue: 5, Volume: 61, May 1942, pp. 272-279.

[2] Peter Fox-Penner, *Smart Power: Climate Change, the Smart Grid, and the Future of Electric Utilities*, Island Press, 2005.

[3] G. T. Heydt "The next generation of power distribution systems," *IEEE Trans. Smart Grid*, vol. 1, no. 3, 2010, pp. 225-235.

[4] M. Hashmi, S. Hanninen, K. Maki, "Survey of smart grid concepts, architectures, and technological demonstrations worldwide," *IEEE PES Conference on Innovative Smart Grid Technologies (ISGT Latin America)*, 2011.

[5] P. M. Costa, M. A. Matos, "Reliability of distribution networks with microgrids," *IEEE in Power Tech, Russia*, 2005, pp. 1-7.

[6] I. S. Bae and J. O. Kim, "Reliability evaluation of customers in a microgrid," *IEEE Transactions on Power Systems*, vol. 23, 2008, pp. 1416-1422.

[7] M.G. Lauby, "Reliability considerations for application of smart grid technologies," *IEEE Power and Energy Society General Meeting*, 2010.

[8] R. E. Barlow, *Mathematical Reliability Theory: From the Beginning to the Present Time*, World Scientific, Singapore, vol. 7, 2002.

[9] IEEE, "IEEE standard computer dictionary: a compilation of IEEE standard computer glossaries," 1990.

[10] A. M. Leite da Silva, A. M. Cassula, R. Billinton, and L. A. F. Manso, "Integrated reliability evaluation of generation, transmission and distribution systems," *Proc. Inst. Elect. Eng. Gen. Transm. Distrib*., vol. 149, no. 1, 2002, pp. 1–6.

[11] R. L. Robinson, D. F. Hall, C. A. Warren, V. G. Werner, "Collecting and categorizing information related to electric power distribution interruption events: customer interruption data collection within the electric power distribution industry," *IEEE Power Engineering Society General Meeting*, October 2006.

[12] V. Werner, D. Hall, R. Robinson, C. Warren, "Collecting and categorizing information related to electric power distribution interruption events: data consistency and categorization for benchmarking surveys," *IEEE Trans. on Power Delivery*, v. 21, No. 1, Jan. 2006, pp. 480–483.

[13] S. Mandal, A. Pahwa, "Optimal selection of conductors for distribution feeders," *IEEE Trans. on Power Systems*, v. 17, No. 1, Feb. 2002, pp. 192–197.

[14] R. E. Brown, S. Gupta, R. D. Christie, S. S. Venkata, R. D. Fletcher, "Automated primary distribution system design: reliability and cost optimization," *IEEE Trans. on Power Delivery*, v. 12, no. 2, Apr. 1997, pp. 1017-1022.

[15] H. L. Willis, *Power Distribution Planning Reference Book*, New York, NY: Marcel Dekker, 1997.

[16] D. A. Kowalewski, "A comparable method for benchmarking the reliability performance of electric utilities," *Proc. IEEE Power Engineering Society Summer Power Meeting*, v. 2, July 2002, pp. 646–649.

[17] S. Knezevic, D. Skrlec, M. Skok, "The impact of reliability indices in the process of planning radial distribution networks," *Proc. International Conference on Using a Computer as a Tool EUROCON*, v. 2, Sept. 2003, pp. 244–248.

[18] N. Balijepalli, S. S. Venkata, R. D. Christie, "Modeling and analysis of distribution reliability indices," *IEEE Trans. on Power Delivery*, v. 19, No. 4, Oct. 2004, pp. 1950–1955.

[19] E. Carpaneto, A. Mosso, A. Ponta, E. Roggero, "Comparison of reliability and availability evaluation techniques for distribution network systems," *Proc. Annual Reliability and Maintainability Symposium*, Jan. 2002, pp. 563–568.

[20] H. Herath, V. Gosbell, S. Perera, "Power quality (PQ) survey reporting: discrete disturbance limits," *IEEE Trans. on Power Delivery*, v. 20, No. 2, April 2005, pp. 851-858.

[21] J. Horak, "Power quality: measurements of sags and interruptions," *Proc. IEEE Transmission and Distribution Conference*, May 2006, pp. 733–739.

[22] M. Al-Muhaini, G. T. Heydt, A. Huynh, "The reliability of power distribution systems as calculated using system theoretic concepts," *IEEE Power and Energy Society General Meeting*, July 2010.

[23] H. Brown, D. A. Haughton, G. T. Heydt, S. Suryanarayanan, "Some elements of design and operation of a smart distribution system," *IEEE PES Transmission and Distribution Conference and Exposition*, April 2010.

[24] A. A. Chowdhury, S. K. Agarwal, D. O. Koval, "Reliability modeling of distributed generation in conventional distribution systems planning and

analysis," *IEEE Transactions on Industry Applications*, v. 39, no. 5, 2003, pp. 1493–1498.

[25] S. Conti, R. Nicolosi, S. A. Rizzo, "Generalized systematic approach to assess distribution system reliability with renewable distributed generators and microgrids," *IEEE Transactions on Power Delivery*, v. 27, Jan. 2012, pp. 261–270,

[26] M. Fotuhi-Firuzabad, A. Rajabi-Ghahnavie, "An analytical method to consider DG impacts on distribution system reliability," *IEEE Transmission and Distribution Conference & Exhibition,* 2005.

[27] AC Nōto, M.G. Dajilva, "Impact of distributed generation on reliability evaluation of radial distribution systems under network constraints," *Proc. of 9th International Conference on Probabilistic Methods Applied to Power Systems*, June 11-15, 2006.

[28] Westinghouse Electric Corp., *The Westinghouse Transmission and Distribution Engineering Handbook*, E. Pittsburgh, PA, 1965.

[29] W. Kersting, *Distribution System Modeling and Analysis*, CRC Press, Boca Raton FL, 2002.

[30] R. Billinton, R. N. Allan, *Reliability Evaluation of Engineering Systems,* Plenum Press, New York, 1992.

[31] R. Ramakumar, *Engineering Reliability Fundamentals and Applications,* Prentice Hall, New Jersey, 1993.

[32] O. Shavuka, K. O. Awodele, S. P. Chowdhury, S. Chowdhury, "Application of predictive reliability analysis techniques in distribution networks," *45th International Universities Power Engineering Conference (UPEC)*, 2010.

[33] T. Gönen, *Electric Power Distribution System Engineering*, 2nd Edition, CRC Press, Boca Raton FL, 2008.

[34] R. Billinton, *Power System Reliability Evaluation*, Gordon and Breach, New York, 1974.

[35] R. Billinton, R. Ringlee, A. Wood, *Power System Reliability Calculations,* MIT Press, Cambridge MA, 1973.

[36] D. Midence, S. Rivera, A. Vargas, "Reliability assessment in power distribution networks by logical and matrix operations," *Proc. IEEE / PES Transmission and Distribution Conference and Exposition Latin America*, August 2008, pp. 1–6.

[37] J. Endrenyi, *Reliability Modeling in Electric Power Systems*, John Wiley & Sons, Toronto, 1978.

[38] Lee. Layton, "Electric System Reliability Indices," available at: http://www.l2eng.com/Reliability_Indices_for_Utilities.pdf.

[39] Joseph H. Eto, Kristina Hamachi LaCommare, "Tracking the Reliability of the U.S. Electric Power System: An Assessment of Publicly Available Information Reported to State Public Utility Commissions," LBNL-1092E report, October 2008.

[40] S. Asgarpoor, M. J. Mathine, "Reliability evaluation of distribution systems with non-exponential down times," *IEEE Trans. Power Syst*., v. 12, 1997, pp. 579-584.

[41] R. Billinton, R. Allan, *Reliability Evaluation of Power Systems*, Plenum Press, New York, 1996.

[42] R. Allan, I. Rondiris, D. Fryer, "An efficient computational technique for evaluating the cut tie sets and common cause failures of complex systems," *IEEE Trans. on Rel.*, v. R-30, 1981, pp. 101-109.

[43] G. B. Jasmon, K. W. Foong, "A method for evaluating all the minimal cuts of a graph," *IEEE Transactions on Reliability*, v. R-36, no. 5, December 1987.

[44] M. Al-Muhaini, G. T. Heydt, "A novel method for evaluating future power distribution system reliability," (*submitted) IEEE Transactions on Power Systems*, June 2012.

[45] A. Konak, "Combining network reductions and simulation to estimate network reliability," *Proceedings of the 2007 Winter Simulation Conference*, 2007, pp. 2301–2305.

[46] Ahmad R. Sharafat, Omid R. Ma'rouzi, "All-terminal network reliability using recursive truncation algorithm," *IEEE Transactions on Reliability*, 2009, pp. 338-347.

[47] M. Al-Muhaini, G. T. Heydt, "Minimal cut sets, Petri nets, and prime number encoding in distribution system reliability evaluation," *proceedings of the 2012 IEEE Power and Energy Society T&D conference*, May 2012.

[48] C. A. Petri, "Kommunikation mit Automaten," Bonn: Institut fur lnstrumentelle Mathematik, Schriften des IIM, Nr. 3, 1962. Also, English translation, "Communication with Auto- mata," New York: Griffiss Air Force Base.Tech. Rep. RADC- TR-65-377, v. 1, 1966.

[49] G. S. Hura, "Use of Petri Nets for System Reliability Evaluation," in *New Trends in Reliability Evaluation*, K. B. Misra, Ed. Amsterdam, Netherlands: Elsevier Science Publishers, pp. 339–368, 1992.

[50] T. Murata, "State equation, controllability, and maximal matchings of Petri nets," *IEEE Trans. Autom. Control*, vol. 22, 1977, p. 412.

[51] Liu Yong, C. Singh, "Reliability evaluation of composite power systems using Markov cut-set method," *IEEE Transaction on Power Systems*, v. 25, no. 2, 2010, pp. 777-785.

[52] C. Singh, "On the behavior of failure frequency bounds." *IEEE Transaction on Reliability*, vol. 26, no. 1, 1977, pp. 63–66.

[53] M. Al-Muhaini, G. T. Heydt, "An algorithm for reliability bounds evaluation for power distribution system," (*submitted) Kuwait Journal of Science and Engineering*, May 2012.

[54] R. N. Allan, R. Billinton, I. Sjariej, L. Goel, K. S. So, "Reliability test system for education purposes - basic distribution system dates and results," *IEEE Transactions on Power Systems*, v. 6, n. 2, May 1991.

[55] IEEE Standard 1366-2003, "Guide for Electric Power Distribution Reliability Indices," Piscataway NJ, March 2003.

[56] G. Pepermans, J. Driesen, D. Haeseldonckx, W. D'haeseleer, and R. Belmans, "Distributed Generation: Definition, Benefits and Issues," Katholieke Universiteit Leuven, 19 August 2003.

[57] W. El-Khattam, M. M. Salama, "Distributed generation technologies, definitions and benefits," *Electric Power Systems Research,* v. 71, Oct. 2004, pp. 119-128.

[58] M. Werven, M. Scheepers, "Dispower - the changing role of energy suppliers and distribution system operators in the deployment of distributed generation in liberalised electricity markets," Ecn Report Ecn-C--05-048, NL, 2005.

[59] A. Chambers, *Distributed Generation: A Nontechnical Guide*, Pennwell, Tulsa, OK, P. 283.

[60] R. Ramakumar, P. Chiradeja, "Distributed generation and renewable energy systems," *Proc. IEEE Energy Conversion Engineering Conf.*, 2002, pp. 716-724.

[61] An Arthur D. Little, *Distributed Generation: System Interfaces*, White Paper, Arthur D. Little Inc., 1999.

[62] S. Häggmark, V. Neimane, Axelsson, *et al*, "Aspects of different distributed generation technologies," CDOGUnet WP 3, Vattenfall Utveckling Ab, 2003.

[63] P. P. Barker, R. W. de Mello, "Determining the impact of distributed generation on power systems: part 1- radial distribution systems," *Proc. IEEE PES Summer Meeting*, v. 3, 2000, pp. 1645-1656.

[64] T. E. McDermott, R. C. Dugan, "PQ, reliability and DG", *IEEE Ind. Appl. Mag.*, vol. 9, no. 5, 2003, pp. 17-23.

[65] R. E. Brown, L. A. Freeman, "Analyzing the reliability impact of distributed generation," *Proceedings of the IEEE Summer Meeting*, July 2001, pp. 1013-1018.

[66] E. Vidya Sagar, P. V. N. Prasad, "Impact of DG on radial distribution system reliability," *Fifteenth National Power Systems Conference (NPSC)*, IIT Bombay, December 2008.

[67] R. Billinton, Bagen, "A sequential simulation method for the generating capacity adequacy evaluation of small stand-alone wind energy conversion systems," *Proc. IEEE Can. Conf. Electrical and Computer Engineering-CCECE 2002*, v. 1, 2002, pp. 72.

[68] R. Billinton, H. Chen, R. Ghajar, "Time-series models for reliability evaluation of power systems including wind energy" *Microelectronics and Reliability*, v. 36, 1996, pp. 1253-61.

[69] R. Karki, R. Billinton, "Cost-effective wind energy utilization for reliable power supply," *IEEE Transactions on Energy Conversion*, v. 19, 2004, pp. 435-440.

[70] National Renewable Energy Laboratory (NREL), The 1991- 2005 National Solar Radiation Data Base (NSRDB), available at: http://www.ncdc.noaa.gov/oa/reds/index.html#nsrdb

[71] National Renewable Energy Laboratory (NREL), Western Wind Dataset, available at: http://www.nrel.gov/wind/integrationdatasets/

[72] A. Jonnavithula, "Composite system reliability evaluation using sequential Monte Carlo simulation," Ph. D. Thesis, University of Saskatchewan, 1997.

[73] A. Sankarakrishnan, R. Billinton, "Sequential Monte Carlo simulation for composite power system reliability analysis with time varying loads," *IEEE Transactions on Power Systems*, v. 10, no. 3, August 1995, pp. 1540-1545.

[74] P. Wang, R. Billinton, "Time sequential distribution system reliability worth analysis considering time varying load and cost models," *IEEE Transactions on Power Delivery*, v.14, no. 3, Jul 1999, pp. 1046-1051.

[75] G. T. Heydt, T. J. Graf, "Distribution system reliability evaluation using enhanced samples in a Monte Carlo approach," *IEEE Transactions on Power Systems*, v. 25, No. 4, November 2010, pp. 2006–2008.

APPENDIX A

ALTERNATIVE MEASURES OF DISTRIBUTION SYSTEM RELIABILITY

The most common reliability indices used in distribution systems are SAIDI and SAIFI. They reflect the reliability of the system in terms of the frequency and duration of sustained interruptions. The Customer average interruption duration index (CAIDI) is also used to evaluate the average response time of each utility to clear the fault and restore the service to each customer. Other indices that can be used to evaluate the reliability performance of the distribution system may include [39]:

- Customer average interruption duration index (CAIDI)
- Average service availability index (ASAI)
- Average service unavailability index (ASUI)
- Energy not supplied (ENS) (also termed 'energy unserved')

These indices may not be as widespread in use for utilities and customers as SAIFI, SAIDI and CAIDI, but they can be useful measures in some complex systems and specific applications. CAIDI is the average duration of each interruption seen by each interrupted customer. CAIDI captures the average time that the utility responds by measuring the average time to restore service. The difference between SAIDI and CAIDI is that in SAIDI the total duration of all interruptions averaged by the total number of customers connected to the system. CAIDI, on the other hand, is only averaged by the customers interrupted in each outage event.

$$CAIDI = \frac{Sum\ of\ all\ customer\ interruptions\ durations}{Total\ number\ of\ customer\ interruptions} = \frac{SAIDI}{SAIFI} \qquad (A.1)$$

The ASAI is the measure of service availability during a given period. It is calculated by dividing the number of hours when service available to the customers by the total number of demand hours for all customers.

$$ASAI = \frac{Total\ number\ of\ hours\ availability}{Total\ demand\ hours}$$

$$ASAI = \frac{8760 - SAIDI}{8760} \tag{A.2}$$

Similarly, ASUI can be calculated from the ASAI,

$$ASUI = \frac{Total\ number\ of\ hours\ unavailability}{Total\ demand\ hours}$$

$$ASUI = 1 - ASAI = \frac{SAIDI}{8760} \tag{A.3}$$

To report the total energy not supplied by the system during the outages, ENS can be used and calculated as,

$$ENS = Total\ energy\ not\ supplied$$

$$ENS = \sum P_{avg,i} AID_i \tag{A.4}$$

where P_{avg} can be calculated as,

$$P_{avg} = \frac{Total\ annual\ energy\ demanded}{8760} \tag{A.5}$$

APPENDIX B

RBTS RELIABILITY DATA

Tables B.1 – B.6 document the system data for the RBTS [58].

Table B.1 Lines reliability data – RBTS Bus 2

Section number	Length (km)	Overhead Lines			Underground Cables		
		Failure rate (f/y)	Repair rate (r/y)	Repair Time (h)	Failure rate (f/y)	Repair rate (r/y)	Repair Time (h)
2, 6, 10, 14, 17, 21, 25, 28, 30, 34	0.60	0.03900	1752	5	0.024	292	30
1, 4, 7, 9, 12, 16, 19, 22, 24, 27, 29, 32, 35	0.75	0.04875	1752	5	0.030	292	30
3, 5, 8, 11, 13, 15, 18, 20, 23, 26, 31, 33, 36	0.80	0.05200	1752	5	0.032	292	30

Table B.2 Transformers reliability data – RBTS Bus 2

Component	Type	Failure Rate (f/y)	Repair Rate (r/y)	Repair time (h)	Replacing Rate (r/y)	Replacing time (h)
37-56	11/0.415	0.015	43.8	200	876	10

Table B.3 Load data – RBTS Bus 2

Loads	Feeder	Type	Average load (MW)	Peak Load (MW)	Number of customers
1	F1	Residential	0.535	0.8668	210
2	F1	Residential	0.535	0.8668	210
3	F1	Residential	0.535	0.8668	210
4	F1	Gov/Inst	0.566	0.9167	1
5	F1	Gov/Inst	0.566	0.9167	1
6	F1	Commercial	0.454	0.75	10
7	F1	Commercial	0.454	0.75	10
8	F2	Small user	1	1.6279	1
9	F2	Small user	1.15	1.8721	1
10	F3	Residential	0.535	0.8668	210
11	F3	Residential	0.535	0.8668	210
12	F3	Residential	0.45	0.7291	200
13	F3	Gov/Inst	0.566	0.9167	1
14	F3	Gov/Inst	0.566	0.9167	1
15	F3	Commercial	0.454	0.75	10
16	F4	Commercial	0.454	0.75	10
17	F4	Residential	0.45	0.7291	200
18	F4	Residential	0.45	0.7291	200
19	F4	Residential	0.45	0.7291	200
20	F4	Gov/Inst	0.566	0.9167	1
21	F4	Gov/Inst	0.566	0.9167	1
22	F4	Commercial	0.454	0.75	10

Table B.4 Transformers reliability data – RBTS Bus 4

Type	Voltage level (kV)	Failure Rate (f/y)	Repair Rate (r/y)	Repair time (h)	Replacing Rate (r/y)	Replacing time (h)
Transformers	33/11	0.015	-	-	584	15
	11/0.415	0.015	43.8	200	876	10

Table B.5 Lines reliability data – RBTS Bus 4

Section	Voltage level (kV)	Length (km)	Overhead Lines			Underground Cables		
			Failure rate (f/y)	Repair rate (r/y)	Repair Time (h)	Failure rate (f/y)	Repair rate (r/y)	Repair Time (h)
2, 6, 10, 14, 17, 21, 25, 28, 30, 34, 38, 41, 43, 46, 49, 51, 55, 58, 61, 64, 67	11	0.60	0.03900	1752	5	0.024	292	30
1, 4, 7, 9, 12, 16, 19, 22, 24, 27, 29, 32, 35, 37, 40, 42, 45, 48, 50, 53, 56, 60, 63, 65	11	0.75	0.04875	1752	5	0.030	292	30
3, 5, 8, 11, 13, 15, 18, 20, 23, 26, 31, 33, 36, 39, 44, 47, 52, 54, 57, 59, 62, 66	11	0.80	0.05200	1752	5	0.032	292	30
68, 69	33	15	0.69	1095	8	-	-	-
70, 71	33	10	0.46	1095	8	-	-	-

Table B.6 Load data – RBTS Bus 4

Loads	Feeder	Type	Average load (MW)	Peak Load (MW)	Number of customers
1	F1	Residential	0.545	0.8869	220
2	F1	Residential	0.545	0.8869	220
3	F1	Residential	0.545	0.8869	220
4	F1	Residential	0.545	0.8869	220
5	F1	Residential	0.500	0.8137	200
6	F1	Commercial	0.415	0.6714	10
7	F1	Commercial	0.415	0.6714	10
8	F2	Small user	1	1.63	1
9	F2	Small user	1.5	2.445	1
10	F2	Small user	1	1.63	1
11	F3	Residential	0.545	0.8869	220
12	F3	Residential	0.545	0.8869	220
13	F3	Residential	0.545	0.8869	220
14	F3	Residential	0.500	0.8137	200
15	F3	Residential	0.500	0.8137	200
16	F3	Commercial	0.415	0.6714	10
17	F3	Commercial	0.415	0.6714	10
18	F4	Residential	0.545	0.8869	220
19	F4	Residential	0.545	0.8869	220
20	F4	Residential	0.545	0.8869	220
21	F4	Residential	0.545	0.8869	220
22	F4	Residential	0.500	0.8137	200
23	F4	Residential	0.500	0.8137	200
24	F4	Commercial	0.415	0.6714	10
25	F4	Commercial	0.415	0.6714	10
26	F5	Small user	1	1.63	1
27	F5	Small user	1	1.63	1
28	F5	Small user	1	1.63	1
29	F6	Small user	1	1.63	1
30	F6	Small user	1	1.63	1
31	F6	Small user	1.5	2.445	1
32	F7	Residential	0.545	0.8869	220
33	F7	Residential	0.545	0.8869	220
34	F7	Residential	0.545	0.8869	220
35	F7	Residential	0.545	0.8869	220
36	F7	Residential	0.500	0.8137	200
37	F7	Residential	0.500	0.8137	200
38	F1	Commercial	0.415	0.6714	10

APPENDIX C

SAMPLE MATLAB CODE

```
%%%%%%%%%%%%%%%% THE MAIN PROGRAM %%%%%%%%%%%%%%%%%%%%%%%%%%%%%%

%% PROGRAM USES SUB-ROUTINES TO EVALUATE THE DISTRIBUTION SYSTEM
RELIABILITY USING EMCS ALGORITHM.

%%THE SUB-ROUTINES INCLUDE:
%%REDUCTION TECHNIQUES
%%PRIME NUMBER ENCODING
%%CREATING MASTER LIST
%%FINDING TIE SETS USING PETRI NETS CONCEPT
%%FINDING CUT SETS USING PRIME NUMBER ENCODING
%%BUILDING THE MARKOV TRANSITION MATRIX
%%BUILDING Q-MATRIX AND P-MATRIX
%%CALCULATING MTTF
%%CALCULATING THE STEADY STATE PROBABILITIES
%%CALCULATING THE LOAD INDICES

%% AUTHOR: ALMUHAINI, MOHAMMAD
%% REFERENCE: PhD DISSERTATION
%% DATE: AUGUST 2012

%%%%%%%%%%%%%%%%%%%%%%%%%%%%%%%%%%%%%%%%%%%%%%%%%%%%%%%%%%%%%%%%%%%

clear; clc

[A1, LL, LLL, FRR, RRR, NumberOfCustomers,AveragePower] =
inputRBTSBUS2;
maxcutset=3;
glimit=5;
ss=primes(100);

for loads=1:length(LL)

clearvars -except A1 RRR FRR AveragePower NumberOfCustomers vaa
maxcutset states nodes lines ss glimit Availability
Unavailability MeanTimeToFailure Frequency TotalFrequency
NumberOfNodes NumberOfLines NumberOfStates MasterList CutSets LL
LLL FailureRate loads
A=A1;
FR=FRR; RR=RRR;
L=LL(loads);
s=size(A);
x=s(1,2); xx=s(1,1);
M=zeros(xx,1);
M(1,1)=1;M(L,1)=1;

%%REDUCTION TECHNIQUES
[A,L,M] = loadsred(A,LLL,L,M);
A=sparse(A);
s=size(A);
x=s(1,2); xx=s(1,1);
va=zeros(3,x);
va(1,:)=1:x;
va(2,:)=1:x;
```

```
xxz=x;
[M, A,x,xx,RR,FR,L, va,nodes,lines, states] = reduction2(A,RR,FR,
M,L, xxz, va,nodes,lines, states,loads);

%%PRIME NUMBER ENCODING
xx2=1:x;
aa=(2^x);
[ng, gul, sss, sss2,l1]= primeindex(x,ss,glimit);

%%CREATING MASTER LIST
[eeeee, eee2]  = mlist2(maxcutset, aa, x, ss, sss, xx2, glimit,
gul, ng, l1);

%%FINDING TIE SETS USING PETRI NETS CONCEPT
siz=size(eee2); aa=siz(1,1);
[eee2, tiepath, enc,enc2]  = pathsets(M, A, aa, x, xx, sss, eee2,
ng, l1);

%%FINDING CUT SETS USING PRIME NUMBER ENCODING
[eee2, eeeee, cutset]  = cutsets(aa, x , eee2, eeeee, ng);

%%BUILDING THE MARKOV TRANSITION MATRIX
[aaa, qmatrix]  = qmat(x, eeeee, eee2, sss, RR, FR, ng, sss2);

%%BUILDING Q-MATRIX AND P-MATRIX
[Qmatrix, Pmatrix, PP]  = QPmat(qmatrix, aaa);

%%CALCULATING MTTF
[Qmatrix2, MTTF]  = MTTFF(Pmatrix, eee2, aaa, ng);

%%CALCULATING THE STEADY STATE PROBABILITIES
[xxx]=invv(Qmatrix,PP);

%%CALCULATING THE LOAD INDICES
[AA, UU, freq, tfreq, qmatrix2, qmatrix3,eee4] = AUf(xxx,aaa,
qmatrix, eee2, ng);

cv=size(MTTF); bb=cv(1,1);
FRr=1/MTTF(bb);

Availability(loads,1)=AA;
Unavailability(loads,1)=UU;
MeanTimeToFailure(loads,1)=MTTF(1,1);
FailureRate(loads,1)=FRr(1,1);
TotalFrequency(loads,1)=tfreq;
NumberOfStates(loads,:)=states(:,loads)';
NumberOfLines(loads,:)=lines(:,loads)';
NumberOfNodes(loads,:)=nodes(:,loads)';
vaa(:,:,loads)=va;
end

%loads
Reliability(:,1)=1:length(LL)';
```

```
%Availability
Reliability(:,2)=Availability;
%Unavailability
Reliability(:,3)=Unavailability;
%MTTF
Reliability(:,4)=MeanTimeToFailure;
%Failure Rate
Reliability(:,5)=FailureRate;
% Interruption Frequency
Reliability(:,6)=TotalFrequency;
% Interruption Duration
Reliability(:,7)=Reliability(:,3)*8760;
%Duration/Faiulre
Reliability(:,8)=Reliability(:,7)./Reliability(:,6);
%ENS
Reliability(:,9)=Reliability(:,7).*AveragePower;

%SAIFI
Total(1)=sum(Reliability(:,6).*NumberOfCustomers)/sum(NumberOfCus
tomers);
%SAIDI
Total(2)=sum(Reliability(:,7).*NumberOfCustomers)/sum(NumberOfCus
tomers);
%CAIDI
Total(3)=Total(2)/Total(1);
%ASAI
Total(4)=((sum(NumberOfCustomers*8760))-
sum(Reliability(:,7).*NumberOfCustomers))/(sum(NumberOfCustomers*
8760));
%ASUI
Total(5)=1-Total(4);
%ENS
Total(6)=sum(Reliability(:,7).*AveragePower);
```

APPENDIX D

CHRONOLOGIAL LOAD DATA

Tables D.1 – D.3 document the load data for the RBTS [82, 83].

Table D.1 Weekly residential sector fraction

Week	Weekly Percentage	Week	Weekly Percentage
1	0.922	27	0.815
2	0.96	28	0.876
3	0.938	29	0.861
4	0.894	30	0.94
5	0.94	31	0.782
6	0.901	32	0.836
7	0.892	33	0.86
8	0.866	34	0.789
9	0.8	35	0.786
10	0.797	36	0.765
11	0.775	37	0.84
12	0.787	38	0.755
13	0.764	39	0.784
14	0.81	40	0.784
15	0.781	41	0.803
16	0.86	42	0.804
17	0.814	43	0.86
18	0.897	44	0.941
19	0.93	45	0.945
20	0.94	46	0.969
21	0.916	47	1
22	0.871	48	0.95
23	0.96	49	0.975
24	0.947	50	0.97
25	0.956	51	0.98
26	0.921	52	0.99

Table D.2 Hourly fraction of the sector peak load for residential, commercial, and industrial customers

Hour	Average Residential Day	Average Commercial Day	Industrial
1	0.55	0.01	0.337
2	0.5	0.01	0.337
3	0.43	0.01	0.337
4	0.37	0.01	0.337
5	0.36	0.01	0.337
6	0.38	0.03	0.337
7	0.385	0.04	1
8	0.425	0.25	1
9	0.45	0.85	1
10	0.55	0.9	1
11	0.6	0.91	1
12	0.7	0.92	1
13	0.7	0.985	1
14	0.75	0.975	1
15	0.75	0.88	1
16	0.75	0.865	1
17	0.8	0.89	1
18	0.85	0.9	1
19	0.85	0.9	1
20	0.86	0.64	1
21	0.86	0.6	1
22	0.8	0.42	1
23	0.75	0.4	1
24	0.65	0.025	1

Table D.3 Daily fraction of the residential, commercial, and industrial peak load

Day	Residential	Commercial	Industrial
Monday	0.96	1	1
Tuesday	1	1	1
Wednesday	0.98	1	1
Thursday	0.96	1	1
Friday	0.97	1	1
Saturday	0.83	1	1
Sunday	0.81	1	1